INSTITUTO DE BIOCIÊNCIAS
PROGRAMA DE PÓS-GRADUAÇÃO EM BIOLOGIA ANIMAL

LEANDRO RODRIGUES BORGES

EVOLUÇÃO NO CRÂNIO E MANDÍBULA DE ESPÉCIES DO GÊNERO *CTENOMYS* BLAINVILLE, 1826

PORTO ALEGRE
2019

LEANDRO RODRIGUES BORGES

EVOLUÇÃO NO CRÂNIO E MANDÍBULA DE ESPÉCIES DO GÊNERO *CTENOMYS* BLAINVILLE, 1826

Tese apresentada ao Programa de Pós-Graduação em Biologia Animal, Instituto de Biociências da Universidade Federal do Rio Grande do Sul, como requisito parcial à obtenção do título de Doutor em Biologia Animal.

Área de concentração: Biologia Comparada

Orientador: Prof. Dr. Thales Renato Ochotorena de Freitas

PORTO ALEGRE
2019

LEANDRO RODRIGUES BORGES

EVOLUÇÃO NO CRÂNIO E MANDÍBULA DE ESPÉCIES DO GÊNERO *CTENOMYS* BLAINVILLE, 1826

Aprovada em ____ de _____ de _____.

BANCA EXAMINADORA

_____

Dr/a. Gislene Lopes Gonçalves - UFRGS

_____

Dr. Jorge Reppold Marinho - URI

_____

Dr/a. Maria João Ramos Pereira - UFRGS

AGRADECIMENTOS

Sinceros agradecimentos a todos aqueles que contribuíram para a realização deste trabalho. Em particular:

Ao meu orientador, Thales, pela oportunidade, confiança, amizade, liberdade, e por todas as histórias, ensinamentos biológicos e de vida.

A minha família, por me apoiar sempre e estar presente em todos os momentos.

À Daniele Gerber Dorn pelo amor, equilíbrio, apoio emocional, paciência e confiança.

Ao Programa de Pós-graduação em Biologia Animal e a CAPES pela conceção da bolsa que foi fundamental para minha dedicação exlusiva.

Aos professores do Curso de Ciências Biológicas da URI Campus de Erechim, em especial: Jorge Reppold Marinho, Rodrigo Fornel, Rogério Luis Cansian, Denise Aparecida Martins Sponchiado, Sonia Balvedi Zakrzevski e Elisabete Maria Zanin, pela amizade.

Aos amigos: Bruno Busnello Kubiak, Renan Maestri, Marcelo Malysz e Daniel Galiano, pelas conversas e discussões sempre muito produtivas.

Todos os colegas do Laboratório de Citogenética e evolução (Departamento de genética da UFRGS), que me acolheram tão bem ao longo destes anos, vindo a criar diversas novas amizades.

Aos demais amigos que sempre estiveram presentes!

SUMÁRIO

RESUMO

Os roedores subterrâneos têm sido amplamente estudados, principalmente porque mostram muitas especializações (morfológicas, fisiológicas e comportamentais) relacionadas ao seu habitat. O gênero *Ctenomys* (tuco-tucos) é o mais diverso entre os roedores subterrâneos, com aproximadamente 70 espécies descritas. Estão amplamente distribuídas no Sul da América do Sul, e ocupam uma variedade de tipos de habitats (pastagens, estepes, desertos e dunas de areia). Os tuco-tucos também apresentam morfologia do crânio, corpo e cariótipos altamente diversificados. Este estudo utilizou a morfologia craniana e da mandíbula do gênero *Ctenomys*, para investigar aspectos evolutivos da espécie. Utilizamos aqui técnicas de morfometria geométrica e linear, aliadas a filogenia, o gene *Runx2* e ecologia (densidade aparente do solo) de diferentes espécies do gênero para acessar tais resultados. Não encontramos mudanças significativas nos padrões de integração do crânio, porém houve alta varição da integração morfológica. Também foi revelado alto sinal filogenético com os módulos propostos. O gene *Runx2* aparentemente não parece estar ligado com o alongamento facial dos espécimes de tuco-tucos. Porém não podemos descartar a possibilidade de que as substituições de glutaminas para prolinas possam alterar a funcionalidade proteica e, por extensão, a morfologia do crânio. Para a maioria das espécies investigadas, a correlação entre força da mordida e a densidade do solo não foi clara, e uma baixa correlação geral foi encontrada. As diferentes formas do crânio e mandíbula acessadas, geralmente foram associadas à força de mordida. As diferentes estratégias de escavação podem ser responsáveis pelo padrão encontrado na distribuição das espécies nas diferentes densidades de solo. Onde, em solos com maior densidade, ocorrem espécies com altas e baixas forças de mordida, enquanto em solos de menor densidade foram encontradas apenas espécies com forças de mordida baixas.

PALAVRAS CHAVE: Ctenomyidae, Rodentia, *Ctenomys*, integração morfológica, modularidade, *Runx2*; evolução morfológica.

ABSTRACT

Underground rodents have been extensively studied, mainly because they show many specializations (morphological, physiological and behavioral) related to their habitat. The genus Ctenomys (tuco-tucos) is the most diverse among subterranean rodents, with approximately 70 species described. They are widely distributed in southern South America, and occupy a variety of habitat types (pastures, steppes, deserts and sand dunes). The tuco-tucos also present morphology of the skull, body and highly diversified karyotypes. This study used the cranial and mandibular morphology of the genus Ctenomys to investigate evolutionary aspects of the species. We used here techniques of geometric and linear morphometry, together with phylogeny, the Runx2 gene and ecology (apparent density of soil) of different species of the genus to access such results. We did not find significant changes in the patterns of skull integration, but there was a high variation of the morphological integration. A high phylogenetic signal was also revealed with the proposed modules. The Runx2 gene apparently does not appear to be linked to the facial elongation of the tuco-tucos specimens. However, we can not rule out the possibility that glutamine-to-proline substitutions may alter protein functionality and, by extension, skull morphology. For most species investigated, the correlation between bite force and soil density was unclear, and a low overall correlation was found. The different skull and jaw forms accessed were generally associated with bite force. The different strategies of excavation can be responsible for the pattern found in the distribution of the species in the different soil densities. Where higher density soils occur with high and low bite forces, while in low density soils only species with low bite forces are found.

KEYWORDS: Ctenomyidae, Rodentia, *Ctenomys*, morphological integration, modularity, Runx2; morphological evolution.

Capítulo I

Introdução Geral

Evolução morfológica

A partir das ideias de Darwin, o entendimento de como morfologias complexas se desenvolvem e evoluem tem sido um dos assuntos fundamentais, mas pouco entendido em biologia evolutiva (Futuyma, 2002). Um organismo não é uma simples "impressão" do genoma, para compreender inteiramente a evolução necessitamos de informações sobre o genoma, que leva ao fenótipo via processos de desenvolvimento (Atchley e Hall, 1991; Raff, 1996). A teoria da evolução possui grande destaque na ciência, ela mudou profundamente a visão de mundo e forneceu base para entender a diversidade de formas de vida que habitam nosso planeta (Trevisan et al., 2017).

Em uma perspectiva de longo período de espaço/tempo a evolução biológica é a continuidade de organismos com alterações de linhagens distintas a partir de ancestrais comuns. A história da evolução biológica possui dois elementos principais: a ramificação das linhagens e as alterações dentro das linhagens. A princípio, espécies semelhantes tornam-se cada vez mais distintas, de maneira que transcorrido um determinado período de tempo, elas podem vir a apresentar significativas altercações, como por exemplo: genéticas e morfológicas (Futuyma, 2002).

Os mecanismos de evolução podem ser divididos em microevolução e macroevolução. A microevolução tange às variações nas frequências genéticas intrapopulacionais, perante a atuação da seleção natural e da deriva aleatória (Ridley, 2004). Contrapondo, a macroevolução tange à origem de novas espécies e divisões da hierarquia taxonômica acima do nível da espécie e, além disso, o início de adaptações complexas (*e.g.* morfologia) (Resnick & Ricklefs, 2009).

Uma maneira de explorar a variação na forma dos organismos e por extensão a evolução morfológica seria através do conjunto de técnicas de morfometria geométrica. Esta abordagem é o método que estuda a forma das estruturas biológicas empregando marcos anatômicos (*landmarks*) (Rohlf & Marcus, 1993), dando origem também, aos resultados em relação ao seu tamanho e forma (Peres-Neto, 1995). Utilizando estes marcos anatômicos (homólogos) tem-se um maior conhecimento da morfologia. Eles permitem identificar as variações de forma entre as mesmas estruturas morfológicas dos indivíduos analisados por usar as coordenadas cartesianas. Sejam elas em duas (2D) ou

três (3D) dimensões desses marcos anatômicos (Rohlf, 1999). As análises de forma são todos os atributos de uma configuração de pontos que não se modificam por implicações de tamanho, posição e orientação (Bookstein, 1989).

Integração morfológica

Os estudos de Olson e Miller (1951; 1958) basearam-se na quantificação das correlações entre caracteres de estruturas de diferentes grupos e fontes paleontológicas, com posterior análise qualitativa dos resultados. Baseados em hipóteses de função e desenvolvimento compartilhados entre caracteres, eles procuraram explicar o agrupamento estatístico entre determinados caracteres. Esses autores deram o nome de integração morfológica a esta técnica. Os grupos de correlações em uma estrutura existem em vários níveis, sendo o maior deles o organismo como um todo. No outro extremo, a existência de partes que não compartilham vias de desenvolvimento ou função com nenhuma outra (Wagner et al., 2008). Estes grupos de correlação mais fortes são atualmente denominados módulos (Wagner; Altemberg, 1996; Wagner et al., 2007).

Módulos são conjuntos de caracteres que podem ser: genes, proteínas ou elementos morfológicos altamente integrados entre si e pouco associados com os demais elementos. Em estudos empíricos de evolução morfológica eles são reconhecidos pela presença e correlações entre algumas partes de um organismo e ausência de correlação entre estas e outras partes do mesmo organismo (Berg, 1960). O arranjo modular pode ser considerado o resultado das relações funcionais entre caracteres de um determinado organismo (Falconer e Mackay, 1996).

O crânio é uma estrutura de suma importância para estudos morfológicos devido à complexidade do seu crescimento e as múltiplas funções dos órgãos da cabeça, revelando informações fundamentais sobre os taxas (Cheverud, 1982). Além disso, padrões comuns de desenvolvimento do crânio foram encontrados entre grupos afastados fornecendo a oportunidade para conduzir estudos comparativos em um contexto evolutivo (Moore, 1981; Smith, 1997; Porto et al., 2009). Sendo assim, o crânio de mamíferos é uma das estruturas biológicas mais estudadas no contexto de análises de integração morfológica (*e.g.* Marroig & Cheverud 2001; Ackermann & Cheverud 2004; Goswami 2006; Mitteroecker & Bookstein 2008; Porto et al. 2009; Koyabu et al. 2014).

Inferir o padrão modular de estruturas morfológicas complexas, isto é, entender de que forma alguns caracteres compartilham correlações mais elevadas entre si do que em relação a outros caracteres apresenta papel fundamental no entendimento da evolução

morfológica das espécies. Isso porque esse padrão pode facilitar ou restringir mudanças evolutivas (Schluter, 1996; Marroig e Cheverud, 2005; Pavlicev et al., 2008). Pode ser utilizado como exemplo, o alongamento craniofacial que é um aspecto comum de crescimento pós-natal em mamíferos. Os bebês humanos, assim como a maioria dos outros mamíferos placentários juvenis, têm rostos pequenos em relação ao adulto e cabeças comparativamente arredondadas (Cardini e Polly, 2013). Ou seja, em geral os mamíferos apresentam dois grandes módulos ligados ao crânio: o rostro (face) e a caixa craniana com crescimento diferenciado.

Gene RUNX 2

Os genes Runx são reguladores chave da expressão gênica específica nas principais vias de desenvolvimento ósseo, possivelmente surgiram no início da evolução dos mamíferos (Coffman, 2003; Levanon et al., 2003; Rennert et al., 2003). Nos vertebrados existem diversos genes Runx, por exemplo, os mamíferos possuem três: Runx1, Runx2 e Runx3 (Lund & Lohuizen, 2002). É sugerido que o Runx2 possui importante papel na variação da morfologia dos mamíferos, dentre elas a craniofacial (Sears et al.,2007; Newton et al., 2017). O gene Runx2 abrange aproximadamente 220 pares de base e contém oito exons (Ziros et al., 2008). Possui uma organização genômica semelhante aos outros genes Runx encontrados em mamíferos, o que indica preservação dos mesmos ao longo da evolução (Levanon et al., 1994; Zhang, et al., 1997; Ziros et al., 2008).

O Runx 2 contém vários domínios funcionais, dentre eles, um domínio repetitivo de glutamina (Q), alanina (A) (Ziros et al., 2008). Mudanças no comprimento, ou na proporção, de sequencias de glutaminas para alaninas dentro de Runx2 alteram sua atividade transcricional (Thirunavukkarasu et al., 1998; Pelassa et al., 2003). Fornecendo uma ligação direta entre a variação dentro deste domínio e o comprimento craniofacial (Sears et al.,2007). Tais repetições de codificação de proteínas foram descritas como “botões de ajuste evolucionário”, onde pequenas alterações podem ser associadas à rápida evolução morfológica (King et al., 1997; Kashi & King, 2006). Alguns estudos vêm comprovando esta hopótese (Sears et al.,2007; Williams et al., 2010; Pointer et al., 2012; Ritzman et al., 2017) revelando significativa correlação entre a repetição Q/A e o comprimento facial dentro de linhagens placentárias.

Embora os fatores envolvidos na formação da morfologia do crânio em roedores sejam conhecidos (Borges et al., 2016; Maestri et al., 2016; Marcy et al., 2016; Kubiak et

al., 2018), a base genética causadora da morfologia do crânio permanece pouco compreendida. O fator de transcrição 2 relacionado ao Runt (Runx2) codifica uma proteína essencial para a diferenciação e maturação dos osteoblastos e ossificação intramembranosa e endocondral (Otto et al., 1997; Zhang et al., 2017; Jung et al., 2017). Quando o Runx2 é regulado positivamente, a proliferação de osteoblastos aumenta e o tecido ósseo é alongado, enquanto quando regulado negativamente, a proliferação de osteoblastos diminui e o desenvolvimento ósseo é truncado (Sears et al. 2007).

Sabe-se que mutações no gene Runx2 estão associadas a doenças em humanos, como a displasia cleidocraniana (CCD) (OMIM: 119600) que pode ser causada por exemplo, por mutações não-sinônimas (Quack et al., 1999; Kim et al., 2006; Zhou et al., 1999), deleções (Ott et al., 2010) e repetições em tandem em domínios funcionais da proteína (Mundlos et al., 1997). Considerando o último, repetições em tandem dentro de regiões codificantes de um gene podem promover a regulação fina da expressão gênica, especialmente quando se consideram elementos que regulam tal expressão, como no caso do Runx2, um fator de transcrição (Ziros et al., 2008).

De fato, Sears et al. (2007) descobriram que o gene Runx2 está envolvido no alongamento e encurtamento do rostro de carnívoros, uma vez que o comprimento das repetições de glutamina (Q) e alanina (A), ou seja Q/A, apresenta uma forte correlação com o comprimento do rostro nas raças de cães. Sears et al. (2012) exploraram essa variação em vários táxons de vertebrados e descobriram que essa correlação vale para alguns táxons, e não entre vertebrados em geral.

Roedores do gênero *Ctenomys* Blainville, 1826

O grupo dos roedores é o mais bem sucedido (possui maior riqueza de espécies) entre os mamíferos. Estima-se que 40% das espécies de mamíferos vivos pertença a esse grupo, e se distribuem em todos os ambientes terrestres, exceto a Antártica (Lacher, 2016; Lacey et al., 2000). Entre os roedores terrestres, os que em algum momento da vida utilizam túneis ou escavações abaixo da superfície do solo para realizarem suas atividades essenciais, são denominados fossoriais (Lacey et al., 2000). Esses roedores administram grande parte de suas atividades vitais em galerias abaixo da superfície terrestre e são denominados de roedores subterrâneos (Lacey et al. 2000). Os roedores subterrâneos de diferentes famílias e gêneros distribuídos no mundo são marcados por suas convergências em estrutura e tamanho. Possuem semelhanças entre características corporais e hábitos de vida sugerindo uma evolução convergente na adaptação a este modo de vida (Lacey et

al., 2000), exibindo adaptações morfológicas para a atividade de escavação (Becerra et. al., 2011; Becerra et. al., 2014).

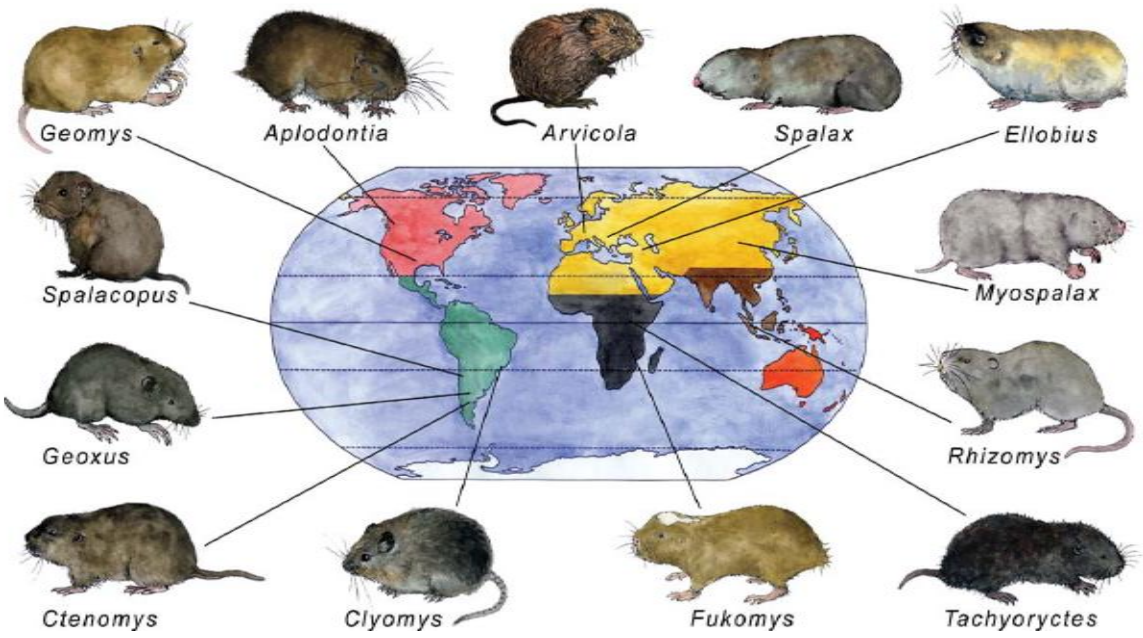

Distribuição de roedores subterrâneos pelo planeta. Diferentes mapas indicam as diferentes regiões zoogeográficas. Apenas gêneros selecionados representando diversas famílias e subfamílias de roedores subterrâneos são representados: *Geomys* (Geomyidae), *Aplodontia* (Aplodontidae), *Arvicola* (Muridae - Arvicolinae), *Spalax* (Muridae - Spalacinae), *Ellobius* (Muridae - Arvicolinae), Myospalax (Muridae - Myospalacinae), *Rhizomys* e *Tachyoryctes* (Muridae -Rhizomyinae), *Fukomys* (Bathyergidae), *Clyomys* (Echimyidae), *Ctenomys* (Octodontidae), *Geoxus* (Muridae - Sigmodontinae), *Spalacopus* (Octodontidae). De acordo com Begall et al., (2007).

Pertencente à família Ctenomyidae, o gênero *Ctenomys* (subordem Hystricognathi) é o mais diversificado entre os gêneros de roedores subterrâneos (Lacey et al., 2000). Encontrados exclusivamente na Região Neotropical, atualmente são descritas aproximadamente 70 espécies (Bidau, 2015; Freitas, 2016). Está presente em registros fósseis em formações do Terciário (Plioceno Superior) na Argentina, indicando sua origem neste ponto há mais de três milhões de anos (Reig et al., 1990; Verzi, 2008). Apresenta ampla distribuição na região Neotropical (Reig et al. 1990) com registros desde o Sul do Peru até a Terra do Fogo na Argentina. Por toda extensão da distribuição, o gênero pode ser encontrado em altitude desde o nível do mar até mais de 3700 metros, nos Andes peruanos (Pearson et al., 1968; Cook et al., 1990; Reig et al., 1990). Tais estimativas recentes têm sido consideradas como evidência de uma especiação em explosão em *Ctenomys*, dada a estruturação filogenética encontrada em muitos estudos independentes (Lessa & Cook, 1998; D'Elía et al., 1999; Slamovits et al., 2001; Castillo

et al., 2005; Parada et al., 2011; Freitas et al., 2012; Gardner et al., 2014). Também apresenta morfologia do crânio e do corpo altamente diversificada, e números cromossômicos de 2n = 10 em *Ctenomys steinbachi* à 2n = 70 em *Ctenomys dorbyigni* (Anderson, 1987; Reig et al., 1990).

Geralmente são encontrados em habitats como desertos, campos naturais, dunas costeiras, montanhas e ambientes florestais (Lacey et al., 2000). Devido ao seu hábito subterrâneo os tuco-tucos desenvolveram adaptações morfológicas. Como corpo robusto e cilíndrico, redução da cauda, redução dos pavilhões auditivos, maior desenvolvimento da musculatura (principalmente dos membros anteriores) e das unhas e abertura bucal atrás dos incisivos que ficam expostos para fora da boca (Nevo, 1979; Reig et al., 1990; Nowak, 1999). Alimentam-se preferencialmente de gramíneas (são herbívoros) e na maioria dos casos são generalistas. Causam influência direta na distribuição de plantas e na modificação das condições do solo, através do revolvimento e aeração da região onde habitam (Zenuto & Busch 1995; Rosi et al. 2000; Del Valle et al. 2001). Os espécimes do gênero costumam distribuir-se em manchas devido a sua alta territorialidade e possuem baixa dispersão (Busch et al. 2000).

Levando em consideração o que foi exposto anteriormente esta Tese analisou as seguintes hipóteses: 1) As espécies do gênero *Ctenomys* que habitam os solos mais compactos ou densos possuem a força da mordida mais forte, o que deve refletir-se na forma do crânio e da mandíbula dos indivíduos; enquanto as espécies que vivem em solos mais macios teriam uma força de mordida menor. 2) A presença de dois (rostro, caixa craniana) e três (rostro, caixa craniana e base crânio) módulos no crânio de espécies do gênero *Ctenomys*. 3) A correlação entre a relação Q/A de um domínio funcional da proteína Runx2 e a morfologia individual do crânio de representantes de um gênero *Ctenomys* e suas as suas implicações evolutivas. Avaliando se o gene Runx2 está diretamente envolvido em diferenças na forma do crânio dentro do gênero.

Objetivos

Este estudo avaliou o grau de integração/independência morfológica de distintos módulos no crânio de espécies do gênero *Ctenomys*. Inicialmente testamos como a dureza do solo afeta a força de mordida, bem como a forma e tamanho dos crânios e mandíbulas de tuco-tucos. Também foram testadas hipóteses modulares, após isso, avaliamos qual a magnitude de integração morfológica que está presente entre os módulos cranianos das diferentes espécies. Compararamos as taxas de magnitude das diferentes espécies e

analisamos as suas consequências evolutivas. E por fim, analisamos a associação entre a relação Q/A de um domínio funcional da proteína Runx2 e a morfologia individual do crânio de representantes do gênero *Ctenomys*.

Objetivo específico

- Verificar como a densidade do solo afeta a força da mordida, bem como a forma e o tamanho do crânio e mandíbula de tuco-tucos.

- Avaliar e comparar os padrões de integração morfológica em espécies morfologicamente diversas, analisando as implicações evolutivas desses padrões e magnitudes de integração para a evolução da morfologia das espécies.

- Explorar a associação entre a relação Q/A de um domínio funcional da proteína Runx2 e a morfologia individual do crânio de representantes do gênero *Ctenomys*, avaliando se o gene Runx2 está diretamente envolvido em diferenças na forma do crânio dentro do gênero.

Capítulo II

Manuscrito publicado no periódico *Journal of Zoology*

Anexo I

The role of soil features in shaping the bite force and related skull and mandible morphology in the subterranean rodents of genus *Ctenomys* (Hystricognathi: Ctenomyidae)

Leandro R. Borges[1], Renan Maestri[2], Bruno B. Kubiak[1], Daniel Galiano[3], Rodrigo Fornel[4], Thales R. O. Freitas[5]

1 Programa de Pós-Graduação em Biologia Animal, Universidade Federal do Rio Grande do Sul, Porto Alegre, RS, Brazil

2 Programa de Pós-Graduação em Ecologia, Universidade Federal do Rio Grande do Sul, Porto Alegre, RS, Brazil

3 Programa de Pós-Graduação em Ciências Ambientais, Universidade Comunitária da Região de Chapecó, Chapecó, SC, Brazil

4 Programa de Pós-Graduação em Ecologia, Universidade Regional Integrada do Alto Uruguai e das Missões, Erechim, RS, Brazil;

5 Departamento de Genética, Universidade Federal do Rio Grande do Sul, Porto Alegre, RS, Brazil.

Correspondence

Leandro Rodrigues Borges, Programa de Pós-Graduação em Biologia Animal, Universidade Federal do Rio Grande do Sul, Porto Alegre, RS, Brazil

Email: lborgesbiologia@gmail.com

Short title: Bite force in genus *Ctenomys*

Abstract

For rodents that live underground, digging in highly compacted soils requires a higher energy expenditure than digging in poorly compacted soils. We tested how soil hardness affects the bite force as well as the shape and size of the skulls and mandibles of tuco-tucos. Our hypothesis is that species that inhabit harder soils would show a stronger bite force, which should be reflected in the shape of the skull and mandible; while species living in softer soils should have a weaker bite force. We used 24 species of the genus *Ctenomys* to measure bite force (through the incisor strength formula) and quantify the shape and size of the skull and mandible. Information on soil bulk density in the regions occupied by each species was obtained from the literature. We used a combination of geometric morphometric and comparative methods to test our hypothesis. A phylogenetic linear regression (PGLS) between bite force (N) and centroid size was used to account for the dependence of bite force on size. We employed a series of two-block partial least-squares analyses to uncover the covariation between bite force and the shape of the skull and mandible. Finally, we ran five independent PGLS analyses to assess the influence of bulk density on bite force, skull shape, and mandible shape, taking into account phylogenetic non-independence. Species with higher bite forces tend to inhabit more-compact soils. However, for most species, the relationship between bite force and soil bulk density was unclear, resulting in a low overall correlation. Nonetheless, differences in skull and mandible shapes were generally associated with bite force (r= 0.60). In denser soils, species with high and low bite forces occur; whereas in lower density soils we found only species with weak bite forces. Differences in the excavation strategies among species may be responsible for this pattern.

Keywords

Functional morphology, geometric morphometrics, morphological evolution, phylogenetic comparative methods, rodent skull, soil hardness, subterranean niche, tuco-tucos.

Introduction

Knowledge of the factors that guide morphological diversification is of great interest for evolutionary biology (Wainwright, 2007; Diniz-Filho *et al*., 2009). The morphological variation among species is influenced mainly by two factors, ecology (e.g. environmental variables, biotic interactions) and evolutionary history (Viguier, 2002; Caumul & Polly, 2005; Wiens & Graham, 2005). The ecomorphological concept assumes that a correlation exists between the morphology and the ecology of organisms; that is, the mechanical demands imposed by ecological traits can be reflected in morphological changes in the system involved (Huey *et al*., 2003). Mammals possess a variety of body forms, which are often considered to be specific adaptations for specific environments and particular ways of life (Hildebrand, 1985; Biewener, 2003). Simultaneously, the history of lineages contributes to maintain phylogenetically close species with similar niche characteristics. This phylogenetic niche conservatism is accentuated in small-range mammals living in the tropics (Cooper *et al*., 2011).

Subterranean rodents have been extensively studied, particularly because they show many specializations (morphological, physiological and behavioral) related to their habitat (Nevo, 1999; Begall *et al*., 2007). The genus *Ctenomys* (tuco-tucos) is the most diverse among subterranean rodents (Lacey *et al*., 2000). The approximately 70 described species (Gardner *et al*., 2014; Bidau, 2015) are widely distributed across southern South America. They occupy a wide range of habitat types, especially in open areas including grasslands, steppes, deserts and sand dunes (Redford & Eisenberg, 1992; Bidau, 2006).

A few species occur in forest regions (Gardner *et al*., 2014). These open environments differ widely in the hardness and compaction of the soil, as well as in the amount of resources available. These soil features may influence some aspects of the biology of subterranean rodents (e.g. burrow-system characteristics and excavation strategies) (Reichman *et al*., 1982; Heth, 1989; Rosi *et al*., 2000; Becerra *et al*., 2011; Becerra *et al*., 2014; Lovy *et al*., 2015).

Species of *Ctenomys* possess a range of morphological adaptations for digging, which evolved over the last 15 million years after the group separated from its sister family Octodontidae (Lessa *et al*., 2008). The tuco-tucos, as well as some other subterranean rodents, use their mandibles and incisors to excavate the soil and to sever roots (Hildebrand, 1985; Nevo, 1999). The excavation process involves a high physiological cost, which increases in more-compact soils (Luna & Antinucci, 2006). The upper incisors of subterranean species are more similar to a chisel than are the incisors of species that inhabit the surface. Excavation using chisel-like teeth is described by some authors as executed primarily by the upper incisors, which break up the soil, while the lower incisors mainly move the soil (Hildebrand, 1998). By acting as a tool, applying a strong force in a restricted area, the incisors are closely involved in the excavation process (Hildebrand, 1998; Stein, 2000), helping to break up the substrate and open the way by cutting roots, tubers and the soft parts of plants (Stein, 2000). However, the differences in excavation strategies among species, and the degree to which each species is affected by the soil that it inhabits, remain largely unexplored (Hildebrand, 1998; Stein, 2000).

In view of the empirical association between soil features and the morphology of subterranean species (Mora *et al*., 2003; Lessa *et al*., 2008), we tested how soil hardness affects the bite force as well as the shape and size of the skulls and mandibles of tuco-tucos. The incisor section modulus, a geometrical parameter proportional to bending

strength, may be useful for prediction of bite force when direct measurements are not available (Freeman & Lemen, 2008), and was the index used in this study. Our hypothesis is that species that inhabit harder soils would show a stronger bite force, which should be reflected in the shape of the skull and mandible of individuals; while species living in softer soils would have a weaker bite force.

Materials and methods

Sample

We measured the bite force of 167 individuals belonging to 24 species of the genus *Ctenomys* (Appendix S1), deposited in the Recent mammal collection of the Field Museum of Natural History, Chicago, Illinois, USA, and in the Departamento de Genética, Universidade Federal do Rio Grande do Sul, Porto Alegre, Brazil. Only adult specimens were considered: juveniles were identified by their small skulls and were excluded. Additionally, we measured the shape and size of the skull and mandible of 1,122 adult specimens for the same 24 species (Appendix S1). These are deposited in the following museums and scientific collections: Departamento de Genética, Universidade Federal do Rio Grande do Sul, Porto Alegre, Brazil (UFRGS); Museo Nacional de História Natural y Antropología, Montevideo, Uruguay (MUNHINA); Museo Argentino de Ciencias Naturales "Bernardino Rivadavia", Buenos Aires, Argentina (MACN); Museo de La Plata, La Plata, Argentina (MLP); Museo de Ciencias Naturales "Lorenzo Scaglia", Mar del Plata, Argentina (MMP); Museum of Vertebrate Zoology, University of California, Berkeley, USA (MVZ); American Museum of Natural History, New York, USA (AMNH); and Field Museum of Natural History, Chicago, USA (FMNH).

Bite force

The bite force was measured for each individual by the method proposed by Freeman & Lemen (2008). We measured the length and width of the inferior incisor (anterior-posterior length and medial-lateral width, respectively), both taken at the base of the incisor. After taking the measurements, we applied the following formula: (Zi =((anterior-posterior length)^2 × (medial-lateral width)) / 6), where Zi is the index of incisor strength. This measure is highly correlated with direct measurements of bite force when measured *in vivo*, with a correlation coefficient of 0.96 (Freeman & Lemen, 2008). Bite-force values were transformed to Newtons (N), using the regression equation of Freeman & Lemen (2008). See Appendix S2 for bite-force values for each species. We then calculated an arithmetic mean of N values for all individuals in each species, and used the mean values for the species in the subsequent analyses.

Geometric morphometrics

Images of each skull in the dorsal, ventral and lateral views, and of the lateral view of the mandible were taken with a digital camera with 3.1 megapixels (2048 × 1536) resolution, in macro function and without flash or zoom. On each image, 29 landmarks (Appendix S3) were digitalized in the dorsal view (Fig. 1a), 30 in the ventral view (Fig. 1b), and 21 in the lateral view of the skull (Fig. 1c) (Fernandes *et al*., 2009); and 13 were digitalized on the mandible (Fig. 1d) (Fornel *et al*., 2010). The anatomical landmarks were digitized using the TPSDig2 software version 2.17 (Rohlf, 2015). The resulting matrices of coordinates were superimposed through a Generalized Procrustes Analysis procedure (GPA), which removes the effects of scale, orientation, and position. The size of each skull (Appendix S2) was assessed as the square root of the sum of the squares of the distance from each landmark to the centroid of the configuration (Bookstein, 1991),

using only the ventral view. We assumed that sexual dimorphism is negligible for the present purposes, because interspecific differences are usually greater than the reported sexual dimorphism in both the size and shape of the skull. The means of shape and size were calculated for all individuals of each species, and used in the subsequent statistical analyses.

Soil compaction

The bulk density (http://soilgrids.org) was chosen as a measurement of soil compaction because it has a direct relationship to soil hardness, as more-compact soils have greater density (Freddi *et al*., 2007; Reinert *et al*., 2008; Gubiani *et al*., 2014). Hengl *et al*. (2014) constructed the soil bulk density variable (kg/m^3) by compiling previously published soil profile data and environmental layers, at 1-km resolution, and using regression-kriging interpolation at non-sampled locations. The depth at which soil bulk density was compiled by Hengl *et al*. (2014) ranged from 0 to 200 cm. We accessed the information on bulk density for each species using the geographical ranges available from the International Union for Conservation of Nature and Natural Resources (IUCN, 2008). For *C. minutus* and *C. ibicuiensis*, the distribution ranges were generated in ArcGIS 10.0 software, based on occurrence records available in the articles by Galiano *et al*. (2014) and Freitas *et al*. (2012), respectively. This was necessary because the information available from the IUCN for *C. minutus* was incorrect (see Galiano *et al*., 2014 for details), and no information was available for the recently described *C. ibicuiensis*. The bulk density was extracted in ArcGIS 10.0 software for each pixel within the range of each species. Next, we calculated the mean densities of the pixels (mean density of soil) included in the distribution of each species, and used the mean density for each species in the subsequent analysis.

Statistical analyses

Phylogenetic relationships among species were based on the dated phylogenetic hypothesis presented by Freitas *et al*. (2012), pruned to cover the 24 species in our sample (Fig. 2). Details of the phylogenetic construction were described by Freitas *et al*. (2012). We used a phylogenetic generalized least-squares regression between bite force (log-transformed) and centroid size (log-transformed) to account for the dependence of bite force on size. Variables were log-transformed to assure normality and a linear relationship between variables. The phylogenetic covariance matrix used as the error term was based on the Brownian expectation (Grafen, 1989). We expected larger-bodied species to have stronger bites (e.g. Freeman & Lemen, 2008; Nogueira *et al*., 2009). To estimate bite force independently of size, we used the residuals of this regression as a bite-force estimate in all subsequent analyses.

We employed a series of two-block partial least-squares analyses (2B-PLS) to find the maximum covariation between bite force and the shape of the skull (in dorsal, ventral and lateral views) and the mandible (Rohlf & Corti, 2000). The significance of this covariation was assessed through 10,000 permutations in MorphoJ 1.06d (Klingenberg, 2011). We then used the PLS shape vectors as new shape variables (because they covary with bite force) to assess the correlation between them and the bulk density, through a phylogenetic generalized least-squares (PGLS) approach as described above.

We ran five independent PGLS analyses to assess the effect of bulk density on bite force (size-corrected), skull shape (PLS shape vectors of dorsal, ventral, and lateral views) and mandible shape (PLS shape vector), taking into account phylogenetic non-independence (Grafen, 1989). The PGLS regressions were performed in the R software (R Core Team, 2015), with the *geomorph* package (Adams & Otarola-Castillo, 2013).

Results

Most of the variation in bite-force data was explained by the variation in size: bite force is positively correlated with centroid size ($F_{1,22}$ = 155.4; r^2 = 0.87; P <0.0001) (Fig. 3). *Ctenomys lewisi*, *C. pearsoni*, *C. steinbachi* and *C. torquatus* showed a stronger bite force than expected for their size. Others including *C. colburni*, *C. ibicuiensis*, *C. magellanicus*, *C. maulinus*, *C. mendocinus*, *C. opimus* and *C. tuconax* showed a weaker bite than expected for their size, deviating from the allometric prediction downward (Fig. 3).

We found a weaker, although positive relationship between bite force and bulk density (r^2= 0.23; Fig. 4a) and between bite force (size-corrected) and bulk density (r^2=0.10; Table 1; Fig. 4b). Some species, such as *C. lewisi* and *C. steinbachi*, with a stronger bite force, were associated with harder soils; while *C. magellanicus*, *C. maulinus* and *C. colburni*, with a weaker bite force, were associated with softer soils. However, most of the species showed less clear patterns of bite force in relation to bulk density. In general, lower values of bulk density were associated with low bite forces, but higher values of bulk density could be associated with both high and low values of bite force.

The PLS shape vectors derived for the dorsal and lateral views of the skull each showed a higher correlation with the residual bite force than would be expected based on chance (dorsal: r = 0.64; P = 0.03; lateral: r = 0.76; P = 0.003) (Figs 5a and 7a, respectively). However, the ventral views of the skull and the mandible did not show a significant correlation with the residual bite force (ventral: r = 0.60; P = 0.07; mandible: r = 0.65; P = 0.055), despite their relatively high correlations (Figs 6a and 8a, respectively).

The PGLS analysis showed a significant association between the PLS shape vectors of the dorsal, ventral and lateral views of the skull, and the bulk density of the soil (Table 1). However, the PLS shape vector of the mandible and the residual bite force did not show an association with bulk density (Table 1).

The shape changes described by the PLS shape vector derived from the skull data showed that negative values of residual bite force are associated with a lateral narrowing and lengthy rostrum (Figs 5b and 6b), a lateral narrowing of the zygomatic arch, and a perceptible expansion of the braincase (Fig. 7b). At the opposite end of the same shape vector, positive values of residual bite force are associated with a wider skull, especially in the rostrum (Figs 5c and 6c); a relative increase in the skull height (Fig. 7c); a more robust zygomatic arch, particularly in the anterior portion; and a wider interparietal region, as revealed by the convex lateral profile of the occipital (Fig. 7c). Regarding the mandible, negative values of residual bite force were associated with a smaller body of the mandible and a depressed coronoid process (Fig. 8b). Structures of the mandible associated with positive values of residual bite force included a larger condyloid process, a bigger body of the mandible, and a high coronoid process (Fig. 8c).

Discussion

For subterranean rodents, digging in harder soils necessitates a greater energy expenditure than digging in less-compacted soils, as found for *C. talarum* by Luna & Antinuchi (2006). In turn, increases in bite force are also probably necessary to couple with harder soils. Our study provided evidence that this relationship may affect rodents at a macroevolutionary level, where different species have different bite forces depending on the hardness of the soil that they occupy. Species with stronger bite forces (e.g. *C. conoveri*, *C. lewisi* and *C. steinbachi*) tend to inhabit more-compact soils. However, for

most species, the relationship between bite force and bulk density was unclear, resulting in a low overall correlation.

The skull of subterranean rodents is generally more massive and robust than that of surface dwellers (Stein, 2000). The skull projections tend to be compressed to facilitate movement in the burrows (Nevo, 1979). These changes facilitate the process of excavation in a variety of soils, which may be hard or soft (Stein, 2000). The different ways used to dig (chisel teeth and raising the head) (Hildebrand, 1998) are reflected in the different cranial morphologies (Lessa & Thaeler, 1989). In this study, we found a covariation between bite force and skull shape: species with a wider skull and a more-robust mandible have a stronger bite force than species with an elongated and less wide skull and mandible, in agreement with other studies of mammals (Van Valkenburgh & Ruff, 1987; Christiansen & Adolfssen, 2005; Nogueira *et al*., 2009).

An important factor that restricts the shape and mechanics of the body is its size (Schmidt-Nielsen, 1984). *Ctenomys conoveri* inhabits a region with very compacted soil, although its skull and mandible are less robust according to the PLS analysis. However, the stronger bite force of *C. conoveri* can be explained by its larger body size, which generates sufficient force to dig in harder soil. This suggests that, during the course of evolution, *C. conoveri* did not change the shape of its skull and mandible to adapt to the more-compact soil, but might have changed its body size. Because variation in size is sometimes considered a more labile feature than shape, it is also more susceptible than shape to environmental changes (Thorpe, 1976; Patton & Brylski, 1987; Cardini & Elton, 2009). The cost of burrowing also increases with body size (Vleck, 1981) which generates a trade-off between size increasing and metabolic economy in burrowing. This may be a constraint for species of *Ctenomys* to become larger, which may explain why just *C. conoveri* evolved to a discrepant size compared to others.

In contrast, *C. lewisi* and *C. steinbachi*, which also live in more-compacted soils and have intermediate body sizes, have robust skulls, which probably reflects an adaptation to the compact soils. The shape of the skull and mandible may have changed to increase their bite force in order to facilitate the process of excavation. According to Lacey *et al*. (2000), the genus *Ctenomys* includes species that are widely distributed in South America, exploiting different types of habitats and different types of soil. This ecological diversity, involving distinct functional requirements, may have driven the differentiation in skull morphology and led to a high rate of speciation in the genus (Mora *et al*., 2003).

Species with both high and low bite forces proved to be present in harder soils, while only species with low bite forces are present in soft soils. This pattern is likely due to the different characteristics of each environment. Environments with lower bulk density (such as sand dunes) have less biomass than higher-density soils (sand fields), as soil density is positively related to the amount of biomass available (food source) (Malizia *et al.*, 1991; Cutrera *et al.*, 2010; see the results of Galiano *et al.*, 2014; Kubiak *et al*., 2015). The greater availability of food is likely a key factor in the choice of habitat, leading species with lower bite forces to inhabit locations with higher soil bulk density. To make this possible, the species can modify their excavation strategies (Hildebrand, 1998; Vassallo, 1998; Stein, 2000; Becerra *et al*., 2011, 2014) and / or change the shape and size of their burrow systems (Reichman *et al*., 1982; Heth, 1989; Rosi *et al*., 2000; Lovy *et al*., 2015) in order to access larger amounts of food in smaller home ranges.

In summary, the 24 species of the genus *Ctenomys* studied here showed variations in their skull shape associated with bite force. Studies on the association between bite force and environmental features are expanding knowledge of the interactions between morphology and the environments where these species occur (Becerra *et al*., 2011, 2013,

2014; Vassallo *et al*., 2015; Verzi *et al*., 2010). Becerra *et al*. (2014) suggested that, probably, intraspecific differences in the bite force of *C. australis* could be explained mainly by differences in muscle development. This evidence of muscle development in the region of the skull and mandible is likely to contribute to understanding of the bite forces of members of the genus *Ctenomys* and other mammals. Studies of the digging behavior of different species would also be important, providing essential information to better understand the correlation between bite force and the environment.

Acknowledgements

We thank Aldo Vassallo and an anonymous reviewer for the helpful suggestions on the manuscript. We are grateful to our colleagues of the Laboratório de Citogenética e Evolução for their support in various stages of this study. Our thanks to all curators and collection managers who provided access to specimens of *Ctenomys*: Enrique González (MUNHINA), Olga B. Vacaro and Esperança A. Varela (MACN), Diego H. Verzi and A. Itatí Olivares (MLP), A. Damián Romero (MMP), James L. Patton, Eileen A. Lacey, and Christopher Conroy (MVZ), Eileen Westwig (AMNH), and Bruce D. Patterson (FMNH). L.R.B and R.M. received student scholarships from the Coordenação de Aperfeiçoamento de Pessoal de Nível Superior (CAPES), and B.B.K. and D.G. received student grants from the Conselho Nacional de Desenvolvimento Científico e Tecnológico (CNPq). T.R.O.F. received research support from CNPq, CAPES and the Fundação de Amparo à Pesquisa do Rio Grande do Sul (FAPERGS).

References

Adams, D.C. & Otárola-Castillo, E. (2013). Application geomorph: an R package for the collection and analysis of geometric morphometric shape data. *Meth. Ecol. Evol*. **4**, 393–399.

Becerra, F., Echeverría, A. & Vassallo, A.I. (2011). Bite force and mandible biomechanics in the subterranean rodent Talas tuco-tuco (*Ctenomys talarum*) (Caviomorpha Octodontoidea). *Can. J. Zool*. **89**, 334-342.

Becerra, F., Casinos, A. & Vassallo, A.I. (2013). Biting performance and skull biomechanics of a chisel tooth digging rodent (*Ctenomys tuconax*; Caviomorpha; Octodontoidea). *J. Exp. Zool. A*, **319**, 74–85.

Becerra, F., Echeverría, A.I., Casinos, A. & Vassallo, A.I. (2014). Another one bites the dust: Bite force and ecology in three caviomorph rodents (Rodentia, Hystricognathi). *J. Exp. Zool A*, **321**, 220–232.

Begall, S., Burda, H. & Schleich, C.E. (2007). *Subterranean rodents: news from underground.* Berlin: Springer Verlag.

Bidau, C.J. (2006). Familia Ctenomyidae. In *Mamíferos de Argentina: sistemática y distribución*: 212–231. Bárquez, R.J., Díaz, M.M., & Ojeda, R.A. (Eds). Tucumán, Argentina: SAREM (Sociedad Argentina para el Estudio de los Mamíferos).

Bidau, C.J. (2015). Family Ctenomyidae Lesson, 1842. In *Mammals of South America*, Vol. 2: 818 – 877. Patton, J.L., Pardiñas, U.F.J. & D'Elía, E. (Eds). Chicago and London: The University of Chicago Press.

Biewener, A.A. (2003). *Animal locomotion*. Oxford, U.K.: Oxford University Press.

Bookstein, F.L. (1991). *Morphometric tools for landmark data: geometry and biology*. London, U.K: Cambridge University Press.

Cardini, A. & Elton, S. (2009). Geographical and taxonomic influences on cranial variation in red colobus monkeys (Primates, Colobinae): introducing a new approach to 'morph' monkeys. *Glob. Ecol. Biogeogr*. **18**, 248-263.

Caumul, R. & Polly, P.D. (2005). Phylogenetic and environmental components of morphological variation: skull, mandible, and molar shape in marmots (Marmota, Rodentia). *Evolution* **59**, 2460–2472.

Christiansen, P. & Adolfssen, J.S. (2005). Bite forces, canine strength and skull allometry in carnivores (Mammalia, Carnivora). *J. Zool*. **266**,133–151.

Cooper, N., Freckleton, R.P. & Jetz, W. (2011). Phylogenetic conservatism of environmental niches in mammals. *Proc. R. Soc. B*, 278, 2384-2391.

Cutrera, A.P., Mora, M.S., Antenucci, C.D. & Vassallo, A.I. (2010). Intra- and interspecific variation in home-range size in sympatric tuco-tucos, *Ctenomys australis* and *Ctenomys talarum*. *J. Mammal*. **91**, 1425-1434.

Diniz-Filho, J.A., Bini, L.M., Rangel, T.F.L.B., Loyola, R.D., Hof, C., Nogués-Bravo, D. & Araújo, M.B. (2009). Partitioning and mapping uncertainties in ensembles of forecasts of species turnover under climate changes. *Ecography* **32**, 1–10.

Felsenstein, J. (1985). Phylogenies and the comparative method. *Am. Nat*. **125**, 1–15.

Fernandes, F.A., Fornel, R., Cordeiro-Estrela, P. & Freitas, T.R.O. (2009). Intra- and interspecific skull variation in two sister species of the subterranean rodent genus *Ctenomys* (Rodentia, Ctenomyidae): coupling geometric morphometrics and chromosomal polymorphism. *Zool. J. Linn. Soc*. **155**, 220-237.

Fornel, R., Cordeiro-Estrela, P. & Freitas, T.R.O. (2010). Skull shape and size variation in *Ctenomys minutus* (Rodentia: Ctenomyidae) in geographical, chromosomal polymorphism, and environmental contexts. *Biol. J. Linn. Soc*. **101**, 705-720.

Freddi, O.S., Centurion, J.F., Beutler, A.N., Aratani, R.G., Leonel, C.L. & Silva, A.P. (2007). Soil compaction and least limiting water range on development and productivity of maize. *Bragantia*, Campinas **66**, 477-486.

Freeman, P.W. & Lemen, C.A. (2008). A Simple Morphological Predictor of Bite Force in Rodents. *J. Zool*. **275**, 418–422.

Freitas, T.R.O., Fernandes, F.A., Fornel R., & Roratto P.A. (2012). An endemic new species of tuco-tuco, genus *Ctenomys* (Rodentia: Ctenomyidae), with a restricted geographic distribution in southern Brazil. *J. Mammal*. **93**, 1355-1367.

Futuyma, D. J. Biologia evolutiva. Ribeirão Preto: FUNPEC – RP, 2002.

Galiano, D., Kubiak, B.B., Overbeck, G.E. & Freitas, T.R.O. (2014). Effects of rodents on plant cover, soil hardness, and soil nutrient content: a case study on tuco-tucos (*Ctenomys minutus*). *Acta Theriol*. **59**, 583–587.

Gardner, S.L., Salazar-Bravo, J. & Cook, J.A. (2014). New Species of *Ctenomys* Blainville 1826 (Rodentia: Ctenomyidae) from the Lowlands and Central Valleys of Bolivia. *Faculty Publications from the Harold W. Manter Laboratory of Parasitology*. Paper 722.

Garland, T. & Ives, A.R. (2000). Using the past to predict the present: confidence intervals for regression equations in phylogenetic comparative methods. *Am. Nat*. **155**, 346–364.

Goswami, A. & Polly, P.D. (2010). Methods for studying morphological integration and modularity. In *Quantitative Methods in Paleobiology. Paleontological Society Short Course*. Alroy, J. & Hunt, G. (Eds.). *Paleontol. Soc. Pap.* **16**, 213–243.

Grafen, A. (1989). The phylogenetic regression. *Phil. Trans. R. Soc. Lond. B Biol. Sci.* **326(1233)**, 119–157.

Gubiani, P.I., Reinert, D.J. & Reichert, J.M. (2014). Critical values of soil bulk density evaluated by boundary conditions *Ciênc. Rural* **44**, 994-1000.

Hengl, T., Jesus, J.M., MacMillan, R.A., Batjes, N.H., Heuvelink, G.B.M., Ribeiro, E., Samuel-Rosa, A., Kempen, B., Leenaars, J.G.B., Walsh, M.G. & Ruiperez Gonzalez, M. (2014). SoilGrids1km — Global Soil Information Based on Automated Mapping. *PLoS ONE* **9**, e105992.

Heth, G. (1989). Burrow patterns of the mole-rat *Spalax ehrenbergi* in two soil types (terra-rossa and rendzina) in Mount Carmel. Israel. *J. Zool*. **217**, 39-56.

Hildebrand, M. (1985). Digging of quadrupeds. In *Functional vertebrate morphology*: 89–109. Hildebrand, M., Bramble, M., Liem, K.F. & Wake, D.B. (Eds.). Cambridge, Massachusetts: The Belknap Press of Harvard University Press.

Hildebrand, M. (1998). *Analysis of vertebrate structure*. 5th edn. New York: Wiley.

Huey, R.B., Hertz, P.E. & Sinervo, B. (2003). Behavioral drive versus behavioral inertia in evolution: a null model approach. *Am. Nat*. **161**, 357–366.

IUCN (2008). Red List. Available at http://www.iucnredlist.org/technical-documents/spatial-data

Klingenberg, C.P. (2011). MorphoJ: an integrated software package for geometric morphometrics. *Mol. Ecol. Resour*. **11**, 353–357.

Kubiak, B.B., Galiano, D. & Freitas, T.R.O. (2015). Sharing the Space: Distribution, Habitat Segregation and Delimitation of a New Sympatric Area of Subterranean Rodents. *PLoS ONE* **10**, e0123220.

Lacey, E.A., Patton, J.L. & Cameron, G.N. (2000). *Life underground*. Chicago and London: The University of Chicago Press.

Lessa, E. & Thaeler, C. (1989). A reassessment of morphological specialization for digging in pocket gophers. *J. Mammal.* **70**, 689-698.

Lessa, E.P., Vassallo, A.I., Verzi, D.H. & Mora, M.S. (2008). Evolution of morphological adaptations for digging in living and extinct ctenomyid and octodontid rodents (Caviomorpha, Octodontoidea). *Biol. J. Linn. Soc*. **95**, 267–283.

Lövy, M., Šklíba, J., Hrouzková, E., Dvořáková, V., Nevo, E. & Šumbera, R. (2015). Habitat and Burrow System Characteristics of the Blind Mole Rat *Spalax galili* in an Area of Supposed Sympatric Speciation. *PLoS ONE* **10**, e0133157.

Luna, F. & Antinuchi, C.D. (2006). Cost of foraging in the subterranean rodent *Ctenomys talarum*: effect of soil hardness. *Can. J. Zool.* **84,** 661–667.

Malizia, A.I., Vassallo, A.I. & Busch, C. (1991). Population and habitat characteristics of two sympatric species of *Ctenomys* (Rodentia: Octodontidae). *Acta Theriol.* **36**, 87–94.

Mora, M., Olivares, A.I. & Vassallo, A.I. (2003). Size, shape and structural versatility of the skull of the subterranean rodent *Ctenomys* (Rodentia, Caviomorpha): functional and morphological analysis. *Biol. J. Linn. Soc.* **78**, 85–96.

Nevo, E. (1979). Adaptive Convergence and Divergence of Subterranean Mammals. *Ann. Rev. Ecol. Syst.* **10**, 269-308.

Nevo, E. (1999). *Mosaic evolution of subterranean mammals – Regression, progression, and global convergence*. New York: Oxford University Press.

Nogueira, M.R., Peracchi, A.L. & Monteiro, L.R. (2009). Morphological correlates of bite force and diet in the skull and mandible of phyllostomid bats. *Funct. Ecol.* **23**, 715–723.

Patton, J.L. & Brylski, P.V. (1987). Pocket gophers in alfalfa fields: causes and consequences of habitat-related body size variation. *Am. Nat.* **130**, 493–506.

Redford, K.H. & Eisenberg, J.F. (1992). *Mammals of the Neotropics*. Vol. 2. *The Southern Cone: Chile, Argentina, Uruguay, Paraguay.* Chicago: University of Chicago Press.

Reichman, O.J., Whitham, T.G. & Ruffner, G.A. (1982). Adaptive geometry of burrow spacing in two pocket gopher populations. *Ecology* **63**, 687-695.

Reinert, D.J., Albuquerque, J.A., Reichert, J.M., Aita, C. & Andrada, M.M.C. (2008). Bulk density critical limits for normal root growth of cover crops. *Rev. Bras. Ciênc. Solo* **32**, 1805-1816.

Rohlf, F.J. (2015). The tps series of software. *Hystrix, Ital. J. Mammal.* 26: 9-12.

Rohlf, F.J. & Corti, M. (2000). Use of two-block partial least-squares to study covariation in shape. *Syst. Biol.* **49**, 740–753.

Rosi, M.I., Cona, M.I., Videla, F., Puig, S. & Roig, V.G. (2000). Architecture of *Ctenomys mendocinus* (Rodentia) burrows from two habitats differing in abundance and complexity of vegetation. *Acta Theriol.* **45**, 491-505.

Schmidt-Nielsen, K. (1984). *Scaling: why is animal size so important?* Cambridge, U.K.: Cambridge University Press.

Stein, B. (2000). Morphology of subterranean rodents. In *Life underground: the biology of subterranean rodents*: 19–61. Lacey, E.A., Patton, J.L. & Cameron, G.N. (Eds.). Chicago: University of Chicago Press.

Thorpe, R.S. (1976). Biometric analysis of geographic variation and racial affinities. *Biol. Rev*. **51**, 407–452.

Van Valkenburgh, B. & Ruff, C.B. (1987). Canine tooth strength and killing behaviour in large carnivores. *J. Zool*. **212**, 379–397.

Verzi, D.H., Álvarez, A., Olivares, A.I., Morgan, C.C. & Vassallo, A.I. (2010). Ontogenetic trajectories of key morphofunctional cranial traits in South American subterranean ctenomyid rodents. *J. Mammal*. **91**, 1508-1516.

Viguier, B. (2002). Is the morphological disparity of lemur skulls (Primates) controlled by phylogeny and/or environmental constraints? *Biol. J. Linn. Soc.* **76**, 577–590.

Vleck, D. (1981). Burrow structure and foraging costs in the fossorial rodent, *Thomomys bottae*. *Oecologia* **49**, 391-396.

Wainwright, P.C. (2007). Functional versus morphological diversity in macroevolution. *Annu. Rev. Ecol. Evol. Syst*. **38**, 381–401.

Wiens, J.J. & Graham, C.H. (2005). Niche conservatism: integrating evolution, ecology, and conservation biology. *Annu. Rev. Ecol. Evol. Syst.* **36**, 519–539.

Tables

Table 1 Phylogenetic regressions between residual bite forces and the shapes of the skull and mandible, with the soil bulk density of the 24 species of *Ctenomys* found in the Neotropical region.

	F	R^2	*P*
Residual bite force			
Bulk	2.51	0.10	0.41
Dorsal PLS shape vector			
Bulk	11.04	0.33	0.001
Ventral PLS shape vector			
Bulk	9.45	0.30	0.001
Lateral PLS shape vector			
Bulk	8.30	0.27	0.001
Mandible PLS shape vector			
Bulk	0.086	0.003	0.874

Figure Legends

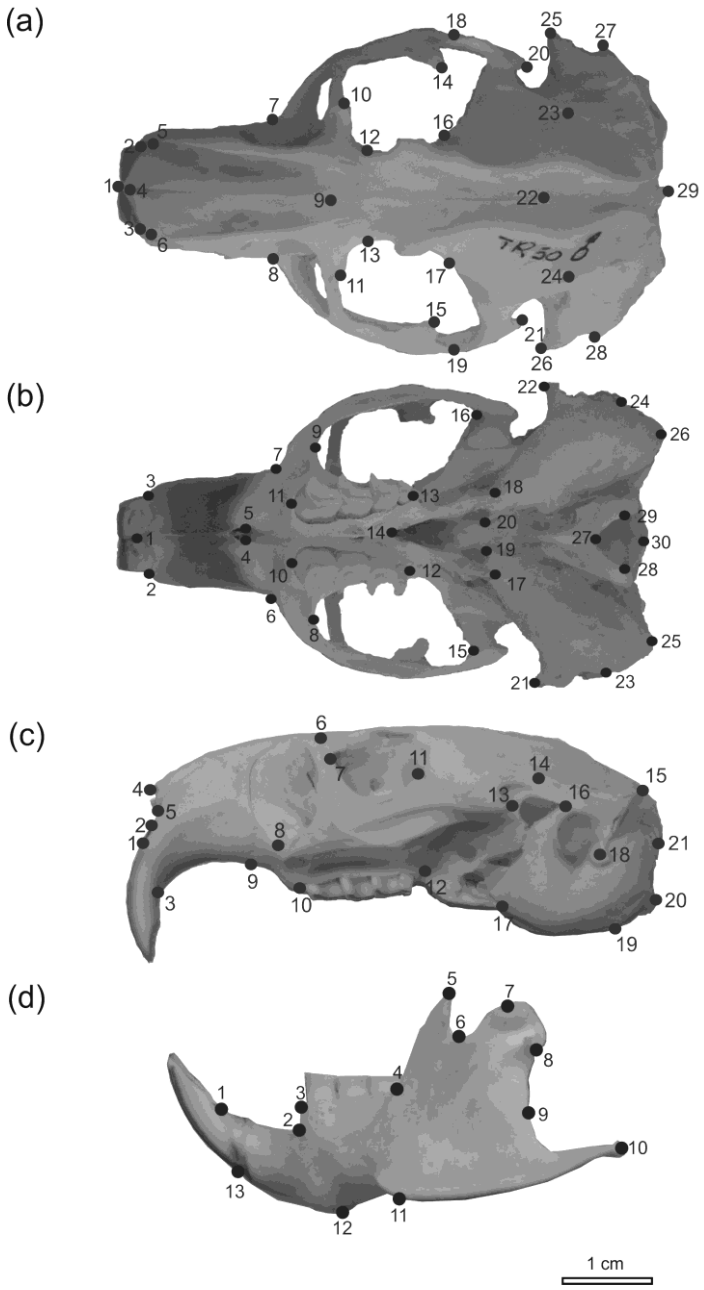

Figure 1 Landmarks used to capture shape from the dorsal, ventral and lateral views of the skull and left side of the mandible, as showed in *Ctenomys flamarioni*.

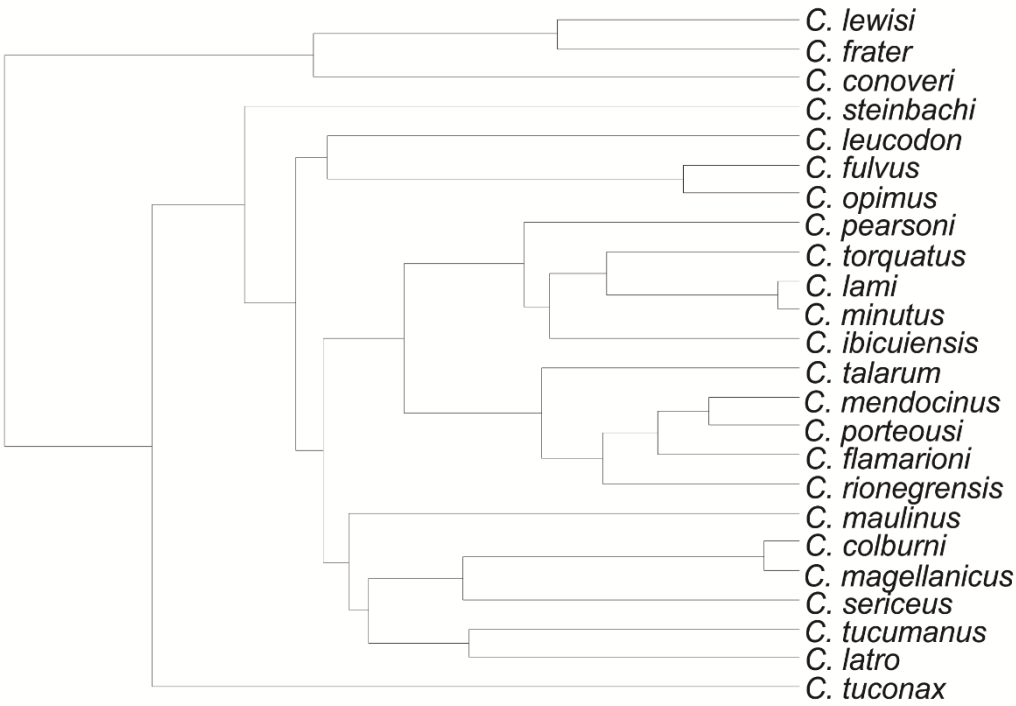

Figure 2 Phylogenetic relationships among species in the genus *Ctenomys*, based on molecular data (Freitas et al., 2012). The original tree was edited to exclude species not investigated here.

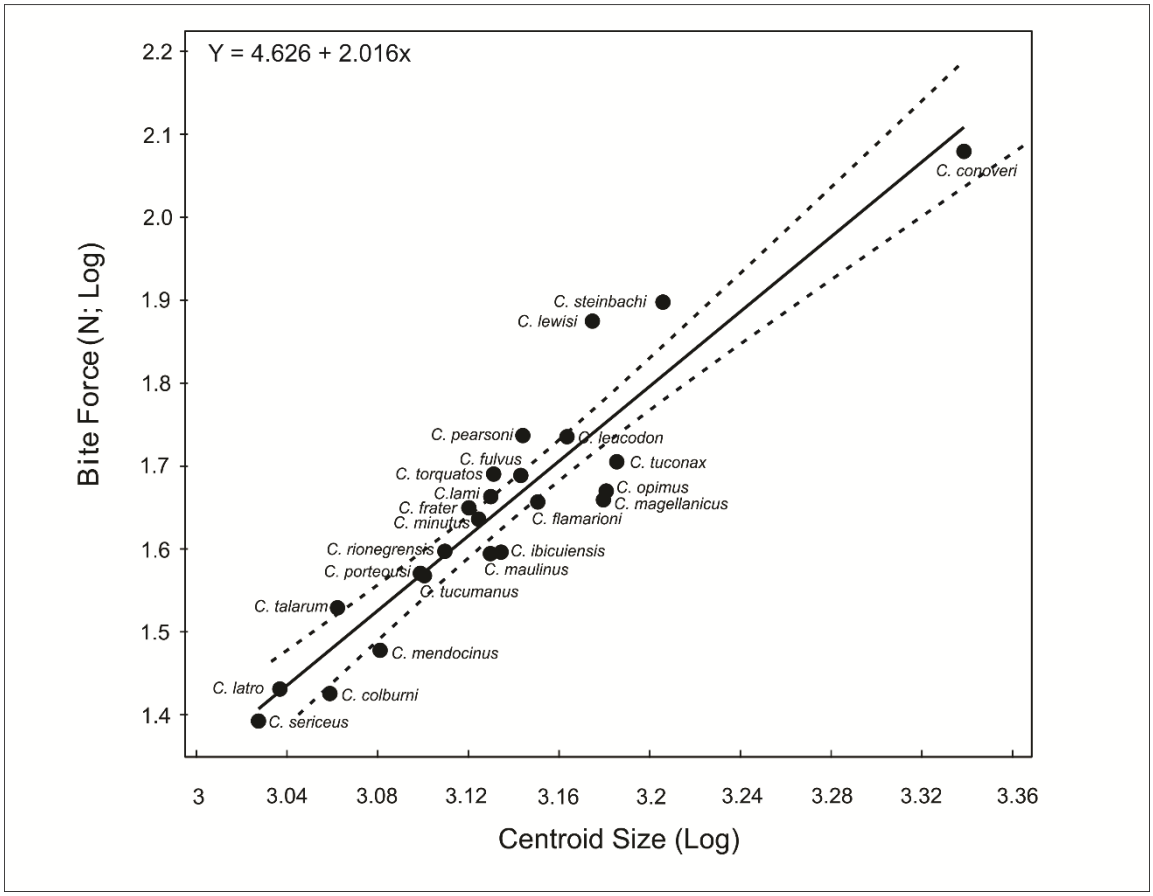

Figure 3 Regression analysis between the bite force (N = Newtons) and the centroid size (log) of 24 species of *Ctenomys*. The dashed lines represent 95% confidence intervals for the predicted line of the phylogenetic generalized least-squares regression.

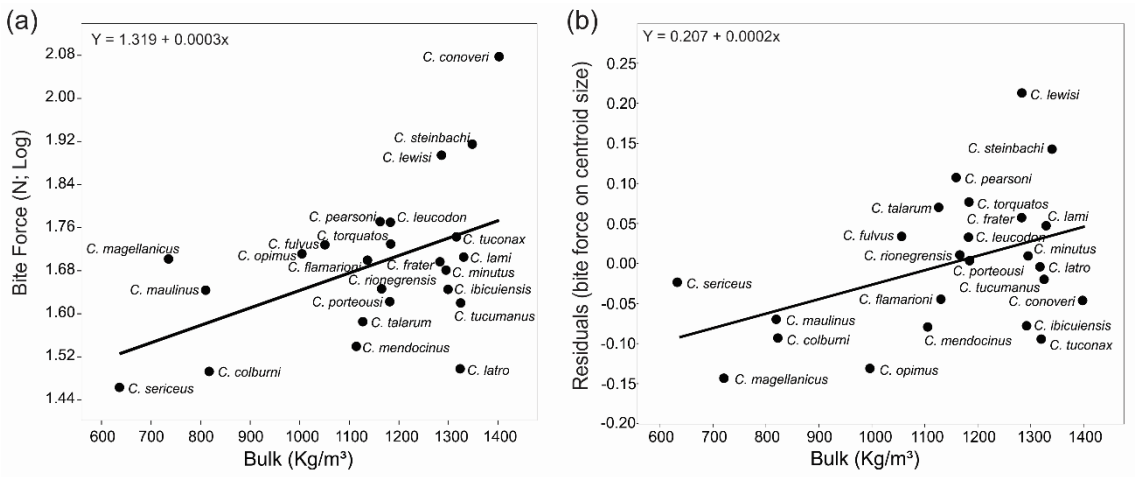

Figure 4 Regression of bite force (residuals of bite force on centroid size) on soil bulk density for 24 species of *Ctenomys*.

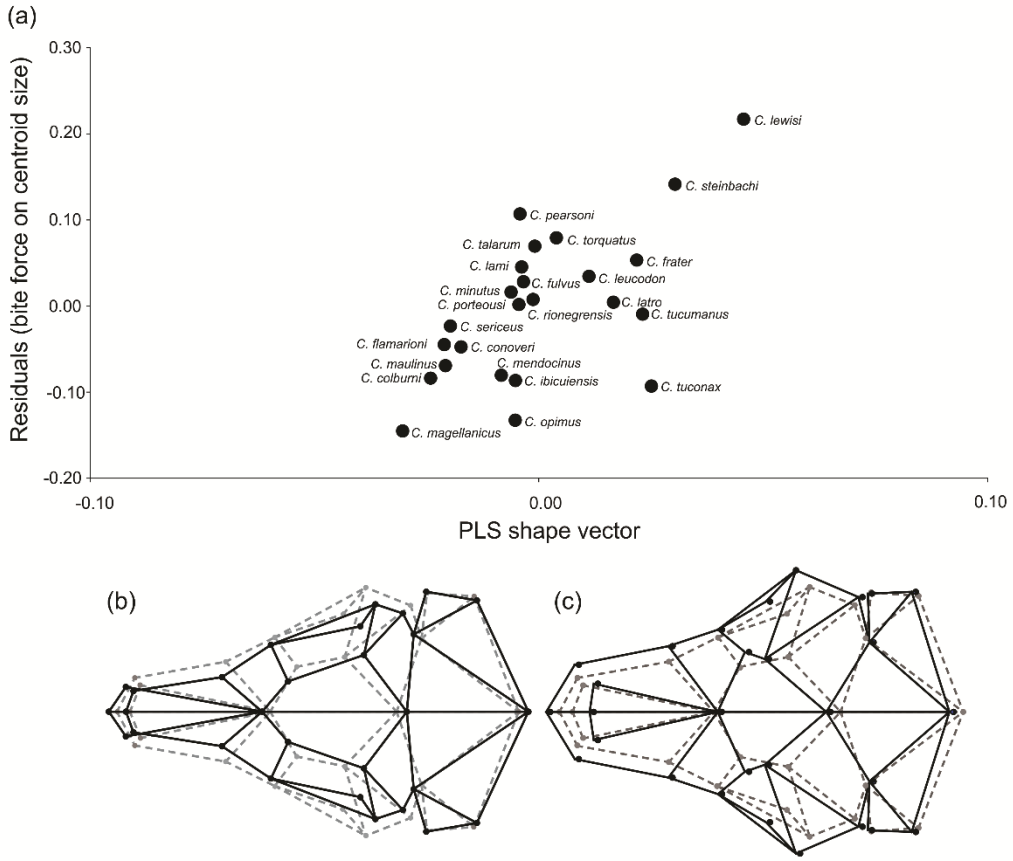

Figure 5 (a) First pair of vectors of a two-block partial least-squares analysis for the association between bite force (residuals of bite force on centroid size) and skull shape in dorsal view for 24 species of *Ctenomys*. Representation of conformational changes associated with (b) negative and (c) positive vectors of PLS (dashed gray lines correspond to the mean shape, and solid black lines correspond to the shape associated with positive and negative scores).

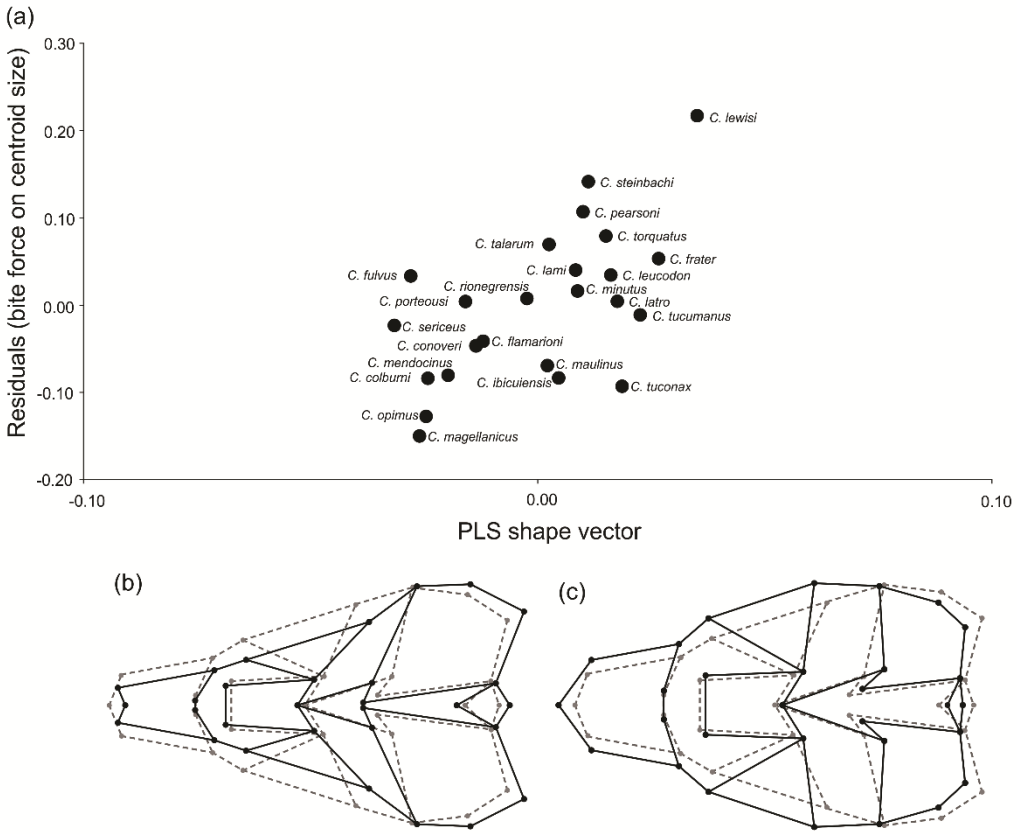

Figure 6 (a) First pair of vectors of a two-block partial least-squares analysis for the association between bite force (residuals of bite force on centroid size) and skull shape in ventral view for 24 species of *Ctenomys*. Representation of conformational changes associated with (b) negative and (c) positive vectors of PLS (dashed gray lines correspond to the mean shape, and solid black lines correspond to the shape associated with positive and negative scores).

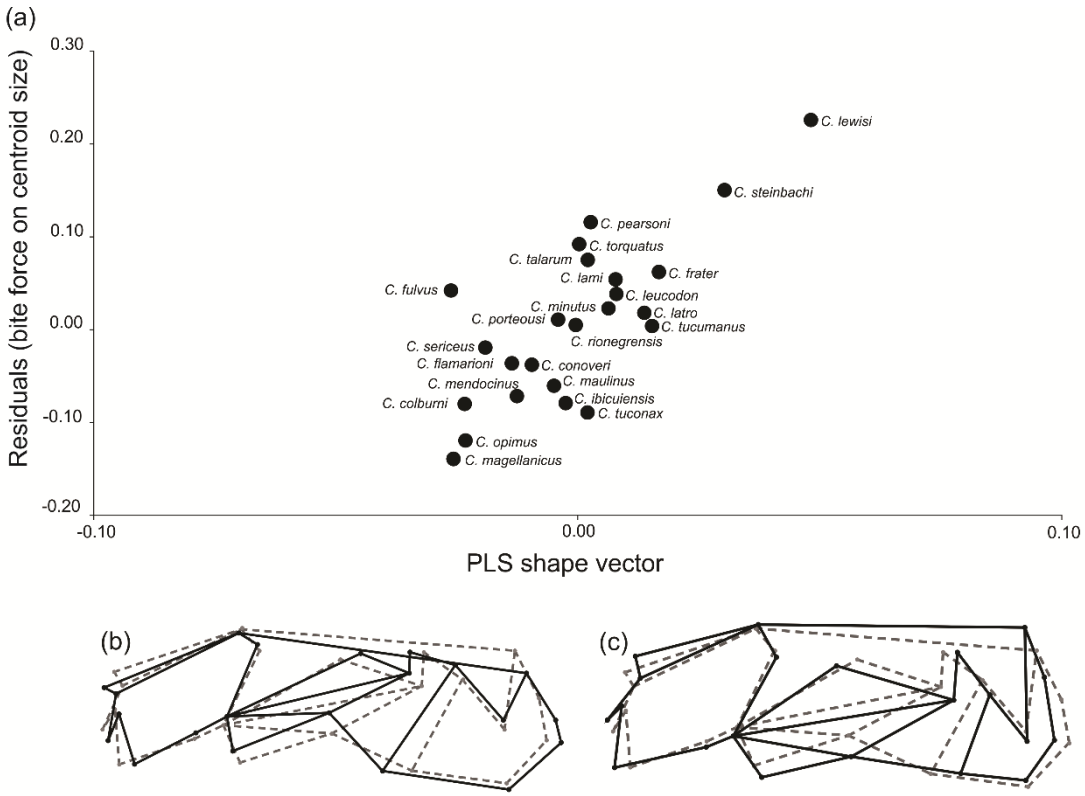

Figure 7 (a) First pair of vectors of a two-block partial least-squares analysis for the association between bite force (residuals of bite force on centroid size) and skull shape in lateral view for 24 species of *Ctenomys*. Representation of conformational changes associated with (b) negative and (c) positive vectors of PLS (dashed gray lines correspond to the mean shape, and solid black lines correspond to the shape associated with positive and negative scores).

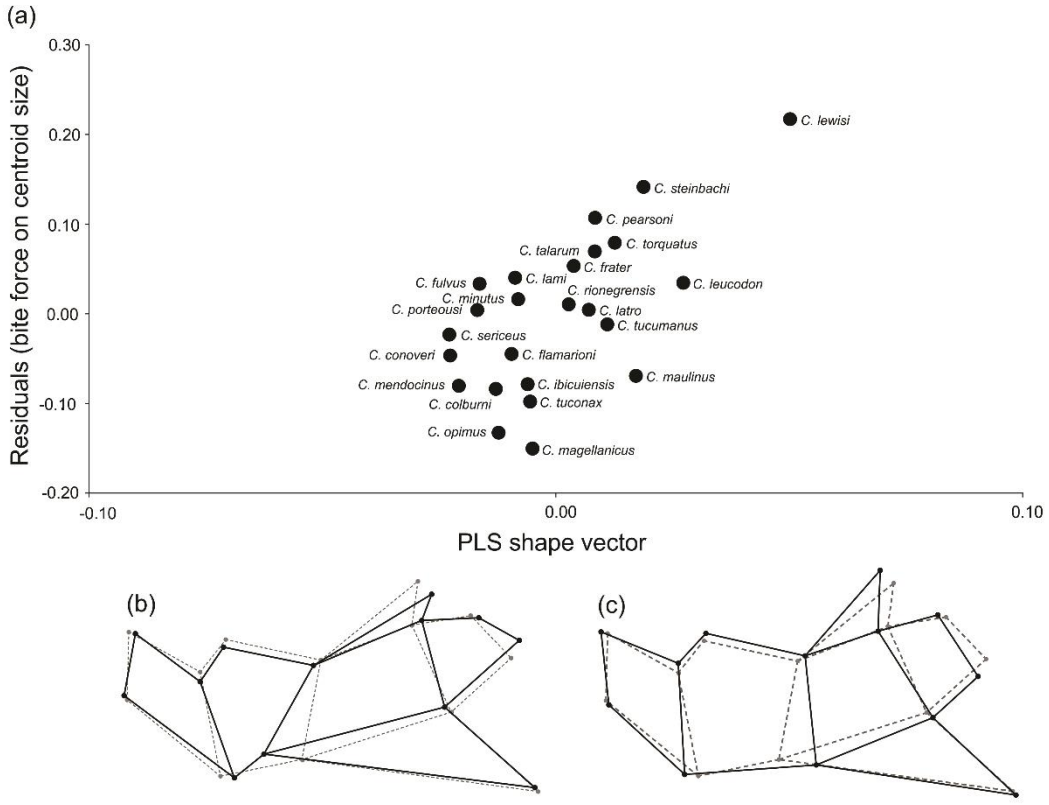

Figure 8 (a) First pair of vectors of a two-block partial least-squares analysis for the association between bite force (residuals of bite force on centroid size) and skull shape in mandible view for 24 species of *Ctenomys*. Representation of conformational changes associated with (b) negative and (c) positive vectors of PLS (dashed gray lines correspond to the mean shape, and solid black lines correspond to the shape associated with positive and negative scores).

Supporting Information

The role of soil features in shaping the bite force and related skull and mandible morphology in the subterranean rodents of genus *Ctenomys* (Hystricognathi: Ctenomyidae)

Leandro R. Borges, Renan Maestri, Bruno B. Kubiak, Daniel Galiano, Rodrigo Fornel, Thales R. O. Freitas

Appendix S1

List of species of *Ctenomys* and sample size used to investigate the skull and mandible shape, and the number of individuals used to measure the incisor strength index (bite force).

Species	**Number of individuals**				
	Dorsal	**Ventral**	**Lateral**	**Mandible**	**Bite force**
C. colburni	31	31	30	21	10
C. conoveri	4	4	4	4	1
C. flamarioni	47	47	47	22	13
C. frater	11	11	11	9	11
C. fulvus	22	22	22	20	7
C. ibicuiensis	16	16	16	16	10
C. lami	96	96	89	66	16

C. latro	8	8	8	7	5
C. leucodon	9	9	9	10	3
C. lewisi	13	13	13	13	2
C. magellanicus	23	23	23	19	10
C. maulinus	36	36	36	31	6
C. mendocinus	23	23	23	14	6
C. minutus	210	210	210	111	15
C. opimus	79	78	78	58	10
C. pearsoni	81	78	77	60	3
C. porteousi	35	35	35	24	5
C. rionegrensis	2	2	2	6	3
C. sericeus	2	2	2	2	2
C. steinbachi	12	12	12	15	3
C. talarum	83	83	83	52	1
C. torquatus	237	225	223	126	15
C. tuconax	17	17	17	14	8
C. tucumanus	25	23	23	12	2
Total	1,122	1,104	1,093	732	167

Appendix S2

The 24 species of the genus *Ctenomys* studied, their bite forces (N = Newtons), centroid size values, and bulk density values.

Species	Bite force (N)	Centroid size	Bulk
C. colburni	31.110	1145.230	817.246
C. conoveri	119.574	2180.731	1402.253
C. flamarioni	50.067	1414.423	1136.629
C. frater	49.339	1318.873	1284.703
C. fulvus	53.481	1390.287	1050.736
C. ibicuiensis	44.198	1362.757	1299.183
C. lami	50.735	1348.546	1330.713
C. latro	31.462	1088.543	1323.690
C. leucodon	58.871	1457.072	1182.808
C. lewisi	78.442	1495.157	1285.868
C. magellanicus	50.333	1511.954	735.268
C. maulinus	44.031	1347.953	810.094
C. mendocinus	34.634	1205.162	1114.029
C. minutus	47.981	1331.976	1295.128
C. opimus	51.447	1516.330	1004.323
C. pearsoni	59.043	1393.174	1162.099

C. porteousi	41.932	1255.464	1181.590
C. rionegrensis	44.290	1287.136	1165.072
C. sericeus	29.063	1065.172	636.168
C. steinbachi	82.228	1606.174	1348.102
C. talarum	38.493	1154.095	1127.047
C. torquatos	53.663	1352.479	1183.490
C. tuconax	55.319	1532.604	1316.181
C. tucumanus	41.694	1260.650	1324.646

Appendix S3

Definition of landmarks with numbers and locations for each view of the cranium and mandible of *Ctenomys* (shown in Fig. 1 in the main text).

Dorsal view of the cranium: 1. anterior tip of the suture between premaxillas; 2-3.anterolateral extremity of incisor alveolus; 4. anterior extremity of suture between nasals; 5-6. anteriormost point of suture between nasal and premaxilla; 7-8. anteriormost point of root of zygomatic arch; 9. suture between nasals and frontals; 10-11. anterolateral extremity of lacrimal bone; 12-13. narrowest point between frontals; 14-15. tip of extremity of superior jugal process; 16-17. anterolateral extremity of suture between frontal and squamosal; 18-19. lateral extremity of suture between jugal and squamosal; 20-21. tip of posterior process of jugal; 22. suture between frontals and parietals; 23-24. anterolateral extremity of suture between parietal and squamosal; 25-26. anterior tip of

external auditory meatus; 27-28. point of maximum curvature on mastoid apophysis; 29. posteriormost point of occipital along midsagittal plane.

Ventral view of the cranium: 1. anterior tip of suture between premaxillas; 2-3. anterolateral extremity of incisor alveolus; 4-5. lateral edge of incisive foramen in suture between premaxilla and maxilla; 6-7. anteriormost point of root of zygomatic arch; 8-9. anteriormost point of orbit in inferior zygomatic root; 10-11. anteriormost point of premolar alveolus; 12-13. posterior extremity of III molar alveolus; 14. posterior extremity of suture between palatines; 15-16. anteriormost point of intersection between jugal and squamosal; 17-18. posteriormost point of pterygoid; 19-20. anterior extremity of tympanic bulla; 21-22. anterior tip of external auditory meatus; 23-24. posterior extremity of mastoid apophysis; 25-26. posterior extremity of paraoccipital apophysis; 27. anteriormost point of foramen magnum; 28-29. posterior extremity of occipital condyle in foramen magnum; 30. posteriormost point of foramen magnum along midsagittal plane.

Lateral view of the cranium: 1. anteriormost point of premaxilla; 2. posteriormost point of incisor alveolus; 3. inferiormost point of incisor alveolus; 4. anterior tip of nasal; 5. anteriormost point of suture between nasal and premaxilla; 6. suture between premaxilla, maxilla and frontal in superior zygomatic root; 7. inferiormost point of suture between lacrimal and maxilla; 8. inferiormost point of infraorbital foramen in inferior zygomatic root; 9. inferiormost point of suture between premaxilla and maxilla; 10. anteriormost point of premolar alveolus; 11. extremity of superior jugal process; 12. extremity of inferior jugal process; 13. tip of posterior jugal process; 14. medial point of suture between parietal and squamosal; 15. superior extremity of lambdoidal crest; 16. posterior extremity of postglenoid fossa; 17. inferior extremity in suture between pterygoid and tympanic bulla; 18. inferior extremity of mastoid apophysis; 19.

anteriormost margin of paraoccipital apophysis; 20. posteriormost margin of paraoccipital apophysis; 21. posterior extremity of intersection between occipital and tympanic bulla.

Lateral view of the mandible: 1. upper extremity of anterior border of incisor alveolus; 2. extremity of diastema invagination; 3. anterior edge of premolar alveolus; 4. intersection between molar alveolus and coronoid process; 5. tip of coronoid process; 6. maximum of curvature between coronoid and condylar processes; 7. anterior edge of articular surface of condylar process; 8. tip of postcondyloid process; 9. maximum curvature between condylar and angular processes; 10. tip of angular process; 11. intersection between mandibular body and masseteric crest; 12. posterior extremity of mandibular symphysis; 13. posterior extremity border of incisor alveolus.

Capítulo III

Manuscrito em preparação: *Zoological Journal of the Linnean Society*

Evolutionary patterns of morphological integration in the skull in the subterranean rodents of genus *Ctenomys* (Hystricognathi: Ctenomyidae)

Leandro R. Borges[1], Rafael A. Carvalho[4], Renan Maestri[2], Rodrigo Fornel[3], Thales R. O. Freitas[1,2,4]

1 Programa de Pós-Graduação em Biologia Animal, Universidade Federal do Rio Grande do Sul, Porto Alegre, RS, Brazil

2 Programa de Pós-Graduação em Ecologia, Universidade Federal do Rio Grande do Sul, Porto Alegre, RS, Brazil

3 Programa de Pós-Graduação em Ecologia, Universidade Regional Integrada do Alto Uruguai e das Missões, Erechim, RS, Brazil;

4 Departamento Pós-Graduação em Genética, Universidade Federal do Rio Grande do Sul, Porto Alegre, RS, Brazil.

Abstract

Studies on morphological integration use the mammalian skull as a standard system, considering the heterogeneity of species that the genus *Ctenomys* presents, we used this study to understand the morphological variations of the genus to a greater extent. We evaluated here the patterns of variation of cranial modules among 16 species of rodents of the genus *Ctenomys* and the morphological evolution of these species. We also evaluated how these modules are correlated evolutionarily through tests of phylogenetic signals. We use here a combination of geometric and comparative morphometric

methods. The morphological integration between the proposed modules was evaluated through the Coefficient Ratio (CR). The matrices were adjusted according to repeatability, thus removing sampling bias in the calculation of correlations between matrices. Phenotype matrices of variance/covariance (V/CV) were generated, based on the coordinates of the anatomical landmarks, to measure patterns of morphological integration of each structure in each species. We evaluated the magnitude of morphological integration between the elements of each structure using the MorphoJ software, where we accessed the values of the variance of the eigenvalues (vote). To evaluate the correlation between form and CR values, we performed a series of linear regressions, the same was done for the values of the voting log to investigate the correlation between form and magnitude of integration. Finally, we use a series of analyzes to investigate phylogenetic relationships. Our results do not demonstrate significant changes between magnitude and cranial integration patterns, and morphological integration varied considerably among the tuco-tucos. We found a high phylogenetic sign between the phylogenetic relationships and the proposed modules for the skull.

ADDITIONAL KEYWORDS: Tuco-tucos, rodents, modularity.

Introduction

Morphological integration is the predisposition that some peculiarities that organisms have to diversify in their totality, in a structured configuration, in a determined structure of the organism, or in the organism as a whole (Olson & Miller, 1958; Klingenberg, 2014). There is a tendency for morphological integration to occur in certain structures of the specimens, depending on their degree of integration (*e.g.*, whether they are dependent or independent), thus being called modules. (Klingenberg, 2013). Modules

can be defined as the set of characteristics that can be genes, proteins, and metabolic pathways or morphological elements, that have great integration between them, and little association with other characteristics (Berg, 1960). Modularity is a generalized feature of biological systems that explains both the integration of the organism or structures into a unit and the autonomy between the organism's characteristics (Goswami, 2007; Santana & Lofgren, 2013). The inference of modular patterns in morphological structures plays a fundamental role in understanding their evolution. That is because this pattern can facilitate or restrict evolutionary changes (Schluter, 1996; Marlig & Cheverud, 2005; Pavlicev *et al.*, 2008).

Integration patterns and magnitudes are two aspects of morphological integration and should be analyzed simultaneously (Marroig & Cheverud, 2001; Porto *et al.*, 2009). The patterns correspond to the characters of a certain organism that may be correlated or covary with certain morphological elements of that organism (Marroig & Cheverud, 2001; Porto *et al.*, 2009). The magnitude of integration corresponds to the degree or strength of the associations between the set of characters (Marroig & Cheverud, 2001; Porto *et al.*, 2009). Changes in patterns and magnitudes of integration may alter the way populations respond to a selection process (Marroig *et al.*, 2009).

The difference in size can be considered important, contributing to the pattern and degree of correlation between attributes (Zelditch, 1988; Marroig *et al.*, 2004). There is great variation in size in most organisms, and this variation can be determined by various genetic and ecological factors (*e.g.*, feed, competition, Patton & Brylski, 1987, Maestri *et al.*, 2016, Borges *et al.*, 2017). The size variation may be an integration factor, the larger the variation in size, the larger the correlations tend to be in and between organic structures as a whole, including the correlations within and between the modules (Shirai & Marroig, 2010). Higher associations in the skull are especially interconnected to the

evolutionary responses along the axis of variation of size, although the selection does not only mean variation in size (Marroig *et al.*, 2009).

Some studies on morphological integration use the mammalian skull as a standard system (Willmore *et al.*, 2006; Cardini & Polly, 2013, Alvarez *et al.*, 2015, McIntosh & Cox, 2016), demonstrating that they are good models for such studies. The genus *Ctenomys* is the most diversified genus of the fossorial rodents (Lacey *et al.*, 2000). Found exclusively in the Neotropical Region, approximately 70 species are currently described (Bidau, 2015; Freitas, 2016). There are fossil records in Tertiary (Upper Pliocene) formations in Argentina, indicating their origin at this point more than three million years ago (Reig *et al.*, 1990; Verzi, 2008). The tuco-tucos, in general, are similar to each other and show morphological adaptations related to their habit of life (Reig *et al.*, 1990).

Considering the heterogeneity of species that genus *Ctenomys* presents (Bidau, 2015; Freitas, 2016), we perform the present study in order to understand the morphological variations of the genus to a greater extent. Here, we evaluated the patterns of variation of cranial modules among 16 species of *Ctenomys* and the morphological evolution in their crania. Initially, we tested two and three modular hypotheses. Next, we evaluate the magnitude of the overall integration in the skull. And finally, in order to shed light on the developmental differences between these species, we evaluate how these modules are correlated evolutionarily through tests of phylogenetic signals.

Materials and methods

Sample

We measured the shape and size of the skull of 1,171 adult individuals of 16 species of *Ctenomys* (Table 1). Only adult specimens were considered: juveniles were

identified based on centroid size (Appendix II) and small skulls were excluded (Borges *et al.*, 2017). These are deposited in the following museums and scientific collections: Departamento de Genética, Universidade Federal do Rio Grande do Sul, Porto Alegre, Brazil (UFRGS); National Museum of Natural History and Anthropology, Montevideo, Uruguay (MUNHINA); Argentine Museum of Natural Sciences "Bernardino Rivadavia", Buenos Aires, Argentina (MACN); Museum of La Plata, La Plata, Argentina (MLP); Museum of Natural Sciences "Lorenzo Scaglia", Mar del Plata, Argentina (MMP); Museum of Vertebrate Zoology, University of California, Berkeley, USA (MVZ); American Museum of Natural History, New York, USA (AMNH); and Field Museum of Natural History, Chicago, USA (FMNH).

Geometric morphometrics

The photos of each skull in the ventral view were recorded with a digital camera of 3.1 megapixels (2048 x 1536), in macro function and without flash or zoom. In each image, 30 landmarks (Appendix I) were digitized (Figure 1a; Fernandes et al., 2009). The anatomical landmarks were digitized twice to quantify and minimize measurement errors (Klingenberg et al., 1998), using TPSDig2 software version 2.17 (Rohlf, 2015). The resulting coordinate matrices were overlapped by a Generalized Procrustes Analysis (GPA) procedure, which removes the effects of scale, orientation, and position. The size of each skull was considered as the square root of the sum of the squares of the distance of each reference to the centroid of the configuration (*i.e.*, centroid size; CS; Bookstein, 1991), using only the ventral view. To remove the effect between form, gender and locality, a MANOVA was performed with the R software (R Core Team, 2018).

Matrix estimation, comparison and repeatability

In order to measure patterns of morphological integration of each species (i.e., the structure of covariation), phenotypic matrices of variance/covariance (V/CV) were generated, based on the two-dimensional coordinates of the anatomical landmarks. These matrices were estimated using the General Linear Model (GLM) routine of Systat 11 (SYSTAT Inc., Richmond, CA). In order to compare the patterns of morphological integration beteween the species, we used the random skewers method (Cheverud, 1996), which compares the evolutionary responses of the matrices to randomly generated vectors (Marroig; Cheverud, 2001, Cheverud, Marroig 2007, Porto et al., 2009, Shirai and Marroig, 2010). We use the MATLAB R2011b software to perform the routines.

As an additional step, the matrix correlations were adjusted according to the repeatability (following Porto et al, 2009), thus removing bias from sampling in calculating correlations between matrices. Therefore, when comparing a pair of matrices, the maximum correlation between them was not 1 as expected, but a lower value than that (Cheverud, 1995, 1996). We use the MATLAB R2011b software to calculate repeatability for each especies and correct the matrix correlation values

Modular hypotheses

To evaluate the strength of the association between the two (Cardini & Polly, 2013; Figure1b) and three proposed modules (Alvarez et al., 2015; Figure1c), a covariance ratio (CR) was used that measures the association between the two or three groups of variables, being the measure of integration between parts we used here (Adams, 2016). We also used the RV coefficient (Appendix II), but we chose to show only the CR results, as pearson correlation between the two coefficients yielded high values (r = 0.974, for two modules; r = 0.972, for three modules; see Adams, 2016). The tests were

performed in R software (R Core Team, 2018), with the *geomorph* package (Adams & Otarola-Castillo, 2013).

Magnitude of overall integration

We evaluated the magnitude of morphological integration between the elements of each structure using eigenvalues of the V/CV matrix. We thus adapted the method of variance of the eigenvalues, which is usually based on correlation matrix (V(λ) log; Cheverud et al., 1983) for the V/CV matrix. We then tested the relationsheep between CR of the proposed modules and the magnitude of morphological integration (vote) through a linear regression, using Past software (Hammer et al., 2001).

Shape analyzes

In order to evaluate the association between shape and CR values, we performed a series of linear regressions. Tthe same was done for the logarithmized values of the logarythmzed V(λ) log, to investigate the correlation between shape and magnitude of integration. The significance of this covariation was assessed through 10000 permutations in MorphoJ 1.06d (Klingenberg, 2011).

Phylogenetic relationships

To access the relationships between similarities of the phenotypic matrices (V/CV) and phylogeny (Freitas et al., 2012) we used Principal Coordinate Analysis (PCoA), also known as metric MDS (MDS: multidimensional sizing; as opposed to MDS not metric; Gower, 1966). The tests were performed in R software (R Core Team, 2018), with the geomorf package (Adams & Otarola-Castillo, 2013).

The phylogenetic signal was estimated between phenotypic matrices (V/CV) and phylogeny using K_{mult} (Adams, 2014). This statistic represents a generalization of the univariate K multivariate statistic proposed by Blomberg et al., (2003). The tests were performed in the R (R Core Team, 2018) software, with the *geomorph* package (Adams & Otarola-Castillo, 2013), based on 10000 random permutations.

The phylogenetic relationships between the proposed modules were based on the phylogenetic hypothesis presented by Freitas et al. (2012), adapted for our sample of 16 species. Details of the phylogenetic construction have been described by Freitas et al. (2012). In order to access the phylogenetic signal, the K_{mult} statistical test was used (Blomberg et al., 2003, see Adams, 2014). The tests were performed in R (R Core Team, 2018) software, with the *phytools* package (Revell, 2012).

Results

The species *C. boliviensis* (CR = 1.002; Table 1) and *C. tucumanus* (CR = 0.974) presented a strong association between the two proposed modules, *C. magellanicus* (0.922) also presented a strong association, but it was not significant. *C. minutus* (CR = 0.662), *C. pearsoni* (CR = 0.667) and *C. lami* (CR = 0.668) revealed significant independence between the modules. The species *C. tucumanus* (CR = 0.971) presented a strong association between the three proposed modules, *C. boliviensis* (CR = 1.029, p = 0.085) also presented, but it was not significant. However, *C. lami* (CR = 0.587), *C. pearsoni* (CR = 0.608) and *C. torquatus* (CR = 0.598) revealed significant independence between the three modules. As for the CR values for the corrected skull size between the two proposed modules, *C. porteousi* (CR = 0.831) and C. *tucumanus* (CR = 0.817) presented strong and significant *C. magellanicus* (CR = 0.833) association. The proposed modules for *C. minutus* (CR = 0.619), *C. pearsoni* (CR = 0.632), *C. lami* (CR = 0.641),

C. talarum (CR = 0.662), *C. torquatus* (OR = 0.693) revealed significant independence. For the values revealed with the skull size corrected between the three modules, *C. tucumanos* (CR = 0.814) showed a strong and significant association. The species *C. lami* (CR = 0.543), *C. minutus* (CR = 0.535) and *C. torquatus* (CR = 0.552) presented significant independence between the three modules.

All comparisons between matrices were significant (p <0.001). The matrix correlation patterns (V/CV) of the skull were similar among the species tested (Table 3). The highest value was for the correlation of the *C. minutus* and *C. torquatus* matrices (0.879), and the lowest crude correlation value was found between *C. magellanicus* and *C. porteousi* (0.396). The mean of all gross correlations between cranial correlation matrices was 0.712. With the adjustment of the correlations for repeatability, the values increased, on average, 5.8%. The highest value continued for the correlation between *C. minutus* and *C. torquatus* (0.908), as well as the lower value for *C. magellanicus* and *C. porteousi* (0.451). The mean of all correlations increased to 0.770. Correlation patterns were found to be different among the species tested for the skull with corrected size (Table 3). All comparisons between matrices (V/CV) were significant (p <0.001). The highest value was for the correlation of the *C. haigi* and *C. torquatus* matrices (0.863) and the lowest gross correlation value was found between *C. magellanicus* and *C. tucumanus* (0.317). The mean of all gross correlations among cranial correlation matrices was 0.675. By adjusting the correlations for repeatability, values increased by an average of 8%. The highest value continued for the correlation between *C. haigi* and *C. torquatus* (0.910), as well as the lower value for *C. magellanicus* and *C. tucumanus* (0.396). The mean of all correlations increased to 0.755. The magnitudes of morphological integration were relatively high (Table 4), with a higher value for *C. tucumanos* (V(λ) log = -7,604) and a lower value for *C. torquatus* (V(λ) log = -9,211).

We found a strong and significant association between the two ($r = 0.864$, $r^2 = 0.746$, $t = 6.418$, $p = 0.0001$, Table 5) and three ($r = 0.807$, $r^2 = 0.651$, $t = 5.112$, $p = 0.0002$) proposed skull modules and V(λ) log. As to the corrected skull size, it was revealed a strong and significant association between the two ($r = 0.773$, $r^2 = 0.598$, $t = 4.567$, $p = 0.0004$) and three ($r = 0.720$, $r^2 = 0.519$, 3,886, $p = 0.002$) proposed skull modules and V(λ) log.

The shape vectors showed a weak and significant association for CR 2 cs values (Appendix V; $R^2 = 0.15$; $p = 0.04$). For the shape vectors and values of CR 2 (Appendix III; $R^2 = 0.08$, $p = 0.2$), CR 3 (Appendix IV; $R^2 = 0.06$, $p = 0.3$), CR 3 cs (Appendix VI; $R^2 = 0.10$, $p = 0.1$) there was no significant association. As for shape vectors and magnitude patterns (Appendix VII; $R^2 = 0.07$, $p = 0.3$), there was also no significant association.

It was explained 64.82% (PcoA 1 = 48.75% and PcoA 2 = 16.07%) of the association between the magnitudes of morphological integration and phylogenetic relationships through the two axes of PcoA (Figure 2). However, the two axes of PcoA for corrected skull size (Figure 3) accounted for 75.49% (PcoA 1 = 66.08% and PcoA 2 = 9.41%) of the association between magnitudes of morphological integration and phylogenetic relationships. K_{mult} revealed weak and non-significant ($K = 0.296$, $p = 0.367$) between matrices (V/CV) and phylogenetic relationships. For the corrected skull size test, it was also low and not significant ($K = 0.37592$; $p =: 0.274$). For the association between phylogenetic relationships and all proposed modules, the K_{mult} test proved to be strong and significant (two modules: $K = 1.453$, $p = 0.001$, Appendix VIII, three modules: $K = 1.873$, $p = 0.001$, Appendix IX; of the skull corrected with two modules $K = 0.869$, $p = 0.01$ Appendix X, three modules $K = 0.811$, $p = 0.01$, Appendix XI).

Discussion

Morphological integration varied considerably among the Tuco-tucos, following the variation between the groups of mammals (Porto et al., 2009). Our results do not demonstrate significant changes between the patterns and cranial integration in 16 studied species of the genus *Ctenomys*. The cranial modules showed high CR values for some species, suggesting relatively high levels of integration between skull and face and skull base, cranial box and face (Klingenberg, 2009, Drake & Klingenberg, 2010, Alvarez *et al.*, 2015). In this paper, we propose the conservation of developmental mechanisms (Drake & Klingenberg 2010; Alvarez *et al.*, 2015), coinciding with the theory of morphological integration (Berg, 1960, Cheverud, 1984, Wagner & Altenberg, 1996).

The matrix correlations were similar, and the magnitudes of integration evolved fast (Porto *et al.*, 2009; Shirai & Marroig, 2010). With this, modularity can also evolve considerably. After correcting the variation (isometric and allometric) of the skull size, the values of integration magnitude reduced, as well as the CR values, evidencing the influence of size and modular patterns. Allometry can be considered important in the growth process that includes the integration of different modules into a functional structure, such as the mammalian skull (Huxley & Teissier, 1936). Therefore, size variation can be considered as a general integration factor (Shirai & Marroig, 2010). Allometry, as a result of proportional changes in certain structures of a given organism concerning size, may facilitate the rapid origin of differences between closely related species (Bininda-Emonds *et al.*, 2003; Sánchez-Villagra, 2010; Porto *et al.*, 2009; Cardini & Polly, 2013). A large part of the integration magnitude between the morphological elements can be attributed to the variation in size, the higher the influence of the size variation, the more restricted the responses to natural selection (Porto *et al.*, 2013).

However, it may facilitate the evolutionary response along the lines of least evolutionary resistance (Marroig & Cheverud, 2005; Marroig *et al.*, 2010).

The species diversity of the genus *Ctenomys* (Bidau, 2015; Freitas, 2016) offers a unique opportunity to study the diversification of the genus on a large scale, by macro and microevolutionary mechanisms (Becerra *et al.*, 2014, Borges *et al.*, 2017, Kubiak *et al.*, 2018). The covariance between structures determines the influence that the selection of a characteristic produces correlated responses in other characteristics (Cheverud, 1982; Wagner *et al.*, 2007; Hallgrímsson *et al.*, 2009). As proposed by Olson and Miller (1958), organisms can be integrated to function as a whole. However, this integration is not uniform throughout the organism (Klingenberg, 2009). In this study, we found a covariation between the morphological integration between two proposed modules for the skull with the corrected size and the shape of the skull. However, we did not find the same pattern for the other modules and the magnitude patterns.

When we evaluated the correlation between integration magnitudes and phylogenetic relationships, a moderate association was revealed between them. After removing the effect of skull size, these patterns became even more evident when this association became strong. That indicates that there may be an association between these patterns. Porto *et al.*, (2013), when removing the variation of size, found that the modularity patterns became more evident and modules not detected, became consistent. The values of K_{mult} smaller than 1 can show adaptive evolution since these values would indicate that distantly related species are converging in some values of characteristics (Álvarez *et al.*, 2015). Although not significant we found K_{mult} values low. What suggests that genetic drift and natural selection fluctuated over time are not enterely responsible for the possible correlation between magnitude patterns and phylogeny. We found a high phylogenetic signal between the phylogenetic relationships and the proposed modules for

the skull; they have the same magnitude of modularity. Torquatus group (see Parada *et al.*, 2011 for more details) seems to have created a break in the general integration and to have generated another degree of modularity. The *C. boliviensis* species belonging to the Boliviensis group, the most basal group in the phylogeny revealed a greater integration of the cranium, remained high even with the removal of the cranial size effect. Such findings demonstrate the possibility that there was also evolution of the modularity of the skulls along with the evolution of the group.

Our study was of great importance for understanding the mechanisms of integration and modularity in rodents of the genus *Ctenomys*. Our results shed light on this subject hitherto not addressed to the group. Future works may address how the environment and phylogenetic relationships interfere with the development of integration and the modularity of the skull.

Acknowledgments

We are grateful to our colleagues of the Laboratório de Citogenética e Evolução for their support in various stages of this study. Our thanks to all curators and collection managers who provided access to specimens of Ctenomys: Enrique González (MUNHINA), Olga B. Vacaro and Esperança A. Varela (MACN), Diego H. Verzi and A. Itatí Olivares (MLP), A. Damián Romero (MMP), James L. Patton, Eileen A. Lacey and Christopher Conroy (MVZ), Eileen Westwig (AMNH), and Bruce D. Patterson (FMNH). L.R.B. received student scholarships from the Coordenação de Aperfeiçoamento de Pessoal de Nível Superior (CAPES), and R.A.C. received student grants from the Conselho Nacional de Desenvolvimento Científico e Tecnológico (CNPq). T.R.O.F. received research

support from CNPq, CAPES (Finance Code 001) and the Fundação de Amparo à Pesquisa do Rio Grande do Sul (FAPERGS).

References

Adams, DC, Otárola-Castillo, E. 2013. Application geomorph: an R package for the collection and analysis of geometric morphometric shape data. *Methods in Ecology and Evolution* **4:** 393–399.

Adams, DC. 2014. A Generalized K Statistic for Estimating Phylogenetic Signal from Shape and Other High-Dimensional Multivariate Data. *Systematic Biology* **63:** 685–697.

Adams, DC. 2016. Evaluating modularity in morphometric data: challenges with the RV coefficient and a new test measure. Methods in Ecology and Evolution. **7:** 565–572.

Álvarez, A, Perez, IS, Verzi, DH. 2015. The Role of Evolutionary Integration in the Morphological Evolution of the Skull of Caviomorph Rodents (Rodentia: Hystricomorpha). *Evolutionary Biology* **36:**136–148

Berg, RL. 1960. The ecological significance of correlation Pleiades. *Evolution* **14:** 171-180.

Bidau, CJ. 2015. *Family Ctenomyidae lesson, 1842. In Mammals of South America* Vol. 2: 818–877. Patton, J.L., Pardiñas, U.F.J. & D'Elía, E. (Eds). Chicago and London: The University of Chicago Press.

Bininda-Emonds, ORP, Jeffrey, JE, Richardson, MK. 2003. Is sequence heterochrony an important evolutionary mechanism in mammals? *Journal of Mammalian Evolution* **10:** 335–361.

Blomberg, SP, Garland, T, Ives, AR. 2003. Testing for phylogenetic signal in comparative data: behavioral traits are more labile. *Evolution* **57:** 717–745.

Bookstein, FL. 1991. *Morphometric Tools for Landmark Data: Geometry and Biology.* London, United Kingdom: Cambridge University Press.

Borges LR, Maestri R, Kubiak BB, Galiano D, Fornel R, Freitas TRO. 2017. The role of soil features in shaping the bite force and related skull and mandible morphology in the subterranean rodents of genus Ctenomys (Hystricognathi: Ctenomyidae). *Journal of Zoology* **301:** 108-117.

Blomberg SP, Garland TJr, Ives AR. 2003 Testing for phylogenetic signal in comparative data: Behavioral traits are more labile. *Evolution* **57** 717-745.

Cardini A, Polly PD. 2013. Larger mammals have longer faces because of size-related constraints on skull form. *Nature Communications* **4:** 24-58.

Chernoff, B, Magwene, PM. 1999. *Morphological integration: forty years later.* In E. C. Olson and R. C. Miller (eds.). Morphological Integration. University of Chicago Press, Chicago.

Cheverud, JM. 1984. Quantitative genetics and developmental constraints on evolution by selection. *Journal of Theoretical Biology* **110:** 155-171.

Cheverud, JM. 1989. A comparative analysis of morphological variation patterns in the papionins. *Evolution* **43:** 1737-1747.

Cheverud, JM., Gunter PW; Dow MM. 1989. Methods for the Comparative Analysis of Variation Patterns. *Systematic Zoology* **38:** 201-213.

Cheverud, JM. 1995. Morphological integration in the saddle-back tamarin (*Saguinus fuscicollis*) cranium. *American Naturalist* **145:** 63-89.

Cheverud, JM. 1996. Developmental integration and the evolution of pleiotropy. *American Zoologist* **36:** 44-50.

Cheverud, JM., Marroig, G. 2007. Research Article Comparing covariance matrices: random skewers method compared to the common principal components model. *Genetics and Molecular Biology* **30:** 461–469.

Drake, AG, Klingenberg, CP. 2010. Large-Scale Diversification of Skull Shape in Domestic Dogs: Disparity and Modularity. *The American Naturalist* **175:** 289-301.

Fernandes, FA, Fornel, F, Cordeiro-Estrela, P, Freitas, TRO. 2009. Intra- and interespecific skull variation in two sister species of the subterranean rodent genus

Ctenomys (Rodentia, Ctenomyidae): coupling geometric morphometrics and chromosomal polymorphism. *Zoological Journal of the Linnean Society* **155:** 220-237.

Freitas, TRO, Fernandes, FA, Fornel, R, Roratto, PA. 2012. An endemic new species of tuco-tuco, genus *Ctenomys* (Rodentia: Ctenomyidae), with a restricted geographic distribution in southern Brazil. *Journal of Mammalogy* **93:** 1355–1367.

Freitas, TRO. 2016. *Family Ctenomyidae (Tuco-tucos). Handbook of the Mammals of the World* Volume 6 Lagomorphs and Rodents I. In: Don E. Wilson; Thomas E. Lacher, Jr; Russell A. Mittermeier. (Org.). 6ed.Barcelona: Lynx Edicions Publications,

Goswami, A. 2007. Cranial modularity and sequence heterochrony in mammals. *Evolution & Development* **9:** 290–298.

Gower, JC. 1966. Some Distance Properties of Latent Root and Vector Methods used in Multivariate Analysis. *Biometrika* **53:** 325-338.

Hammer, O; Harper, DAT, Ryan, PD. 2001. PAST: Paleontological Statistic software package for education and data analysis. *Paleontologia Eletronica* **4:** 1-9.

Huxley, JS, Teissier, G. 1936. Terminology of relative growth. *Nature* **137:** 780-781.

Klingenberg CP, McIntyre GS, Zaklan SD. 1998. Left-right asymmetry of fly wings and the evolution of body axes. *Proceedings of the Royal Society of London B.* **265:** 1255–1259.

Klingenberg, CP. 2009. Morphometric integration and modularity in configurations of landmarks: tools for evaluating a-priori hypotheses. *Evolution and Development* **11:** 405–421.

Klingenberg, CP. 2011. MorphoJ: an integrated software package for geometric morphometrics. *Molecular Ecology Resources* **11:** 353–357.

Klingenberg, CP. 2013. Cranial integration and modularity: insights into evolution and development from morphometric data. *Hystrix* **24:** 43–58.

Klingenberg CP. 2014. Studying morphological integration and modularity at multiple levels: concepts and analysis. *Philosophical Transactions of the Royal Society B* **369:** 20130249.

Lacey, EA, Patton, JL, Cameron, GN. 2000. *Life Underground.* The University of Chicago Press, Chicago and London.

Maestri, R, Patterson, BD, Fornel, R, Monteiro, LR, Freitas, T.R.O. 2016. Diet, bite force and skull morphology in the generalist rodent morphotype. *Journal of Evolutionary Biology* **29:** 2191–2204.

MATLAB, 2011. *R2011b* The Math Works Inc.

Marroig, G, Cheverud, JM. 2001. A comparison of phenotypic variation and covariation patterns and the role of phylogeny, ecology, and ontogeny during cranial evolution of New World Monkeys. *Evolution* **55:** 2576-2600.

Marroig G, Cropp S, Cheverud JM. 2004. Systematics and evolution of the jacchus group of marmosets (Platyrrhini). *American Journal of Physical Anthropology* **123:**11-22.

Marroig G, Cheverud, JM. 2005. Size as a line of least evolutionary resistance: Diet and adaptive morphological radiation in new world monkeys. *Evolution* **59:** 1128-1142.

Marroig, G, Shirai, LT, Porto, A, Oliveira, FB, De Conto, V. 2009. The evolution of modularity in the mammalian skull II: evolutionary consequences. *Evolutionary Biology* **36:** 136–148.

McIntosh, AF; Cox, PG. 2016. The impact of digging on craniodental morphology and integration. *Journal of Evolutionary Biology* **12:** 2383-2394.

Nevo, E. 1979. Adaptive convergence and divergence of subterranean mammals. *Annual Review of Ecology, Evolution, and Systematics* **10:** 269–308.

Nowak, RM. 1999. *Walker's Mammals of the World.* 6th ed. Baltimore (MD): The Johns Hopkins University Press.

Olson, EC, Miller, RL. 1958. *Morphological integration.* Chicago: University of Chicago Press.

Parada, A, D'elia, G, Bidau., C, Lessa, LP. 2011. Species groups and the evolutionary diversification of tuco-tucos, genus *Ctenomys (*Rodentia: Ctenomyidae). *Journal of Mammalogy* **91:** 1313-1321.

Patton JL, Brylski PV. 1987. Pocket gophers in alfalfa fields: causes and consequences of habitat-related body size variation. *American Naturalist* **130:** 493–506.

Pavlicev, MJP, Kenney-Hunt, EA, Norgard, CC, Roseman, JBW, Cheverud, JM. 2008. Genetic variation in pleiotropy: Differential epistasis as a source of variation in the allometric relationship between long bone lengths and body weight. *Evolution* **62:** 199-213.

Porto A, Oliveira FB, Shirai LT, Conto V, Marroig G. 2009. The Evolution of Modularity in the Mammalian Skull I: Morphological Integration Patterns and Magnitudes. *Evolutionary Biology* **36:** 118–135.

Porto, A, Shirai, L, Oliveira, F, Marroig, G. 2013. Size variation, growth strategies and the evolution of modularity in the mammalian skull. *Evolution* **67:** 3305-3322.

R Core Team. 2018. R: A language and environment for statistical computing. *URL https://www.R-project.org/*. R Foundation for Statistical Computing. Vienna, Austria.

Reig, AO, Busch, C, Ortellis, MO, Contreras, JL. 1990. An overview of evolution, systematica, population biology and molecular biology in *Ctenomys*. In: Nevo, E.; Reig, O.A. (eds) *Biology of subterranean mammals at the organismal and molecular levels.* New York, Allan Liss.

Revell, LJ. 2012. Phytools: an R package for phylogenetic comparative biology (and other things). *Methods in Ecology and Evolution* **3:** 217–223.

Rohlf, FJ. 2015. *TPSDig version 2.17*. State University of New York at Stony Brook.

Sánchez-Villagra, MR. 2010. Developmental palaeontology in synapsids: the fóssil record of ontogeny in mammals and their closest relatives. *Proceedings of the Royal Society B* **277:** 1139–1147.

Santana, SE, Lofgren, SE. 2013. Does nasal echolocation influence the modularity of the mammal skull? *Journal of Evolutionary Biology* **26:** 2520–2526.

Schluter, D. 1996. Adaptive radiation along genetic lines of least resistance. *Evolution* **5:** 1766-1774.

Shirai LT, Marroig G. 2010. Skull Modularity in Neotropical Marsupials and Monkeys: Size Variation and Evolutionary Constraint and Flexibility. *Journal of Experimental Zoology Part B-Molecular and Developmental Evolution.* **314:** 663–683.

Verzi, DH. 2008. Phylogeny and adaptive diversity of rodents of the family Ctenomyidae (Caviomorpha): delimiting lineages and generain the fossil record. *Journal of Zoology* **274:** 386–394.

Wagner, GP, Altenberg, L. 1996. Perspective: Complex adaptations and the evolution of evolvability. *Evolution* **50:** 967-976.

Willmore, KE, Leamy L, Hallgrímsson, B. 2006. Effects of developmental and functional interactions on mouse cranialvariability through late ontogeny. *Evolution e Development* **8:** 550–567.

Zelditch, ML. 1988. Ontogenetic variation in patterns of phenotypic integration in the laboratory rat. *Evolution* **42:** 28–41.

Tables and figures

Table 1. Number of individuals per species, morphological integration between two (CR 2) and three (CR 3) modules proposed for the skull, morphological integration between two (CR 2 cs) and three (CR 3 cs) modules proposed for the skull with the corrected size, for 16 species of the genus *Ctenomys* found in the Neotropical region.

Species	**N**	**CR 2**	**CR 3**	**CR 2 cs**	**CR 3 cs**
C. australis	51	0.859	0.765	0.763	0.608
C. boliviensis	60	1.002	1.029*	0.746	0.687
C. colburni	31	0.860	0.864	0.778	0.716
C. flamarioni	47	0.812	0.707	0.782	0.674

C. haigi	77	0.870	0.796	0.765	0.692
C. lami	96	0.668	0.587	0.641	0.543
C. magellanicus	23	0.922*	0.872	0.833	0.776
C. maulinus	34	0.865	0.897	0.770	0.791
C. mendocinus	22	0.808	0.795	0.796	0.781
C. minutus	210	0.662	0.612	0.619	0.535
C. opimus	78	0.812	0.766	0.693	0.661
C. pearsoni	78	0.667	0.608	0.632	0.555
C. porteousi	33	0.868	0.694	0.831	0.646
C. talarum	83	0.733	0.675	0.662	0.617
C. torquatus	225	0.738	0.598	0.692	0.552
C. tucumanus	23	0.974	0.971	0.817	0.814

*$p > 0.05$.

Table 2. Matrix of similarity between matrices of (V/CV), for 16 species of the genus *Ctenomys*. The observed gross correlations are on the lower diagonal and the adjusted ones are on the upper diagonal. Repeatability is bold in diagonal.

Sp	***C.aus***	***C.bol***	***C.col***	***C.fla***	***C.hai***	***C.lam***	***C.mag***	***C.mau***	***C.men***	***C.min***	***C.opi***	***C.pea***	***C.por***	***C.tal***	***C.tor***	***C.tuc***
C.aus	**0.927**	0.735	0.775	0.746	0.869	0.768	0.719	0.713	0.713	0.791	0.822	0.763	0.652	0.875	0.845	0.605
C.bol	0.688	**0.945**	0.650	0.726	0.796	0.641	0.593	0.711	0.667	0.733	0.832	0.641	0.594	0.774	0.726	0.760
C.col	0.698	0.591	**0.876**	0.646	0.838	0.749	0.601	0.670	0.687	0.787	0.775	0.693	0.653	0.754	0.818	0.585
C.fla	0.684	0.673	0.576	**0.909**	0.766	0.740	0.667	0.685	0.622	0.790	0.781	0.736	0.695	0.806	0.821	0.691
C.hai	0.812	0.751	0.761	0.708	**0.942**	0.767	0.692	0.730	0.758	0.846	0.868	0.773	0.729	0.844	0.897	0.645
C.lam	0.718	0.605	0.681	0.685	0.723	**0.944**	0.652	0.663	0.691	0.826	0.779	0.777	0.639	0.855	0.846	0.574
C.mag	0.647	0.539	0.525	0.595	0.628	0.592	**0.873**	0.618	0.682	0.694	0.712	0.632	0.451	0.712	0.715	0.568
C.mag	0.638	0.643	0.583	0.607	0.659	0.599	0.537	**0.864**	0.678	0.793	0.806	0.751	0.575	0.784	0.782	0.707
C.men	0.635	0.600	0.595	0.549	0.681	0.621	0.590	0.583	**0.857**	0.768	0.785	0.691	0.582	0.769	0.772	0.592
C.min	0.750	0.702	0.726	0.742	0.809	0.791	0.639	0.726	0.701	**0.970**	0.879	0.822	0.747	0.877	0.908	0.679
C.opi	0.758	0.774	0.694	0.713	0.807	0.725	0.637	0.717	0.696	0.829	**0.917**	0.817	0.700	0.886	0.878	0.753

C.pea	0.705	0.598	0.622	0.673	0.720	0.724	0.567	0.670	0.614	0.777	0.751	**0.921**	0.720	0.826	0.854	0.589
C.por	0.590	0.543	0.575	0.622	0.665	0.583	0.396	0.502	0.506	0.691	0.630	0.649	**0.883**	0.767	0.769	0.507
C.tal	0.769	0.686	0.644	0.702	0.748	0.758	0.608	0.665	0.650	0.789	0.775	0.724	0.658	**0.833**	0.872	0.752
C.tor	0.799	0.694	0.752	0.769	0.855	0.807	0.657	0.714	0.703	0.879	0.826	0.806	0.710	0.782	**0.966**	0.667
C.tuc	0.536	0.680	0.504	0.606	0.576	0.513	0.489	0.605	0.505	0.615	0.663	0.520	0.438	0.632	0.603	**0.846**

$p < 0.001$.

Table 3. Matrix of similarity between matrices of (V/CV), with corrected skull size, for 16 species of the genus *Ctenomys*. The observed gross correlations are on the lower diagonal and the adjusted ones are on the upper diagonal. Repeatability is in bold diagonal.

Sp	***C.aus***	***C.bol***	***C.col***	***C.fla***	***C.hai***	***C.lam***	***C.mag***	***C.mau***	***C.men***	***C.min***	***C.opi***	***C.pea***	***C.por***	***C.tal***	***C.tor***	***C.tuc***
C.aus	**0.912**	0.747	0.742	0.688	0.820	0.765	0.655	0.687	0.680	0.773	0.812	0.794	0.633	0.860	0.839	0.559
C.bol	0.676	**0.899**	0.678	0.726	0.788	0.757	0.580	0.702	0.679	0.786	0.812	0.772	0.721	0.880	0.787	0.584
C.col	0.650	0.589	**0.842**	0.616	0.796	0.721	0.612	0.666	0.692	0.771	0.770	0.723	0.686	0.754	0.809	0.435
C.fla	0.622	0.653	0.535	**0.898**	0.743	0.709	0.669	0.633	0.572	0.767	0.752	0.712	0.710	0.771	0.790	0.464
C.hai	0.756	0.721	0.704	0.679	**0.931**	0.786	0.660	0.732	0.733	0.859	0.861	0.853	0.814	0.903	0.910	0.523
C.lam	0.709	0.696	0.641	0.652	0.736	**0.941**	0.626	0.613	0.645	0.795	0.740	0.763	0.686	0.878	0.838	0.491
C.mag	0.583	0.512	0.523	0.591	0.594	0.566	**0.868**	0.573	0.658	0.667	0.695	0.669	0.562	0.721	0.676	0.396
C.mag	0.604	0.612	0.562	0.552	0.650	0.547	0.492	**0.847**	0.600	0.722	0.716	0.728	0.677	0.759	0.741	0.463
C.men	0.598	0.592	0.584	0.498	0.650	0.575	0.564	0.508	**0.846**	0.717	0.718	0.682	0.593	0.751	0.734	0.469
C.min	0.726	0.733	0.696	0.714	0.815	0.758	0.611	0.653	0.648	**0.967**	0.866	0.828	0.810	0.880	0.887	0.560
C.opi	0.740	0.736	0.675	0.680	0.793	0.686	0.618	0.629	0.630	0.813	**0.912**	0.840	0.730	0.872	0.868	0.573
C.pea	0.727	0.702	0.636	0.646	0.788	0.709	0.598	0.642	0.601	0.780	0.769	**0.919**	0.765	0.849	0.868	0.515
C.por	0.563	0.637	0.586	0.627	0.732	0.620	0.488	0.581	0.508	0.742	0.650	0.683	**0.868**	0.829	0.805	0.483
C.tal	0.715	0.726	0.601	0.635	0.757	0.741	0.584	0.608	0.601	0.752	0.724	0.708	0.672	**0.756**	0.895	0.675
C.tor	0.787	0.733	0.729	0.735	0.863	0.798	0.618	0.670	0.663	0.857	0.814	0.818	0.737	0.764	**0.965**	0.571
C.tuc	0.459	0.475	0.342	0.377	0.433	0.409	0.317	0.366	0.370	0.473	0.470	0.423	0.387	0.504	0.482	**0.737**

$p < 0.001$.

Table 4. Magnitude of general morphological integration V (λ) log, for 16 species of the genus Ctenomys found in the Neotropical region.

Espécie	V (λ) log
C. australis	-8.640
C. boliviensis	-8.063
C. colburni	-8.449
C. flamarioni	-8.754
C. haigi	-8.483
C. lami	-9.041
C. magellanicus	-8.379
C. maulinus	-8.652
C. mendocinus	-8.515
C. minutus	-9.020
C. opimus	-9.078
C. pearsoni	-9.028
C. porteousi	-8.237
C. talarum	-9.096
C. torquatus	-9.211
C. tucumanus	-7.604

Table 5. Association between morphological integration between two (CR 2) and three (CR 3) modules proposed for the skull, and morphological integration between two (CR 2 cs) and three (CR 3 cs) modules proposed for the skull with the size corrected and magnitude of morphological integration (vote log), for 16 species of the genus Ctenomys found in the Neotropical region.

	r	***r²***	***t***	***p***
CR 2 x V (λ) log	0.864	0.746	6.418	0.0001

CR 3 x V (λ) log	0.807	0.651	5.112	0.0002
CR 2 cs x V (λ) log	0.773	0.598	4.567	0.0004
CR 3 cs x V (λ) log	0.720	0.519	3.886	0.002

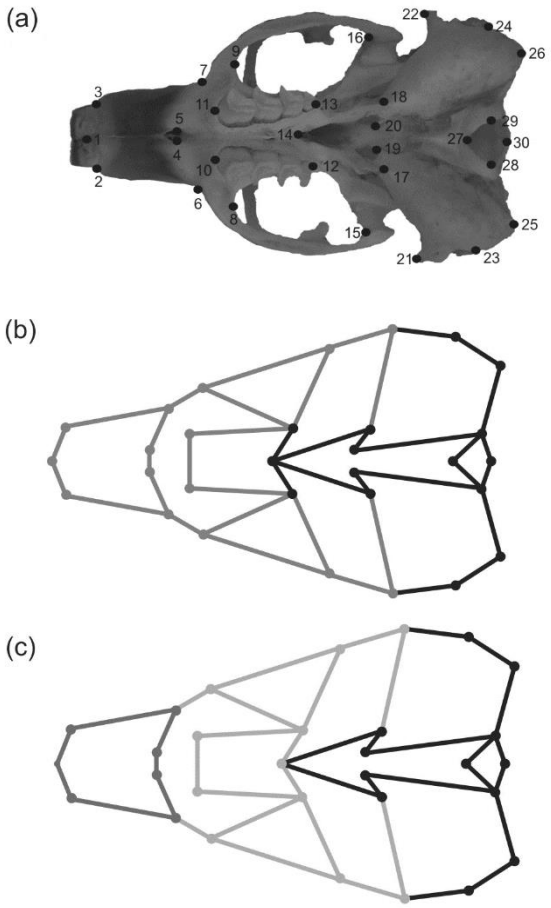

Figure 1: Landmarks used to capture the ventral view of the skull (a) as shown in *Ctenomys flamarioni*. Two (b) and three (c) proposed modules for the skull of the 16 species of the genus Ctenomys found in the Neotropical region.

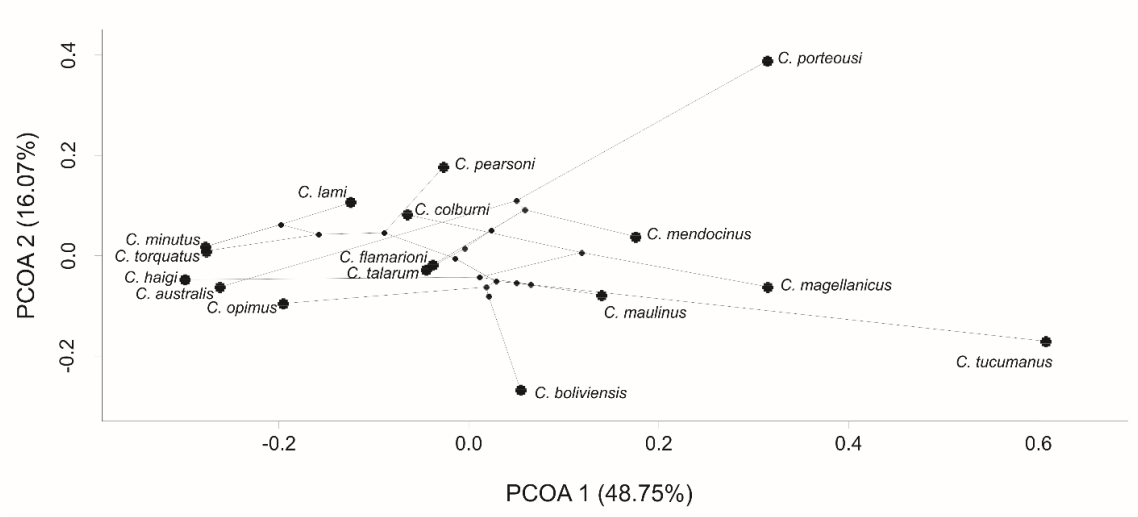

Figure 2. Principal coordinate analysis (PCoA) between phenotypic matrices (V/CV) and phylogenetic relationships among 16 species of the genus *Ctenomys*. Based on molecular data (Freitas et al., 2012), the original tree was edited to exclude species not investigated here. The percentage of variation explained by PCOA1 and PCOA2 is indicated on the axis.

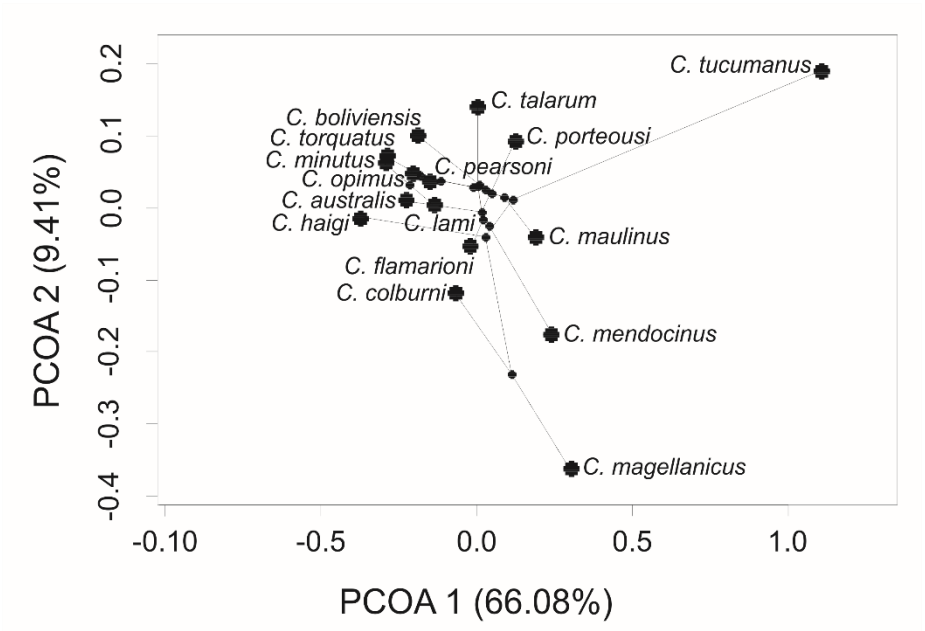

Figure 3. Principal coordinate analysis (PCoA) between phenotypic matrices (V/CV) and phylogenetic relationships among 16 species of the genus *Ctenomys*, for the skull with corrected size. Based on molecular data (Freitas et al., 2012), the original tree was edited

to exclude species not investigated here. The percentage of variation explained by PCOA1 and PCOA2 is indicated on the axis.

Supplementary material

Appendix I

Definition of landmarks with numbers and locations for ventral view of the skull of the genus Ctenomys (shown in Fig. 1a).

1. anterior tip of suture between premaxillas; 2-3. anterolateral extremity of incisor alveolus; 4-5. lateral edge of incisive foramen in suture between premaxilla and maxilla; 6-7. anteriormost point of root of zygomatic arch; 8-9. anteriormost point of orbit in inferior zygomatic root;10-11. anteriormost point of premolar alveolus; 12-13. posterior extremity of III molar alveolus; 14. posterior extremity of suture between palatines; 15-16. anteriormost point of intersection between jugal and squamosal; 17-18. posteriormost point of pterygoid; 19-20. anterior extremity of tympanic bulla; 21-22. anterior tip of external auditory meatus; 23-24. posterior extremity of mastoid apophysis; 25-26. posterior extremity of paraoccipital apophysis; 27. anteriormost point of foramen magnum; 28-29. posterior extremity of occipital condyle in foramen magnum; 30. posteriormost point of foramen magnum along midsagittal plane.

Appendix II

Number of individuals per species (N), centroid size (CS), morphological integration between two (RV 2) and three (RV 3) proposed modules for the skull, morphological integration between two (RV 2 cs) and three (RV 3 cs) modules proposed

for the skull with corrected size, for 16 species of the genus Ctenomys found in the Neotropical region.

Species	**N**	**CS**	**RV 2**	**RV 3**	**RV 2 cs**	**RV 3 cs**
C. australis	51	1597,322	0,531	0,384	0,404	0,242
C. boliviensis	60	1648,801	0,831	0,791	0,339	0,273
C. colburni	31	1145,232	0,616	0,526	0,468	0,363
C. flamarioni	47	1414,423	0,513	0,362	0,494	0,342
C. haigi	77	1287,431	0,599	0,472	0,422	0,304
C. lami	96	1348,546	0,288	0,207	0,261	0,175
C. magellanicus	23	1511,954	0,599	0,485	0,500	0,412
C. maulinus	34	1347,953	0,573	0,520	0,519	0,390
C. mendocinus	22	1205,162	0,496	0,437	0,467	0,401
C. minutus	210	1331,976	0,294	0,230	0,245	0,173
C. opimus	78	1516,331	0,487	0,410	0,329	0,273
C. pearsoni	78	1393,174	0,231	0,261	0,300	0,221
C. porteousi	33	1255,464	0,586	0,353	0,507	0,306
C. talarum	83	1154,095	0,396	0,306	0,336	0,239
C. torquatus	225	1352,479	0,371	0,233	0,298	0,181
C. tucumanus	23	1260,651	0,863	0,780	0,605	0,526

Appendix III

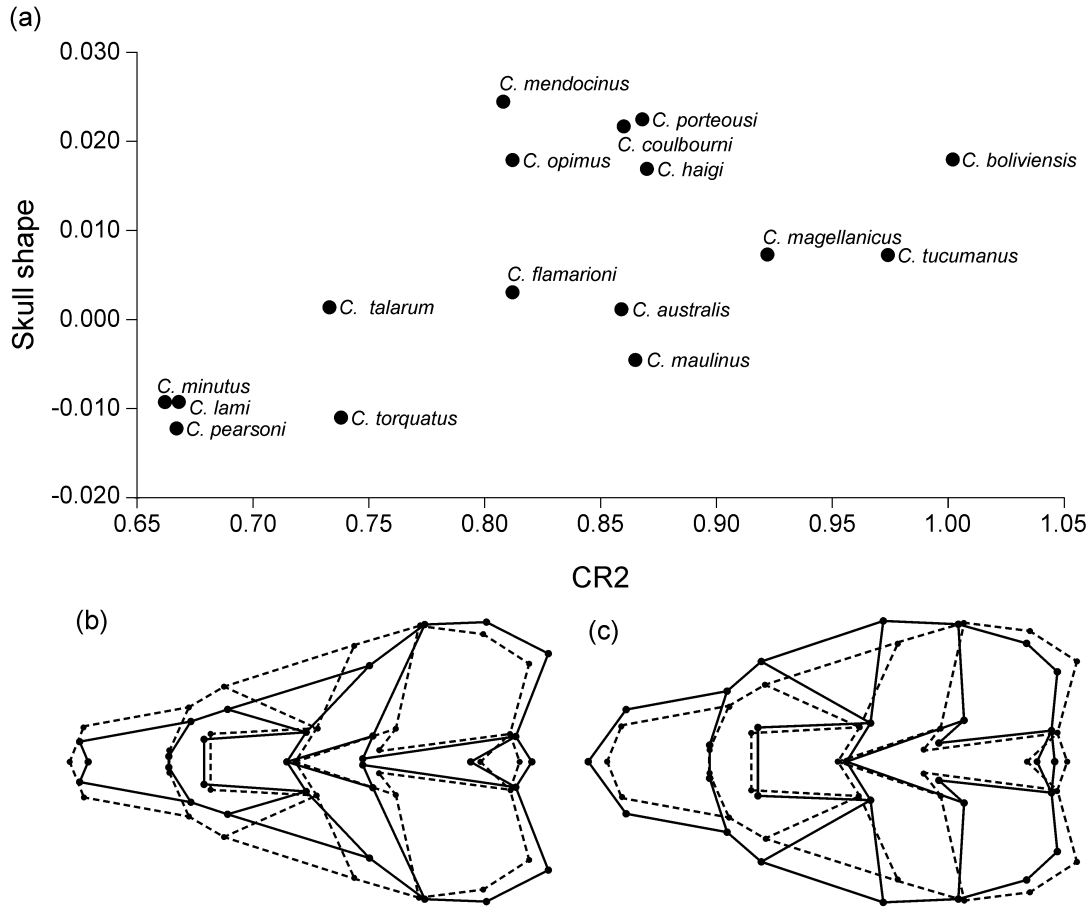

Regression analysis between skull shape and morphological integration between two proposed skull modules (CR 2) for 16 *Ctenomys* species. Representation of conformational changes associated with (b) negative and (c) positive vectors (dashed lines correspond to the mean shape, and solid black lines correspond to the form associated with positive and negative scores).

Appendix IV

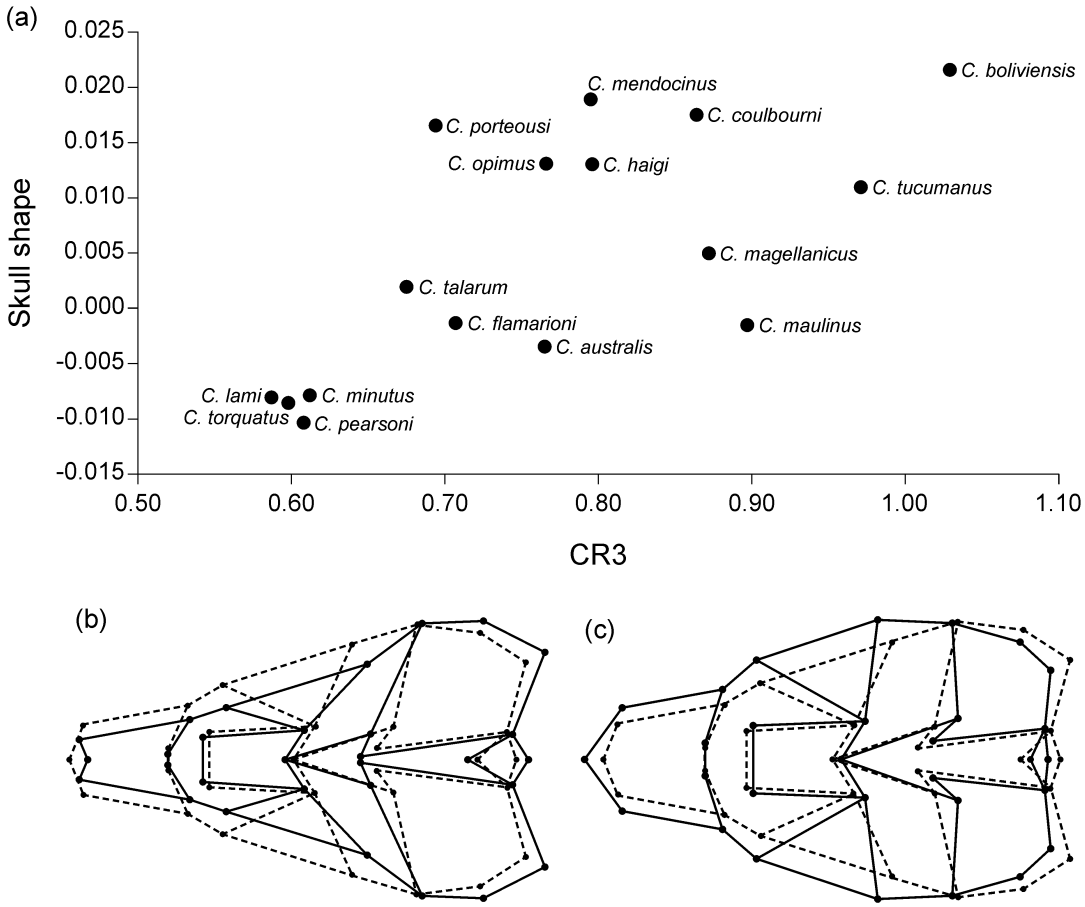

Regression analysis between skull shape and morphological integration between three proposed skull modules (CR 3) for 16 *Ctenomys* species. Representation of conformational changes associated with (b) negative and (c) positive vectors (dashed lines correspond to the mean shape, and solid black lines correspond to the form associated with positive and negative scores).

Appendix V

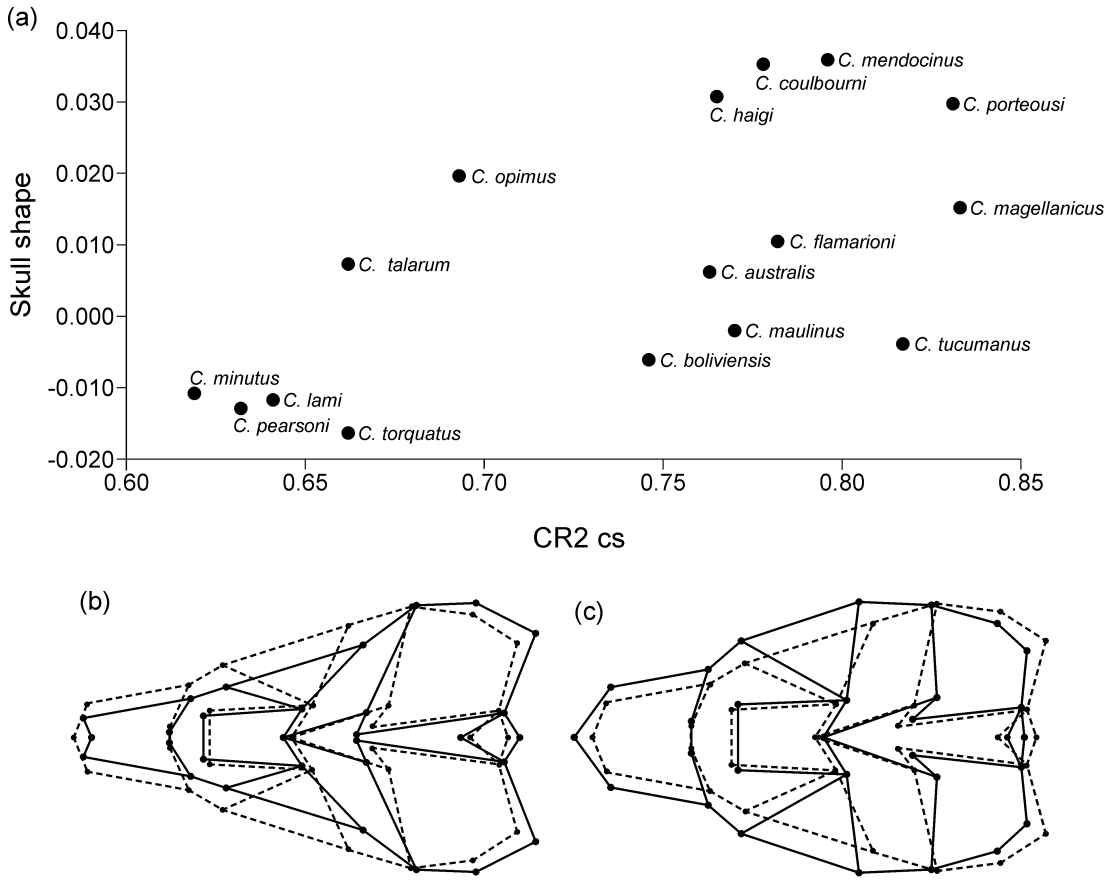

Regression analysis between skull shape and morphological integration between two modules proposed for the skull with the corrected size (CR 2 cs) for 16 *Ctenomys* species. Representation of conformational changes associated with (b) negative and (c) positive vectors (dashed lines correspond to the mean shape, and solid black lines correspond to the form associated with positive and negative scores).

Appendix VI

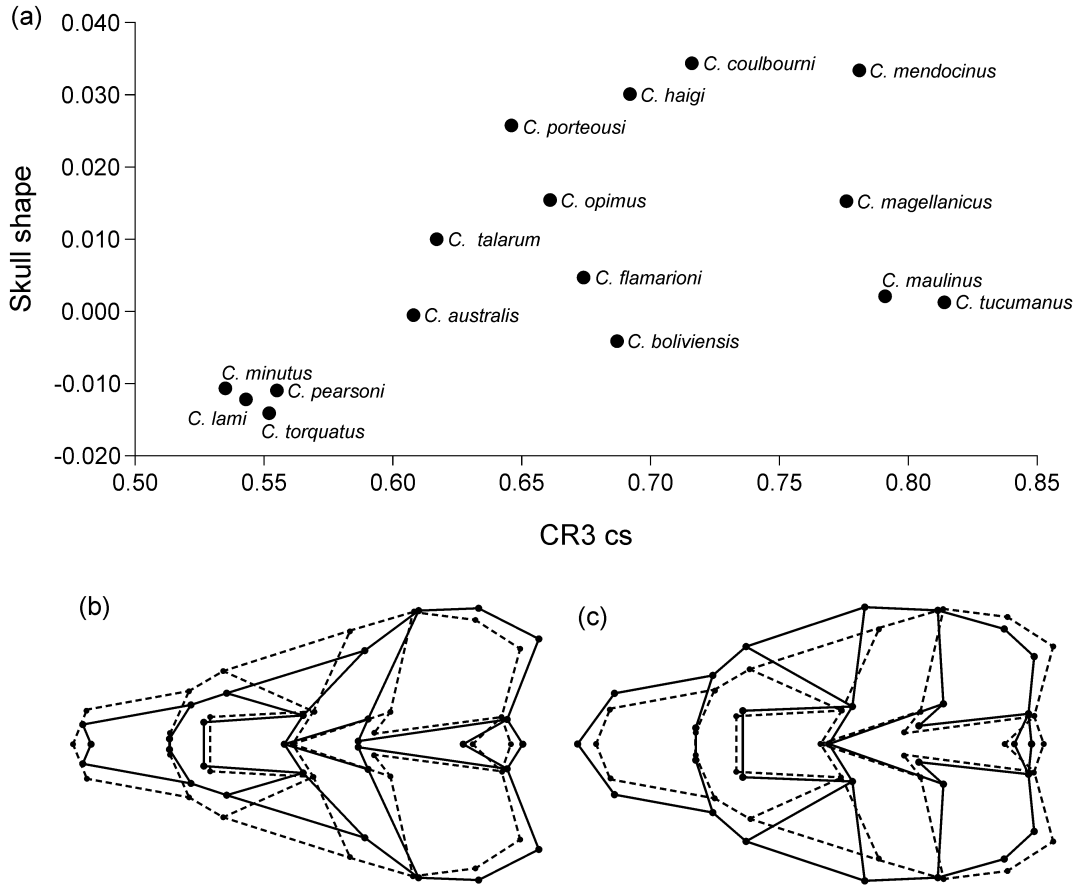

Regression analysis between skull shape and morphological integration between three modules proposed for the skull with the corrected size (CR 3 cs) for 16 *Ctenomys* species. Representation of conformational changes associated with (b) negative and (c) positive vectors (dashed lines correspond to the mean shape, and solid black lines correspond to the form associated with positive and negative scores).

Appendix VII

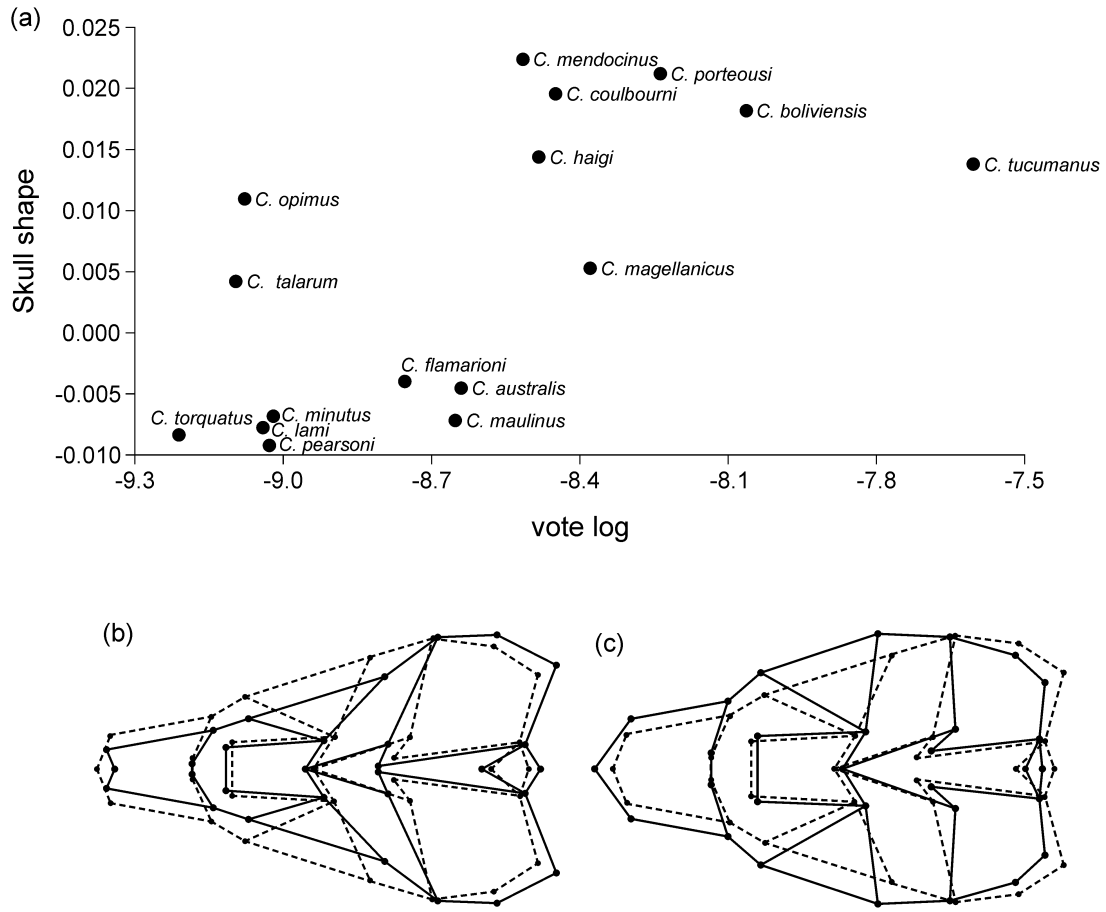

Regression analysis between skull shape and magnitude of morphological integration accessed through variance of the eigenvalues log (vote log) for 16 *Ctenomys* species. Representation of conformational changes associated with (b) negative and (c) positive vectors (dashed lines correspond to the mean shape, and solid black lines correspond to the form associated with positive and negative scores).

Appendix VIII

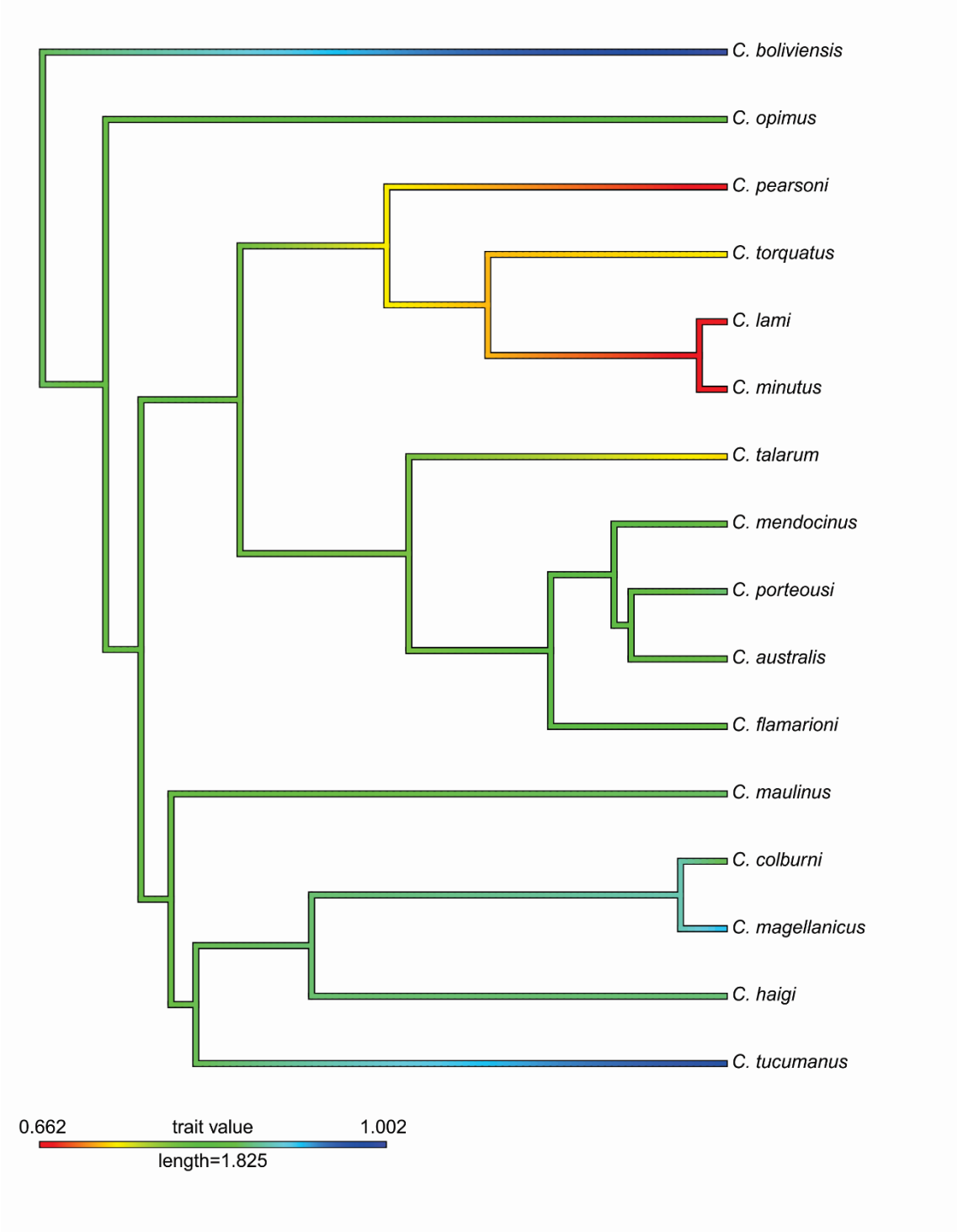

Correlation between the two proposed modules for the skull and phylogenetic relationships among 16 species of the genus *Ctenomys*, based on molecular data (Freitas et al., 2012). The original tree was edited to exclude species not investigated here.

Appendix IX

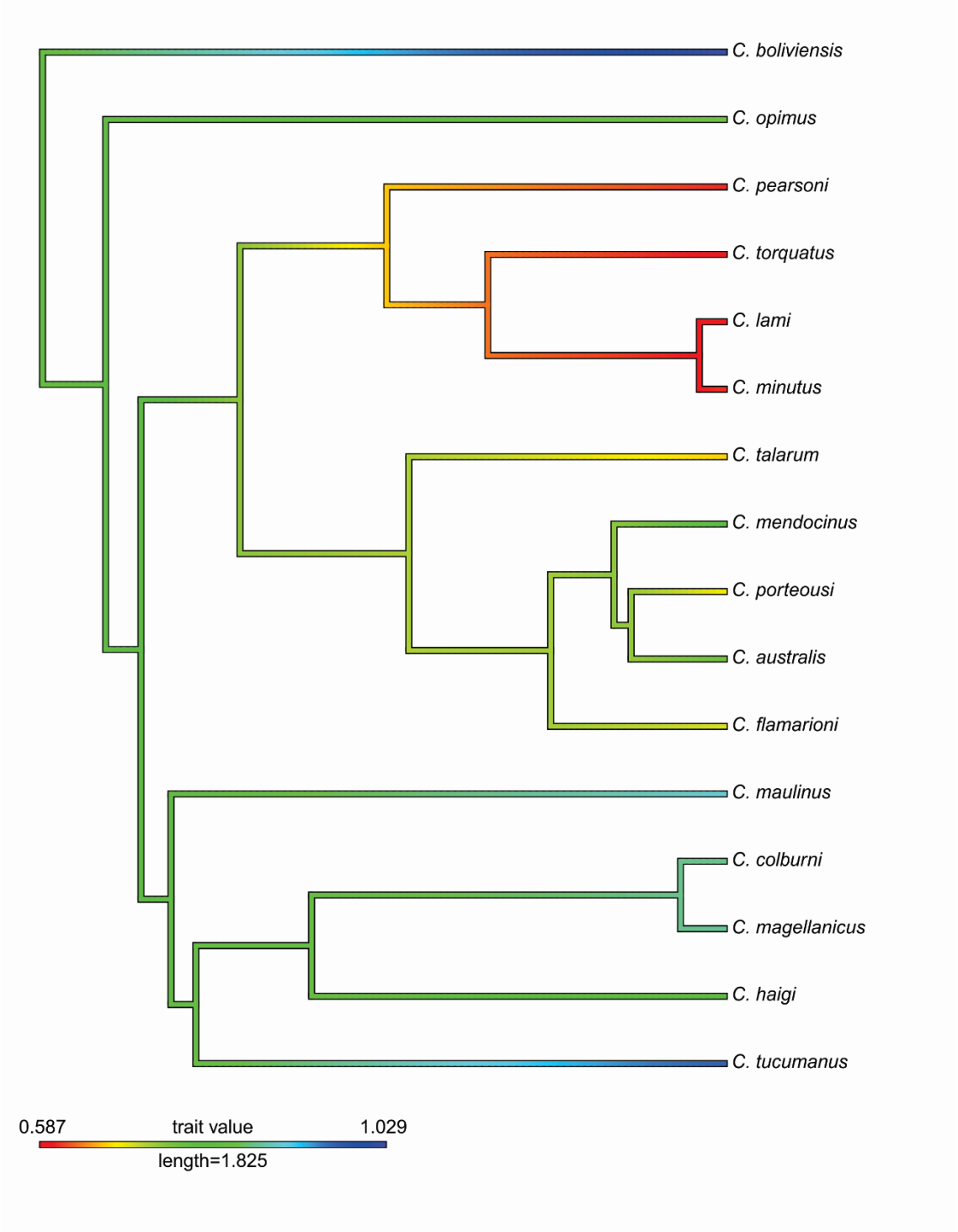

Correlation between the three proposed modules for the skull and the phylogenetic relationships among 16 species of the genus *Ctenomys*, based on molecular data (Freitas et al., 2012). The original tree was edited to exclude species not investigated here.

Appendix X

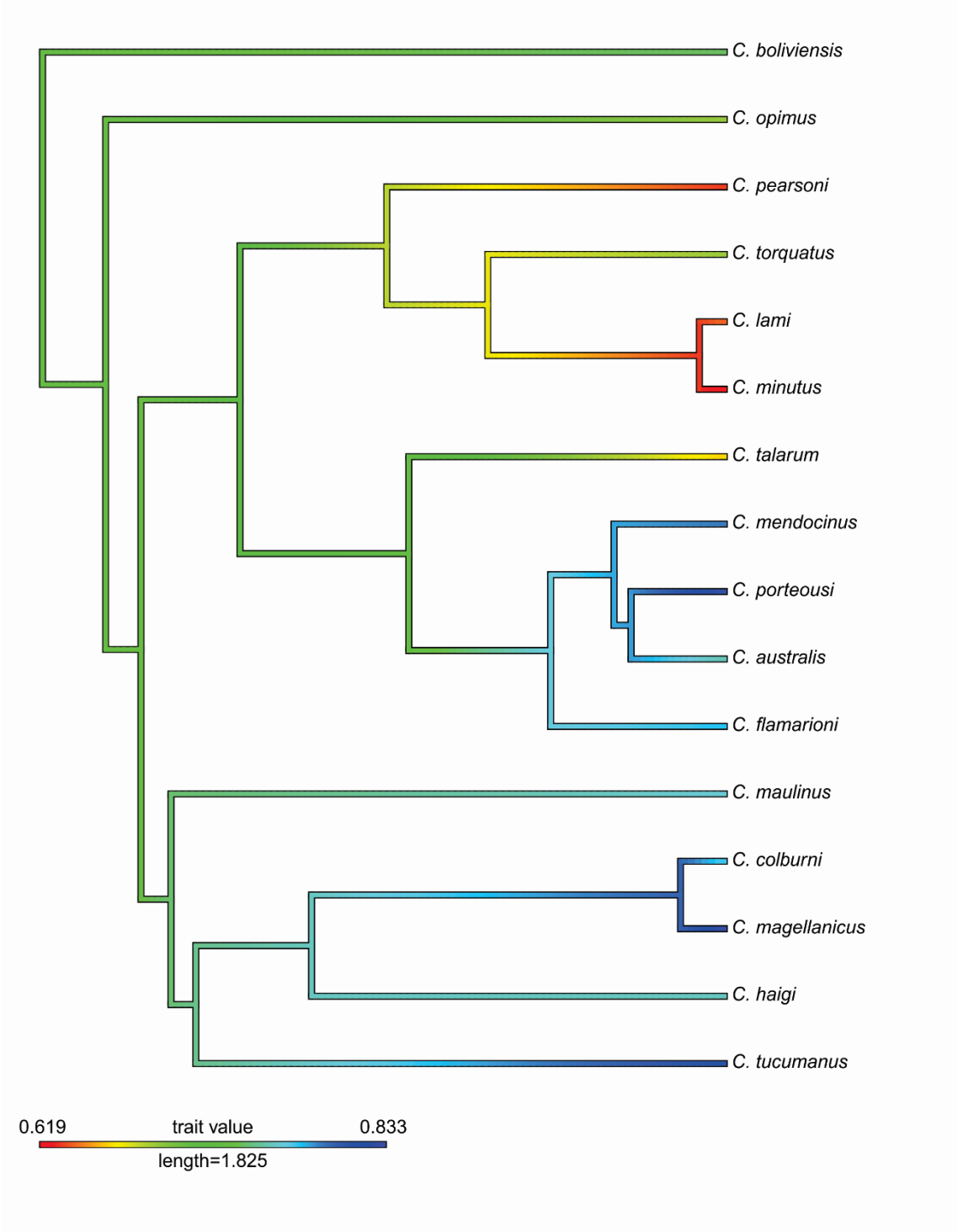

Correlation between the two proposed modules for the skull with corrected size and phylogenetic relationships among 16 species of the genus *Ctenomys*, based on molecular data (Freitas et al., 2012). The original tree was edited to exclude species not investigated here.

Appendix XI

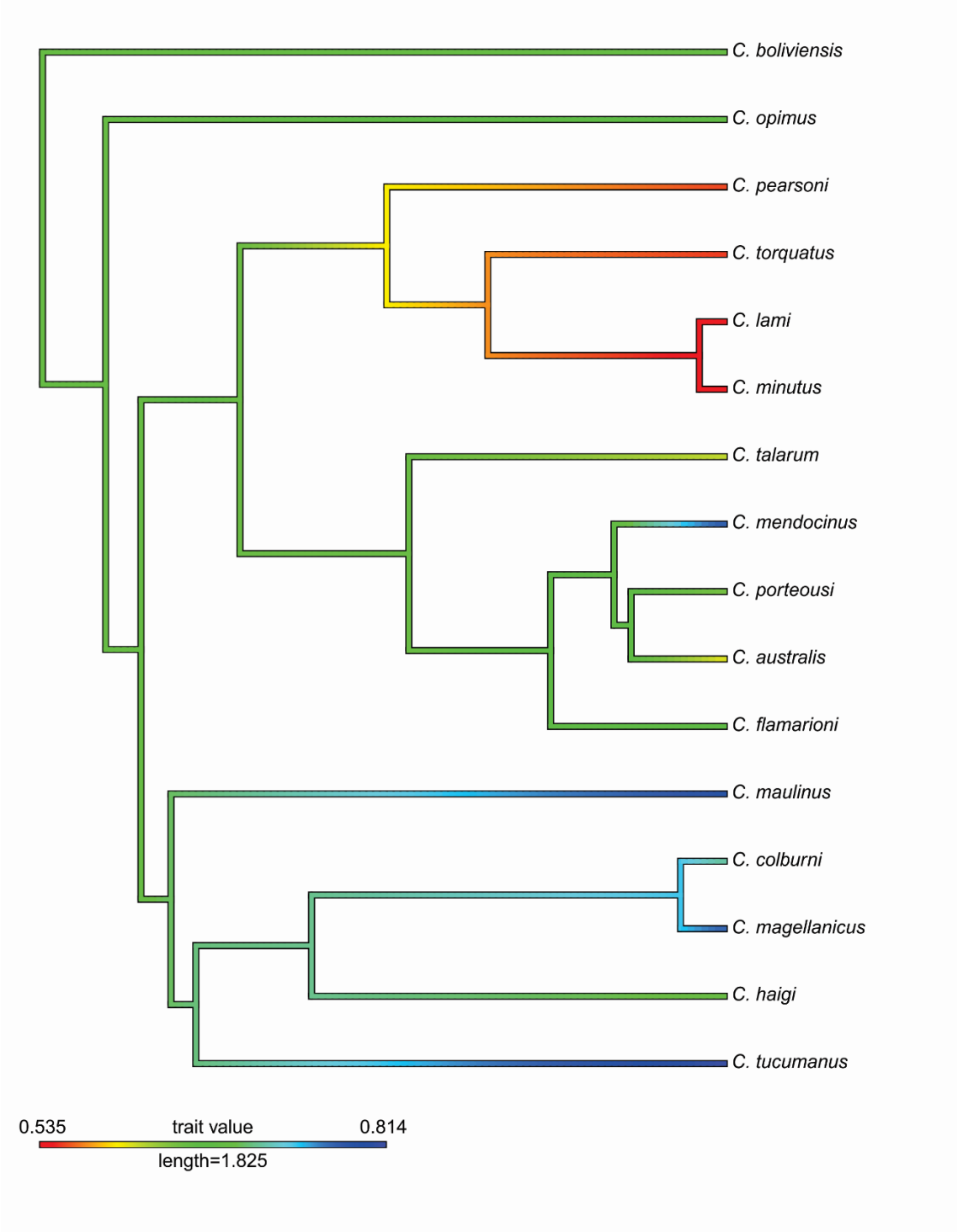

Correlation between the three proposed modules for the skull with corrected size and phylogenetic relationships among 16 species of the genus *Ctenomys*, based on molecular data (Freitas et al., 2012). The original tree was edited to exclude species not investigated here.

Capítulo IV

Manuscrito em preparação: *PNAS*

Searching for genetic basis of skull morphology in subterranean rodents: a case study in tuco-tucos (Hystricognathi: Ctenomyidae).

Borges, L. R.[1], Leipnitz, L. T. [1], Bragatte, M. [1], Maestri, R. [1], Ribas, L. E. J. [1], Fornel, R. [2], Vieira, G.F. [1], Freitas, T. R. O. [1]

1 - Instituto de Biociências da Universidade Federal do Rio Grande do Sul, Av. Bento Gonçalves 9500, 91501-970 Porto Alegre, Brazil.

2 - Programa de Pós-Graduação em Ecologia, Universidade Federal do Rio Grande do Sul, Porto Alegre, RS, Brazil.

Abstract: Skull morphology in rodents is very diverse and defined by a combination of environmental, genetic and demographic factors. Though possible environmental factors that may select for skull shape are well known, the genetic basis of adaption for skull shape in rodents remains poorly understood. The ratio of repetitions of glutamines and alanines (Q/A ratio) in the "coiled coil" domain of Runt related transcription factor 2 (*Runx2*), a transcription factor involved in osteoblast differentiation and several other pathways in bone development, has been correlated with facial length in several dog breeds and some vertebrate genera and may act as an “evolutionary tuning knob”, generating morphological diversity by inducing fine regulation of gene expression. Here we test whether such correlation holds true within *Ctenomys* – a genus of subterranean rodents, which presents high species, karyotype, genetic and morphological diversity, and occupies a wide range of habitats. Results show that the *Runx2* “coiled coil” domain is

mostly conserved between highly divergent species of *Ctenomys*, presenting few non-synonymous amino acid substitutions within the glutamine repetitions, which change glutamines into prolines. In addition, sequences from *Ctenomys* from Midwest and Northern Brazil are identical to predicted sequences of Octodontidae, a family of subterranean rodents, sister to Ctenomyidae. Therefore, the Q/A ratio does not appear to account for differences in facial length between individuals within species or between species, though we cannot rule out the possibility that the Q to P substitutions may alter protein functionality and, by extension, skull morphology, through enhanced or inhibited activity of proteins that Runx2 regulates.

Keywords: Runx2, Ctenomys, tuco-tuco, adaption, development

SIGNIFICANT

The tuco-tucos present morphology of the skull, body and highly diversified karyotypes. We explored here the correlation between the Q/A ratio of a functional domain of the Runx2 protein and the individual skull morphology of specimens of the genus *Ctenomys*, to evaluate whether the Runx2 gene is directly involved differences in skull shape within the genus. We also found a mutation in the Q/A domain of the protein previously unknown in the literature and its potential effects on the structure, function, and interaction of proteins. The Runx2 gene apparently does not appear to be linked to the facial elongation of the tuco-tucus specimens. But we can not rule out the possibility that glutamine-to-proline substitutions may alter protein functionality and, by extension, skull morphology.

Introduction

Tuco tucos (genus *Ctenomys*) are the members of a species-rich genus of subterranean rodents with approximately 70 species described, distributed throughout the Southern half of South America (1, 2), and with a minimum estimated time of origin around 3.5 million years (myr), given the oldest fossil record known for the genus (3). Such recent estimates of origin have been considered as evidence of a burst speciation in *Ctenomys*, given the phylogenetic structuring found in many independent studies (4, 5, 6, 7, 8, 9, 10, 11). The genus also presents highly diverse skull and body morphology, (12, 13, 14,15, 16), and karyotypes ranging from 2n = 10 in *Ctenomys steinbachi* and 2n = 70 in *Ctenomys dorbyigni* (17, 18).

Though factors involved in shaping skull morphology in rodents are well known (15, 19, 20), the causative genetic basis of skull morphology in rodents remains poorly understood. Runt-related transcription factor 2 (*Runx2*) codifies a protein essential to osteoblast differentiation and maturation, and intramembranous and endochondral ossification (21, 22, 23). When *Runx2* is upregulated, proliferation of osteoblasts increases and bone tissue is elongated, while when downregulated, proliferation of osteoblasts decreases and bone development is truncated (24). Mutations in the *Runx2* gene are associated with diseases in humans, such as cleidocranial dysplasia (CCD) (OMIM: 119600), which can be caused by, for example, non-synonymous mutations (25, 26, 27) deletions (28) and tandem repeats in functional domains of the protein (30).

Considering the latter, tandem repeats inside coding regions of a gene can promote fine regulation of gene expression, especially when considering elements that regulate such expression, as in the case of *Runx2*, a transcription factor (29). In fact, Sears (24) have found that the *Runx2* gene is involved in the elongation and shortening of the rostrum

of carnivores, since the length of glutamine (Q) and alanine (A) repeats presents a strong correlation with rostrum length in dog breeds. Pointer (31) explored this variation in several vertebrate taxa and found that this correlation holds true for a few taxa, not across vertebrates in general.

In this paper we explore the correlation between the Q/A ratio of a functional domain of the Runx2 protein and individual skull morphology from representatives of a genus of subterranean rodents (tuco-tucos, *Ctenomys*) to assess whether the *Runx2* gene is directly involved in differences in skull shape within the genus. We also describe a mutation within the Q/A domain of the protein previously unknown in literature and its potential effects on protein structure, function and interaction.

Results

Runx2 sequencing and Q/A ratio analysis – We have successfully amplified and sequenced 174bp of the *Runx2* gene, corresponding to the glutamine/alanine rich domain of the Runx2 protein. The fragment is highly conserved across the individuals sequenced, varying in presence and number of prolines (P) that interrupt the poly-Q sequence (Appendix I). Sequences from individuals representative of species from Midwest and Northern Brazil are identical, with a single proline interrupting the glutamine/alanine rich sequence, while sequences from individuals representative of species from Southern Brazil diverge in number of prolines, which vary from two to three, but are consistent in number of prolines within species (Table 1). All chromatograms were inspected manually to confirm the identity of the prolines as natural polymorphisms and not as sequencing errors.

Comparative analyses - There were significant differences between the specimens with one proline (P1), two prolines (P2) and three prolines (P3) relative to the linear

measurements Nose/Oc-Pat (ANOVA: *d.f.*= 20.9; *F*= 5.85; *p*= 0.01; Figure 1), Nose/CBL (ANOVA: *d.f.*= 20.49; *F*= 12.28; *p*= 0.0003; Figure 2), Face/Oc-Pat (ANOVA: *d.f.*= 20.16; *F*= 7.71; *p*= 0.003; Figure 3) and Face/CBL (ANOVA: *d.f.*= 20.3; *F*= 9.48; *p*= 0.001, Figure 4). Tukey's pairwise comparison confirmed the difference between the linear measurements and some of the revealed prolines groups (see Table 2). The PCA plot (Figure 5) revealed a distribution showing no differences between the P1, P2 and P3 groups of the genus *Ctenomys*. The PC1 score explained 80% of the correlation; PC 2= 12%; PC 3= 7% and PC 4= 0.01%.

The secondary structure analyses - (Figure 6) indicates that prolines probably interfere in the conformation of the region that impact gene expression of genes regulated by Runx2, disrupting an alpha helix by the insertion of coil portions in the middle of structure. A more profound analyses over the general structure of Runx2 was not possible because no templates with acceptable identity were found, for either the Runx2 gene or the highly conserved region of 128 amino acids, known as runt homology domain.

Hierarchical clustering analyses – the clustering (Appendix II) using measures of the face and nose does not reflect the geographic distribution of the sampled individuals.

Discussion

Our study does not show explicit correlation between the length of the skull of rodents of the genus *Ctenomys* and the gene Runx2. Our results corroborate with Pointer (31), where there is no significant correlation between the face length of non-carnivorous placental mammals and the Runx2 gene. Because it is a pleitropic gene, Runx2 is linked to other functionalities and may be expressed in several different tissues in different organisms and in different stages of embryonic development (*e.g.* early development of the thymus and hypertrophic chondrocytes) in addition to the cranium (32, 33, 34, 35).

Such possiblities for differential expression of Runx2 in time and space are a likely explanation for the lack of correlation between the length of the skull and the Runx2 gene.

While most of the 128 amino acid runt activation domain is conserved across all individuals sequenced, we find previously undocumented alterations within the Q/A region, as mutated nucleotides cause non-synonymous amino acid substitutions, from glutamines (Q) to prolines (P) within the poly-Q region. Such amino acid alterations are correlated with geographic and phylogenetic structuring found within species groups of the genus *Ctenomys* in previous studies (8, 11): species that cluster within the *boliviensis* species group – *e.g. C.* sp. xingu, *C.* sp. central, *C. nattereri* and *C. bicolor*; Mato Grosso (MT) state – all present a single P amino acid within the Q region, while the other species studied, which cluster within the *torquatus* – e.g. *C. torquatus, C. ibicuiensis, C. lami* and *C. minutus*; Rio Grande do Sul (RS) state – and *mendocinus – C. flamarioni*; RS state – species groups present two (*C. lami*, *C. minutus* and *C. flamarioni*) and three (*C. torquatus* and *C. ibicuiensis*) Ps substituting Qs. Interestingly enough, the *boliviensis* species group is one of the first species groups to have originated from a common ancestor for the genus, and present the same number of prolines shown in Runx2 sequences predicted for specimens of *Octodon degus*, a species representative of the family Octodontidae, which is a sister family to Ctenomyidae.

The averages cluster analyses further evidence a geographic/phylogenetic pattern of structure, as species from MT state are separated from those from RS state when heavily weighting prolines as causative of individual clustering (one, two and three prolines weighting 1, 2 and 3 respectively); reducing the weight given for each proline, however, failed to recover the complete phylogenetic structuring expected, based on the available phylogenetic data, separating only the individuals whose species presented three prolines (*e.g. C. torquatus* and *C. ibicuiensis*). Furthermore, when considering the

morphological measures only, no visible pattern of structuring is found, neither by species or species groups.

Though pure phylogenetic structuring does not explain the proline pattern found in species from the RS state in Brazil, as two and three prolines occur within the *torquatus* species group, that pattern may be explained by environmental pressures because *C. ibicuiensis* and *C. torquatus*, which present three prolines each, are located in the Pampa biome (central, southwestern, western and northwestern RS, and Uruguay) while *C. lami*, *C. minutus* and *C. flamarioni* inhabit areas within the coastal plains (southeastern, eastern and northeastern RS); both regions are highly differentiated in both biotic and abiotic factors (36, 37, 38). Alternatively, the *torquatus* and *mendocinus* species groups, though monophyletic and highly differentiated, are sister groups within the *Ctenomys* phylogeny, sharing a most recent common ancestor (MRCA) (11)*;* this common recent origin might explain why two prolines are found within both species groups, considering a demographic hypothesis for the Q/A repeat patterns.

When correlation between the number of prolines and the length of the skull was evaluated, significant differences were found, suggesting that variation in proline number may influence the shape of the skulls in *Ctenomys* by altering the functionality of the Runx2 gene (29, 39, 40, 41). However, we can not confirm that the substitutions of Qs for Ps directly influence in the length of the skulls in the specific case of Tuco-tucos, as skull length does not appear to scale with the increase in number of prolines.

Conclusions

All things considered, the body of evidence we present argues that Runx2 is not likely to be a determining factor in skull morphology in the genus *Ctenomys* as is the case in many dog breeds (24) and some vertebrate genus (31), but we cannot rule out that the

Runx2 gene may contribute to the overall regulation of body development, cranium included, since the Runx2 gene is highly regulated by other transcription factors and has different specific expressions (32, 33, 42). Although Runx2 does not seem to be the major factor involved in skull size in *Ctenomys*, investigating candidate development genes such as Runx2 opens the way to new research possibilities concerning genes regarding facial growth/stretching, such as the investigation of Hox genes. We also note the discovery of a new, widespread, mutation within the Q/A repeat region, which may be responsible for altering the functionality of the Q/A domain of the Runx2 protein, likely inhibiting activity because the mutations interrupt the an alpha helix within the protein's domain. Developing structure models for the Runx2 protein is detrimental to further investigate the effect of the novel mutations found and detect to what extent they alter protein function in *Ctenomys* and consequently body development.

Material and Methods

Sample information and DNA extraction - Liver tissues of 36 specimens of *Ctenomys* (Table 1, Appendix III), representative of seven species and two lineages were selected for DNA extraction based on three criteria: i) tissue samples must be well preserved in order to extract genomic DNA with good quality, ii) all tissue samples came from specimens with a preserved skull, to allow for morphological and molecular comparisons as defined in Pointer (31) and iii) all individuals selected were males, in order to block for possible sexual dimorphism effects on skull shape. All individuals are housed at Laboratório de Citogenética e Evolução under individual collection numbers. A detailed description of the individuals, species, species groups analyzed *sensu* (8), and individual collection numbers is shown in Appendix I. Five additional predicted sequences from *Octodon degus* derived from genomic projects (GenBank Accession

numbers: XM012515902, XM012515909, XM012515909, XM012515918 and XM012515919) were used as outgroups. We have extracted DNA from all specimens using the CTAB DNA extraction protocol (43) with modifications. We tested all DNA extractions for quality in 1.5% agarose gels and quantified the extractions using NanoDrop (ThermoFisher Scientific). We diluted working solutions to 50ng/ul of DNA from purified extractions for posterior analysis.

Runx2 amplification, sequencing and molecular analysis - We have sequenced 36 individuals for a fragment of the *Runx2* gene, which translates into the poly glutamine/alanine domain of the protein Runx2. We have amplified DNA fragments through a nested PCR with two sets of primers: an external set (Sears_EXT-F: 5'-TTG TGA TGC GTA TTC CCG TA-3'; Sears_EXT-R: 5'-ACS GAG CAC AGG AAG TTG GG-3') and an internal set (Sears_INT-F: 5'-ATC CGA GCA CCA GCC GGC GGC GCT TCA G-3'; Sears_INT-R: 5'-GTG GTC VGC GAT GAT CTC SAC-3') (24) as described by Pointer (31): in the external PCR, we used 100ng (2.0ul) of purified genomic DNA, 24.0ul of sterile water, 4.0 ul of 10x PCR Buffer, 3.2ul of 50nM $MgCl_2$ as a PCR cofactor, 0.8ul of 10nm deoxynucleotide tri phosphate (dNTP), 0.8ul of 10mM PCR primers - forward and reverse - 2.0ul of DMSO and 0.4ul of 5U/ul Taq Polymerase (Ludwig Biotec), totaling a 40ul PCR reaction. In the internal (nested) PCR we used the same mix concentrations and volumes as in the external PCR, except for water (27.5ul) and genomic DNA (substituted for 0.5ul of the external PCR product) for amplifying the fragment of interest. Bands approximately 200bp long were extracted from agarose gels, purified and sequenced abroad (Macrogen Inc.). We inspected chromatograms manually using Chromas Lite (Technelysium Inc.). We aligned all sequences using the MUSCLE algorithm (44) implemented in MEGA 7 (45).

Skull morphology measures - We have measured each cranium (Figure 7) for facial length (Face), defined as the measure from the anteroventral margin of the orbit at the lacrimal foramen to the anterior margin of the premaxilla and nasal length (Nose), defined as the measure from the anteroventral margin of the orbit at the lacrimal foramen to the anterolateral margin of the nasal bone, and two proxy measures of skull size: cranial base length (Oc-Pat), defined as the distance from lateral-most point of the occipital condyle to the caudal margin of the palate, and condylobasal or total cranial length (CBL), defined as the distance from the lateral-most point of the occipital condyle to the anterior-most premaxilla, as in Sears (24), using a digital caliper; we then standardize the measures of Face and Nose by dividing those metrics by the Oc-Pat and CBL measures for each cranium, as in Pointer (31).

Comparative analyses - the number of amino acid substitutions from glutamine (Q) to proline (P) (P1 = *Ctenomys bicolor*, *Ctenomys nattereri*, *Ctenomys sp.* central and *Ctenomys sp.* xingu specimens with one proline, P2 = *Ctenomys flamarioni*, *Ctenomys lami* and *Ctenomys minutus* specimens with two prolines, P3 = *Ctenomys ibicuiensis* and *Ctenomys torquatus* specimens with three prolines; was compared to linear measurements of the skull proposed by Sears (24), used here in rodents of the genus *Ctenomys*, through an ANOVA; a principal component analysis (PCA) was carried out among the three different groups of prolines (P1, P2 and P3) and linear measurements of the rodent skull of the genus *Ctenomys*, using software Past (46).

Secondary structure prediction – we further analyzed the influence of secondary structures in protein level, since, as a rule, protein structure is more conserved than sequences (47). We translated DNA sequences from fragments of the Runx2 gene into an amino acid sequences by the Expasy translate tool (48). We selected representative specimens based on the number of proline, *Ctenomys nattereri* (P1), *Ctenomys minutus*

(P2), *Ctenomys torquatus* (P3) and use as standard sequence the *Mus musculus*, a specimen which does not show insertion of prolines. The sequence was retrieved from UniProt (Universal Protein Source) database (ID: Q08775). The secondary structure was predicted by the Psipred online server (49).

Hierarchical clustering analyses – looking for correlations among different species of *Ctenomys* in relation to studied dimension (Face and Nose measurements) obtained by the standardization of Oc-Pat and CBL for each skull. We used the Pvclust an R package for assessing the uncertainty in hierarchical cluster analysis with p-values (50). The parameters used in the analyzes were the agglomerative method used in hierarchical clustering as average or UPGMA (Unweighted Pair Group Method with Arithmetic Mean), the approach to evaluate the distances was the matrix of dissimilarity based on correlation, the procedure for computing covariances in the presence of missing values was pairwise complete observations and reinforcement for each branch was achieved by operating bootstrap analysis with 10,000 replicates.

Acknowledgements

We are grateful to our colleagues of the Laboratório de Citogenética e Evolução for their support in various stages of this study. L.R.B. and L.L received student scholarships from the Coordenação de Aperfeiçoamento de Pessoal de Nível Superior (CAPES). T.R.O.F. received research support from CNPq, CAPES and the Fundação de Amparo à Pesquisa do Rio Grande do Sul (FAPERGS).

References

1. Bidau CJ (2015) Family Ctenomyidae. In Patton, J.L., Pardiñas, U.F.J. & D'Elía, G. Mammals of South America Vol. 2: Rodents. The University of Chicago Press Books.

2. Freitas TRO Family Ctenomyidae (Tuco-tucos). In: Don E. Wilson; Thomas E. Lacher, Jr; Russell A. Mittermeier. (Org.). Handbook of the Mammals of the World - Volume 6 Lagomorphs and Rodents I. 6ed.Barcelona: Lynx Edicions Publications, 2016, 6: 1-900.

3. Verzi DH, Olivares AI, Morgan CC (2009) The oldest South American tuco-tuco (late Pliocene, northwestern Argentina) and the boundaries of the genus *Ctenomys* (Rodentia, Ctenomyidae). *Mammalian Biology* 75:243–252.

4. Lessa EP, Cook, JA (1998) The molecular phylogenetics of tuco-tucos (genus *Ctenomys*, Rodentia: Octodontidae) suggests an early burst of speciation. *Molecular Phylogenetics and Evolution* 9: 88-99.

5. D'Elía G, Lessa EP, Cook JA (1999) Molecular phylogeny of tuco-tucos, genus *Ctenomys* (Rodentia, Octodontidae): Evaluation of the mendocinus species group and the evolution of asymmetric sperm. *Journal of Mammalian Evolution* 6: 19-38.

6. Slamovits CH, Cook JA, Lessa EP, Rossi MS (2001) Recurrent amplification and deletions of satellite DNA accompanied chromosomal diversification in south American tuco-tucos (genus *Ctenomys*, Rodentia: Octodontidae): A phylogenetic approach. *Molecular Biology and Evolution* 18: 1708–1719.

7. Castillo AH, Cortinas MN, Lessa EP (2005) Rapid diversification of south American tuco-tucos (*Ctenomys*; Rodentia, Ctenomyidae): Contrasting mitochondrial and nuclear intron suquences. *Journal of Mammalogy* 86:170–179.

8. Parada A, D'Elía G, Bidau CJ, Lessa EP (2011) Species groups and the evolutionary diversification of tuco-tucos, genus *Ctenomys* (Rodentia: Ctenomyidae). *Journal of Mammalogy* 92:671–682.

9. Freitas TRO, Fernandes FA, Fornel R, Roratto PA (2012) An endemic new species of tuco-tuco, genus *Ctenomys* (Rodentia: Ctenomyidae), with a restricted geographic distribution in southern Brazil. *Journal of Mammalogy* 93: 1355-1367.

10. Gardner SL, Salazar-Bravo J, Cook JA (2014). New species of *Ctenomys* (Rodentia: Ctenomyidae) from the lowlands and central valleys of Bolivia. Special Publication, Museum of Texas Tech University 62:1-34.

11. Leipnitz LT, Fornel R, Ribas LEJ, Kubiak BB, Galiano D, Freitas TRO (2018) Lineages of Tuco-Tucos (Ctenomyidae: Rodentia) from Midwest and Northern Brazil: Late Irradiations of Subterranean Rodents Towards the Amazon Forest. *Journal Of Mammalian Evolution* 25: 1-16.

12. Freitas TRO, Lessa EP (1984) Cytogenetics and morphology of *Ctenomys torquatus* (Rodentia-Octodontidae). *Journal of Mammalogy* 65:637-642.

13. Fernandes FA, Fornel R, Cordeiro-Estrela P, Freitas TRO (2009). Intra- and interspecific skull variation in two sister species of the subterranean rodent genus *Ctenomys* (Rodentia, Ctenomyidae): coupling geometric morphometrics and chromosomal polymorphism. *Zoological Journal of the Linnean Society* 155, 220–237.

14. Fornel R, Cordeiro-Estrela P, Freitas TRO (2010) Skull shape and size variation in *Ctenomys minutus* (Rodentia: Ctenomyidae) in geographical, chromosomal polymorphism, and environmental contexts. *Biological Journal of the Linnean Society* 101, 705–720.

15. Borges LR, Maestri R, Kubiak BB, Galiano D, Fornel R, Freitas TRO (2016). The role of soil features in shaping the bite force and related skull and mandible morphology

in the subterranean rodents of genus *Ctenomys* (Hystricognathi: Ctenomyidae). *Journal of Zoology* 301: 108–117

16. Kubiak BB, Maestri R, Almeida TS, Borges LR, Galiano D, Fornel R, Freitas TRO (2018) Evolution in action: soil hardness influences morphology in a subterranean rodent (Rodentia: Ctenomyidae). *Biological Journal of the Linnean Society* XX: 1–11.

17. Anderson S, Yates TL, Cook JA (1987) Notes on Bolivian mammals, 4: The genus *Ctenomys* (Rodentia: Ctenomyidae) in the eastern lowlands. American Museum Novitates 2891:1-20.

18. Reig OA, Busch C, Ortells MO, Contreras JR (1990) An overview of evolution, systematics, population biology, cytogenetics, molecular biology and speciation in *Ctenomys*. Pp. 71–96 in Evolution of subterranean mammals at the organismal and molecular levels (E. Nevo and O. A. Reig, eds.). Wiley- Liss, New York.

19. Marcy AE, Hadly EA, Sherratt E, Garland K, Weisbecker V (2016) Getting a head in hard soils: Convergent skull evolution and divergent allometric patterns explain shape variation in a highly diverse genus of pocket gophers (Thomomys). *BMC Evolutionary Biology* 16:207 DOI: 10.1186/s12862-016-0782-1.

20. Maestri R, Fornel R, Gonçalves GL, Geise L, Freitas TRO, Carnaval AC (2016) Predictors of intraspecific morphological variability in a tropical hotspot: comparing the influence of random and non-random factors. *Journal of Biogeography* 43: 2160–2172.

21. Otto F, Thornell AP, Crompton T, Denzel A, Gilmour KC, Rosewell IR, Stamp GW, Beddington RS, Mundlos S, Olsen BR, Selby PB, Owen MJ. (1997) Cbfa1, a candidate gene for cleidocranial dysplasia syndrome, is essential for osteoblast differentiation and bone development. *Cell.* 1997 30:765-771.

22. Zhang T, Tan P, Wang L, Jin N, Li Y, Zhang L, Yang H, Hu Z, Zhang L, Hu C, Li C, Qian K, Zhang C, Huang Y, Li K, Lin H, Wang D (2017) RNALocate: a resource for RNA subcellular localizations. *Nucleic Acids Research* 45: 135-138.

23. Jung YJ, Bae HS, Ryoo HM, Baek SH (2017) A novel RUNX2 mutation in exon 8, G462X, in a patient with Cleidocranial Dysplasia. *Journal of Cellular Biochemistry* 0: 0-0.

24. Sears KE, Goswami A, Flynn JJ, Niswander LA (2007) The correlated evolution of Runx2 tandem repeats, transcriptional activity, and facial length in Carnivora. *Evolution & Development* 96: 555-565.

25. Quack I, Vonderstrass B, Stock M, Avlsworth AS, Becker A, Brueton L, Lee PJ, Majewski F, Mulliken JB, Suri M, Zenker M, Mundlos S, Otto F (1999) Mutation analysis of core binding factor A1 in patients with cleidocranial dysplasia. *American Journal of Human Genetics* 65:1268-1278.

26. Kim D, Yukl ET, Moënne-Loccoz P, Montellano PR (2006) Fungal heme oxygenases: Functional expression and characterization of Hmx1 from Saccharomyces cerevisiae and CaHmx1 from Candida albicans. *Biochemistry* 45: 14772-14780.

27. Zhou G, Chen Y, Zhou L, Thirunayukkarasu K, Hecht J, Chitayat D, Gelb BD, Pirinen S, Berry SA, Greenberg CR, Karsenty G, Lee B (1999) CBFA1 mutation analysis and functional correlation with phenotypic variability in cleidocranial dysplasia. *Human Molecular Genetics* 8: 2311-2316.

28. Ott CE, Leschik G, Trotier F, Brueton L, Brunner HG, Brussel W, Guillen-Navarro E, Haase C, Kohlhase J, Kotzot D, Lane A, Lee-Kirsch MA, Morlot S, Simon MEH, Steichen-Gersdorf E, Tegay DH, Peters H, Mundlos S, Klopocki E (2010) Deletions of the RUNX2 gene are present in about 10% of individuals with cleidocranial dysplasia. *Human Mutation* 31: 1587-1593.

29. Ziros PG, Basdra EK, (2008) Papavassiliou AG. Runx2: of bone and stretch. *International Journal of Biochemistry & Cell Biology* 40: 1659–63.

30. Mundlos S, Otto F, Mundlos C, Mulliken JB, Aylsworth AS, Albright S, Lindhout D, Cole WG, Henn W, Knoll JHM, Owen MJ, Mertelsmann R, Zabel BU, Olsen BR (1997) Mutations involving the transcription factor CBFA1 cause cleidocranial dysplasia. *Cell Press* 89:773-779.

31. Pointer MA, Kamilar JM, Warmuth V, Chester SGB, Delsuc F, Mundy NI, Asher RJ, Bradley BJ (2012) RUNX2 tandem repeats and the evolution of facial length in placental mammals. *BMC Evolutionary Biology* 12:103. DOI: 10.1186/1471-2148-12-103.

32. Komori TH, Yagi H, Nomura S, Yamaguchi A, Sasaki K, Deguchi K, Shimizu Y, Bronson RT, Gao YH, Inada M, Sato M, Okamoto R, Kitamura Y, Yoshiki S, Kishimoto T (1997) Targeted disruption of Cbfa1 results in a complete lack of bone formation owing to maturational arrest of osteoblasts. *Cell* 89: 755–764.

33. Vaillant F, Blyth K, Andrew L, Neil JC, Cameron ER (2002) Enforced expression of Runx2 perturbs T cell development at a stage coincident with β-selection. *Journal of Immunology*.169: 2866–2874.

34. Komori T (2003) Requisite roles of Runx2 and Cbfb in skeletal development. *Journal of Bone and Mineral Metabolism* 21:193-197.

35. Ding M, Lu Y, Abbassi S, Li F, Li X, Song Y, Geoffroy V, Im HJ, Zheng Q (2012) Targeting Runx2 expression in hypertrophic chondrocytes impairs endochondral ossification during early skeletal development. *Journal of Cellular Physiology* 227: 3446-3456.

36. Rambo B (1956). A fisionomia do Rio Grande do Sul. 2ed. Selbach, Porto Alegre.

37. Jarenkow JA, Waechter JL (2001) Composição, estrutura e relações florísticas do componente arbóreo de uma floresta estacional no Rio Grande do Sul, Brasil. *Revista brasileira de Botânica* 24: 263-272.

38. Crawshaw D, Dall´Agnol M, Cordeiro JLP, Hasenack H (2007) Caracterização dos campos Sul-rio-grandenses: uma perspectiva da ecologia da paisagem. *Boletim Gaúcho de Geografia*. 33: 233–252.

39. Otto F, Kanegane H, Mundlos S (2002) Mutations in the RUNX2 Gene in Patients With Cleidocranial Dysplasia. *Human mutation* 19:209-216.

40. Hansen L, Riis AK, Silahtaroglu A, Hove H, Lauridsen E, Eiberg H, Kreiborg S, (2011) RUNX2 analysis of Danish cleidocranial dysplasia families. *Clinical Genetics* 79: 254–263.

41. Jaruga A, Hordyjewska E, Kandzierski G, Tylzanowski P (2016). Cleidocranial dysplasia and RUNX2-clinical phenotype–genotype correlation. *Clinical Genetics* 90: 393-402.

42. Liu T M, Lee EH (2013) Transcriptional Regulatory Cascades in Runx2-Dependent Bone Development. Tissue Engineering. *Part B Reviews* 19: 254–263.

43. Doyle JJ, Doyle JL 1987 A rapid DNA isolation procedure for small quantities of fresh leaf tissue. *Phytochemical Bulletin* 19: 11-15.

44. Edgar R. 2004. MUSCLE: multiple sequence alignment with high accuracy and high throughput. *Nucleic Acids Research* 32:1792–1797.

45. Kumar S, Stecher G, Tamura K (2016). MEGA7: Molecular Evolutionary Genetics Analysis version 7.0 for bigger datasets. *Molecular Biology and Evolution* 33:1870-1874.

46. Hammer O, Harper DAT, Ryan PD 2001 PAST: PaleontologicalStatistic software package for education and data analysis. *Paleontologia Eletronica* 4: 1-9.

47. Illergård K, Ardell DH, Elofsson A (2009) Structure is three to ten times more conserved than sequence—a study of structural response in protein cores. *Proteins: Structure, Function, and Bioinformatics* 77: 499-508.

48. Artimo P, et al. (2012) ExPASy: SIB bioinformatics resource portal. *Nucleic acids research* 40: 597-603.

49. Jones, DT (1999). Protein Secondary Structure Prediction Based on Position-specific Scoring Matrices. *Journal of Molecular Biology* 292: 195-202.

50. Suzuki R, Shimodaira H (2006) Pvclust: an R package for assessing the uncertainty in hierarchical clustering. *Bioinformatics* 22: 1540-1542.

Tables and Figures

Table 1. List of individuals sequenced and measured as in Pointer *et al.* (2012) used in this study. Left to right: species name, individuals per species, number of glutamines (Q), number of alanines (A), number of prolines (P), Runx2 Q/A ratios considering the prolines, Runx2 Q/A ratios not considering prolines, and face length measurements (in cm).

Species	Individuals	Q	A	P	Q/A (+P)	Q/A (-P)	Nose/ Oc-Pat	Nose/ CBL	Face/ Oc-Pat	Face/ CBL
C. bicolor	PB_40_01	16	4	1	4	4.25	0.369	0.318	0.309	0.267
C. bicolor	PB_41_02	16	4	1	4	4.25	0.356	0.321	0.304	0.274
C. bicolor	PB_42_03	16	4	1	4	4.25	0.362	0.295	0.336	0.274
C. flamarioni	TR 30	15	4	2	4.25	3.75	0.391	0.324	0.354	0.293
C. flamarioni	TR 45	15	4	2	4.25	3.75	0.395	0.33	0.359	0.299
C. flamarioni	TR 65	15	4	2	4.25	3.75	0.356	0.316	0.323	0.287
C. flamarioni	TR 203	15	4	2	4.25	3.75	0.355	0.315	0.335	0.298
C. ibicuiensis	TR 1068	14	4	3	4.25	3.5	0.362	0.318	0.319	0.28

C. ibicuiensis	TR 1069	14	4	3	4.25	3.5	0.34	0.295	0.318	0.276
C. ibicuiensis	TR 1070	14	4	3	4.25	3.5	0.355	0.311	0.323	0.283
C. lami	TR 344	15	4	2	4.25	3.75	0.383	0.321	0.347	0.291
C. lami	TR 202	15	4	2	4.25	3.75	0.379	0.318	0.347	0.291
C. minutus	TR 05	15	4	2	4.25	3.75	0.371	0.317	0.319	0.273
C. minutus	TR 35	15	4	2	4.25	3.75	0.348	0.321	0.315	0.291
C. minutus	TR 38	15	4	2	4.25	3.75	0.375	0.319	0.331	0.282
C. minutus	TR 41	15	4	2	4.25	3.75	0.371	0.311	0.333	0.28
C. minutus	TR 46	15	4	2	4.25	3.75	0.354	0.304	0.317	0.272
C. nattereri	CA_06_01	16	4	1	4	4.25	0.359	0.309	0.311	0.267
C. nattereri	CA_07_02	16	4	1	4	4.25	0.326	0.278	0.303	0.258
C. nattereri	CA_08_03	16	4	1	4	4.25	0.336	0.288	0.292	0.251
C. nattereri	CA_09_04	16	4	1	4	4.25	0.352	0.307	0.3	0.262
C. nattereri	SP_77_04	16	4	1	4	4.25	0.332	0.305	0.275	0.252
C. nattereri	SP_78_05	16	4	1	4	4.25	0.358	0.317	0.301	0.267
C. sp. *central*	NM_84_04	16	4	1	4	4.25	0.369	0.31	0.314	0.264
C. sp. *xingu*	NO_50_11	16	4	1	4	4.25	0.319	0.273	0.286	0.245
C. sp. *xingu*	NU1_31_01	16	4	1	4	4.25	0.318	0.282	0.301	0.267
C. sp. *xingu*	NU1_32_02	16	4	1	4	4.25	0.333	0.288	0.316	0.274
C. sp. *xingu*	NU1_33_03	16	4	1	4	4.25	0.369	0.326	0.328	0.291
C. sp. *xingu*	NU2_56_05	16	4	1	4	4.25	0.386	0.336	0.345	0.3
C. sp. *xingu*	FN_67_03	16	4	1	4	4.25	0.351	0.3	0.32	0.274
C. torquatus	TR 906	14	4	3	4.25	3.5	0.353	0.303	0.341	0.293
C. torquatus	TR 910	14	4	3	4.25	3.5	0.324	0.298	0.298	0.274
C. torquatus	TR 947	14	4	3	4.25	3.5	0.365	0.298	0.34	0.277
C. torquatus	TR 951	14	4	3	4.25	3.5	0.343	0.293	0.307	0.261
C. torquatus	TR 956	14	4	3	4.25	3.5	0.368	0.304	0.329	0.272
C. torquatus	TR 960	14	4	3	4.25	3.5	0.349	0.294	0.307	0.258

Table 2. Tukey pairwise among the linear measurements Nose/Oc-Pat, Nose/CBL, Face/Oc-Pat and Face/CBL relative to the specimens with one proline (P1), two prolines (P2) and three prolines (P3) of the genus *Ctenomys* found in the Neotropical region.

Tukey pairwise Nose/Oc-Pat between P1, P2 and P3			
	P1	**P2**	**P3**
P1		0.01*	0.982
P2	4.338		0.04*
P3	0.254	3.545	
Tukey pairwise Nose/CBL between P1, P2 and P3			
	P1	**P2**	**P3**
P1		0.02*	0.947
P2	3.891		0.03*
P3	0.443	3.801	
Tukey pairwise Face/Oc-Pat between P1, P2 and P3			
	P1	**P2**	**P3**
P1		0.001*	0.234
P2	5.641		0.145
P3	2.351	2.736	
Tukey pairwise Face/CBL between P1, P2 and P3			
	P1	**P2**	**P3**
P1		0.001*	0.352
P2	5.777		0.076
P3	1.980	3.199	

*$p<0.05$.

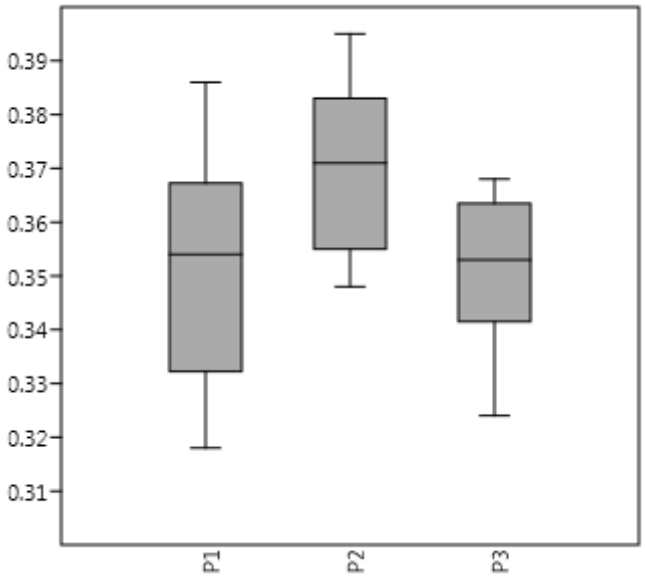

Figures 1. Variation of linear measures Nose/OcPat, specimens with one proline (P1), two prolines (P2) and three prolines (P3) of the genus *Ctenomys* found in the Neotropical region.

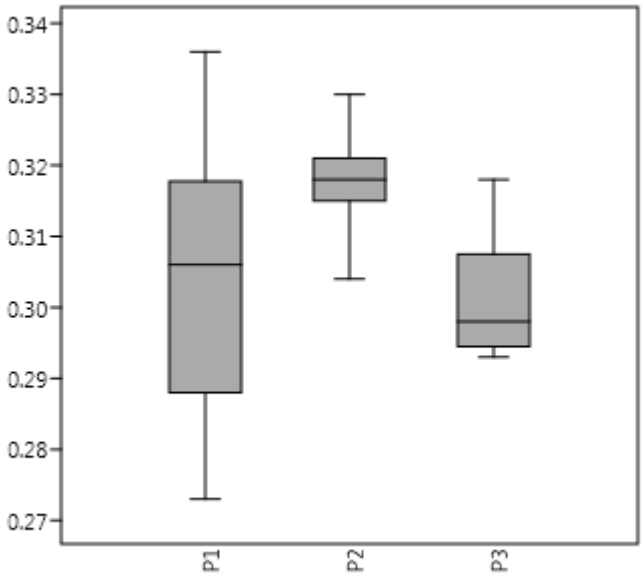

Figure 2. Variation of linear measures Nose/CBL, specimens with one proline (P1), two prolines (P2) and three prolines (P3) of the genus *Ctenomys* found in the Neotropical region.

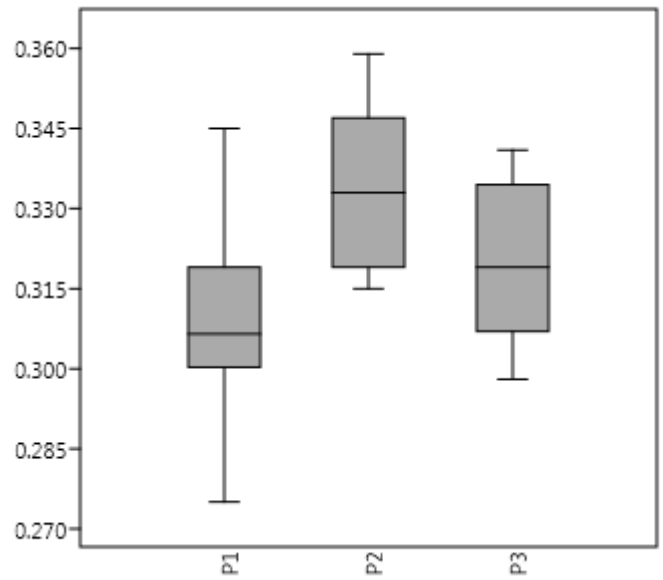

Figure 3. Variation of linear measures Face/OcPat, specimens with one proline (P1), two prolines (P2) and three prolines (P3) of the genus *Ctenomys* found in the Neotropical region.

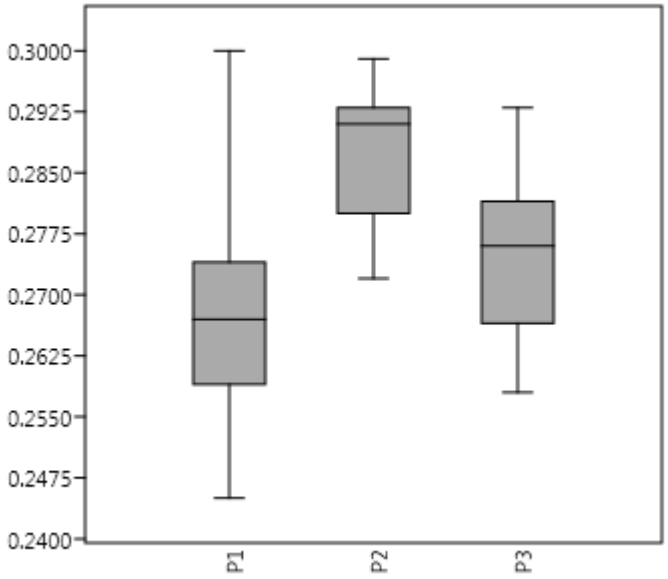

Figure 4. Variation of linear measures Face/CBL, specimens with one proline (P1), two prolines (P2) and three prolines (P3) of the genus *Ctenomys* found in the Neotropical region.

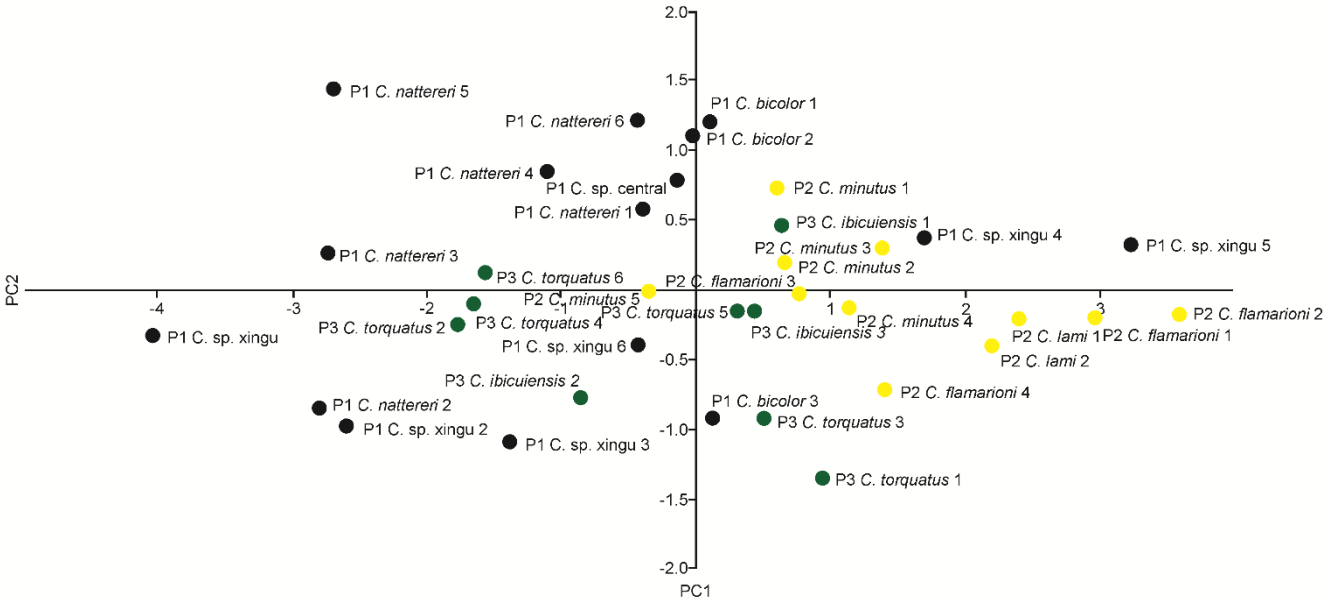

Figure 5. First two axes of principal component analysis (PCA) of the prolines groups (P1= black; P2= green and P3= yellow) and linear measurements of the rodent skull of the genus *Ctenomys* found in the Neotropical region.

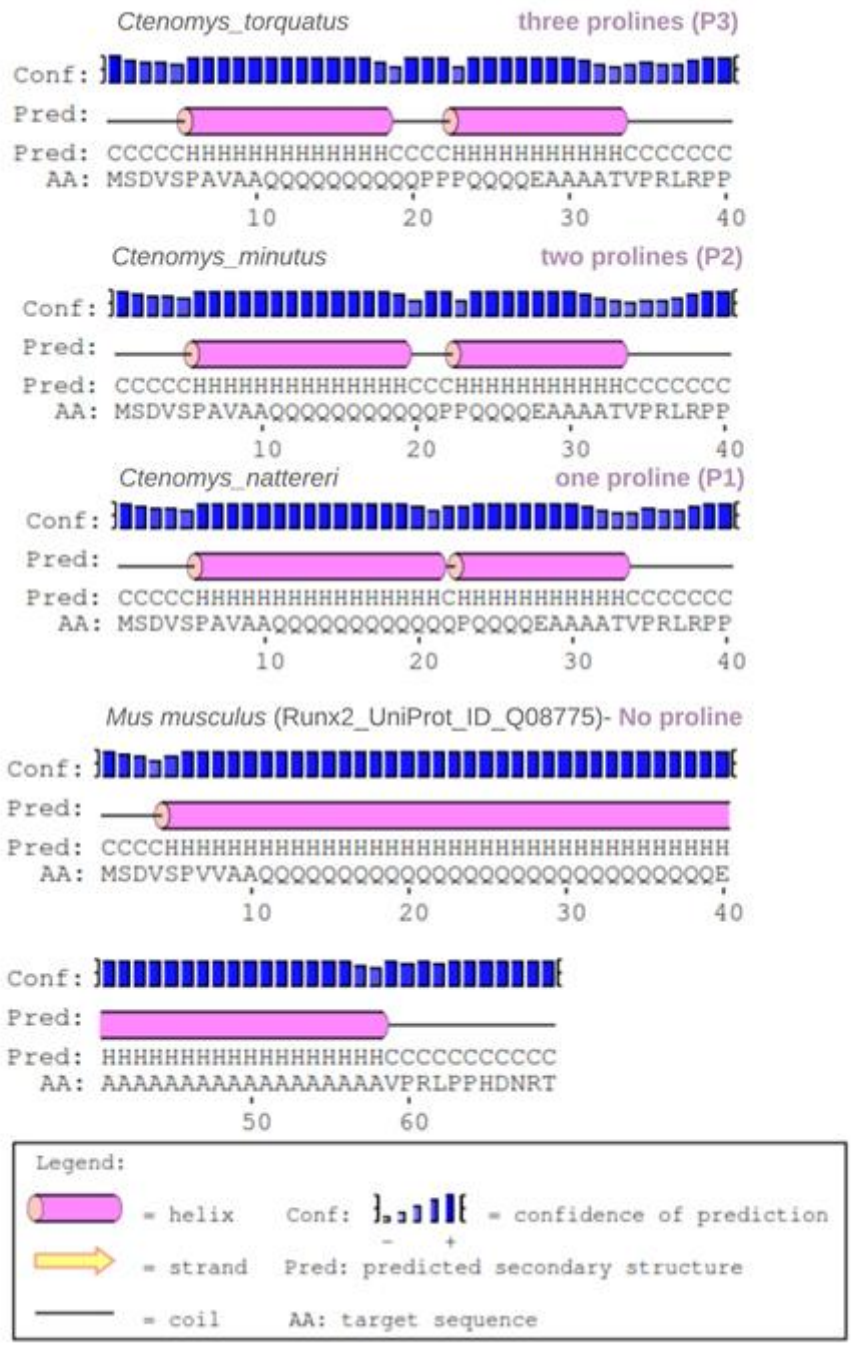

Figure 6. Secondary structure analysis with Psipred tool showing the presumable influence of prolines in the sequence, disrupting an alpha helix by the insertion of coil portions in the middle of the structure.

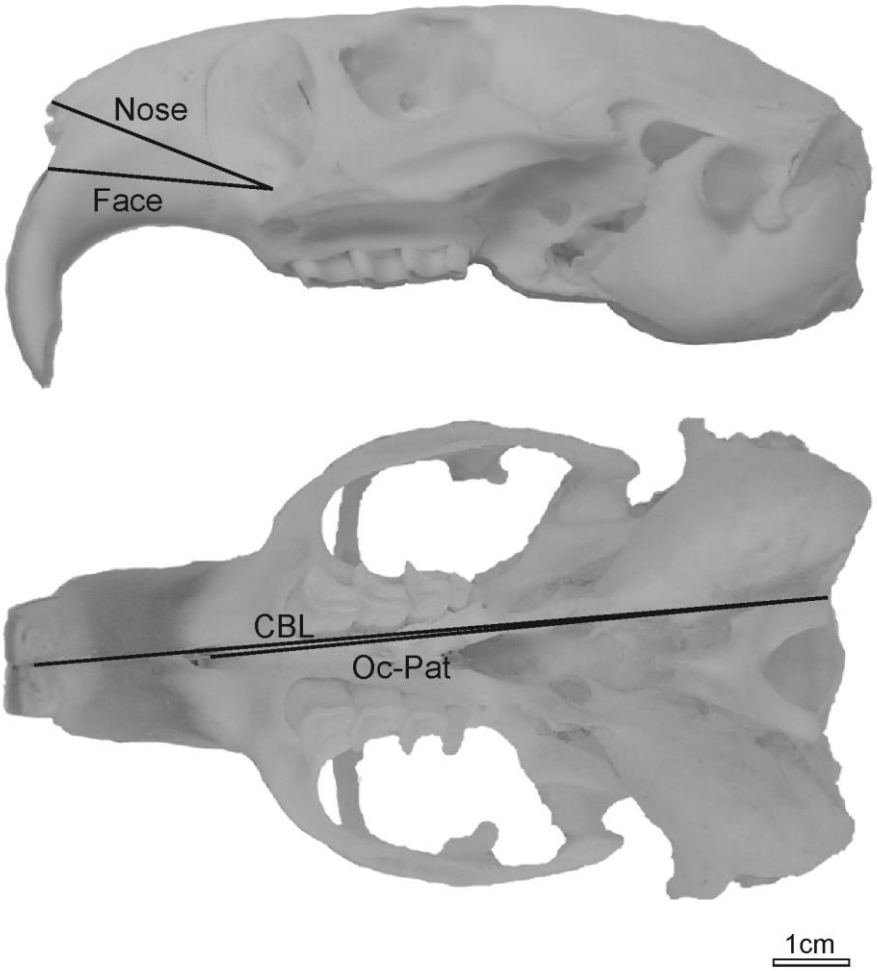

Figure 7. *Ctenomys lami* skull in lateral and ventral views. Nose = anteroventral margin of orbit at lacrimal foramen to anterolateral margin of nasal bone; Face = anteroventral margin of orbit at lacrimal foramen to anterior premaxilla; CBL = distance from lateral-most point of occipital condyle to anterior premaxilla; Oc-Pat = distance from lateral-most point of occipital condyle to caudal margin of palate.

Supplementary material

Appendix I

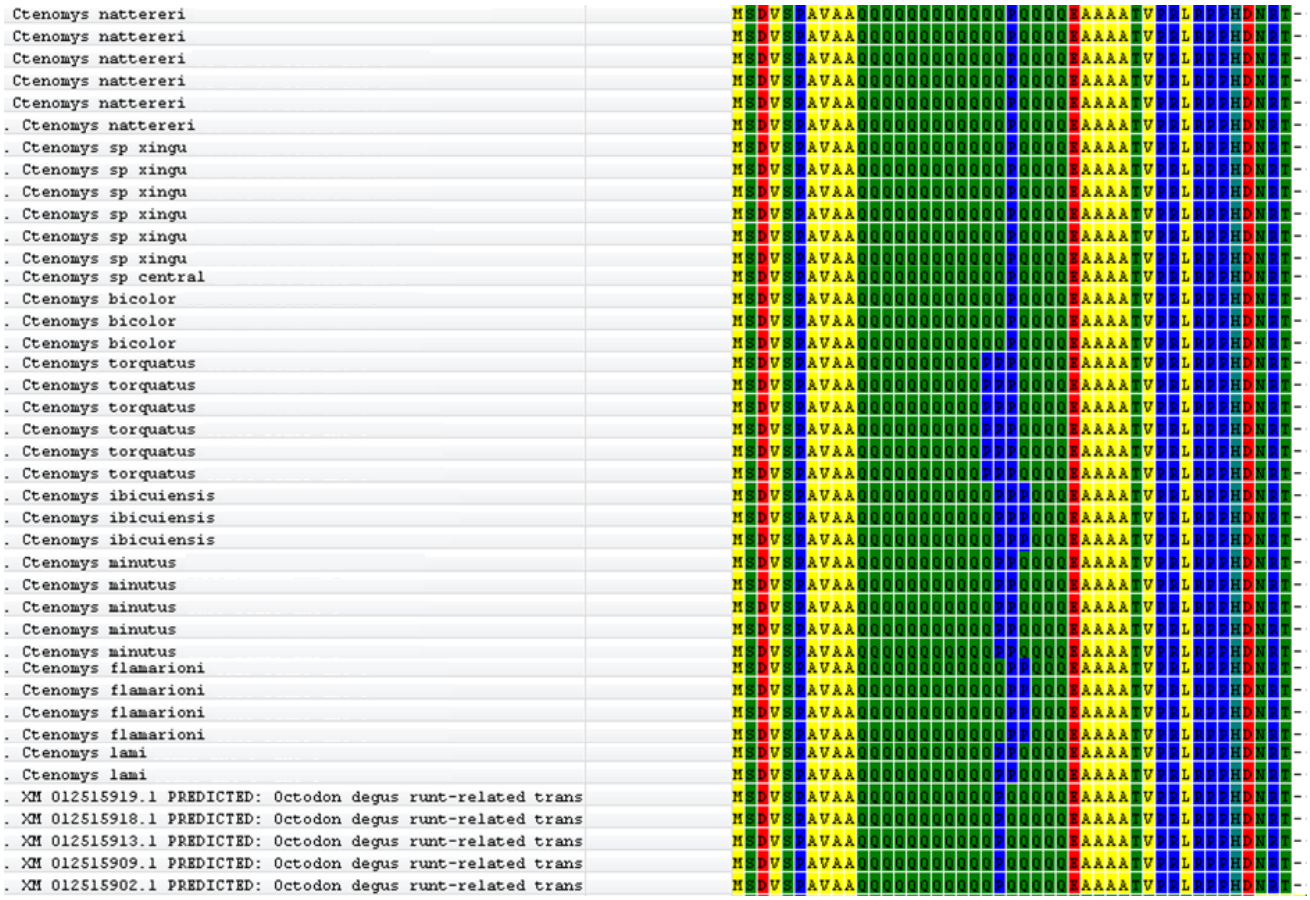

Amino acid alignment of Runx2 showing the Q/A region with flanking sequence of the 36 specimens of the genus *Ctenomys*, found in the Neotropical region. Below are the 5 additional predicted sequences of *Octodon degus* derived from genomic projects used as external groups.

Appendix II

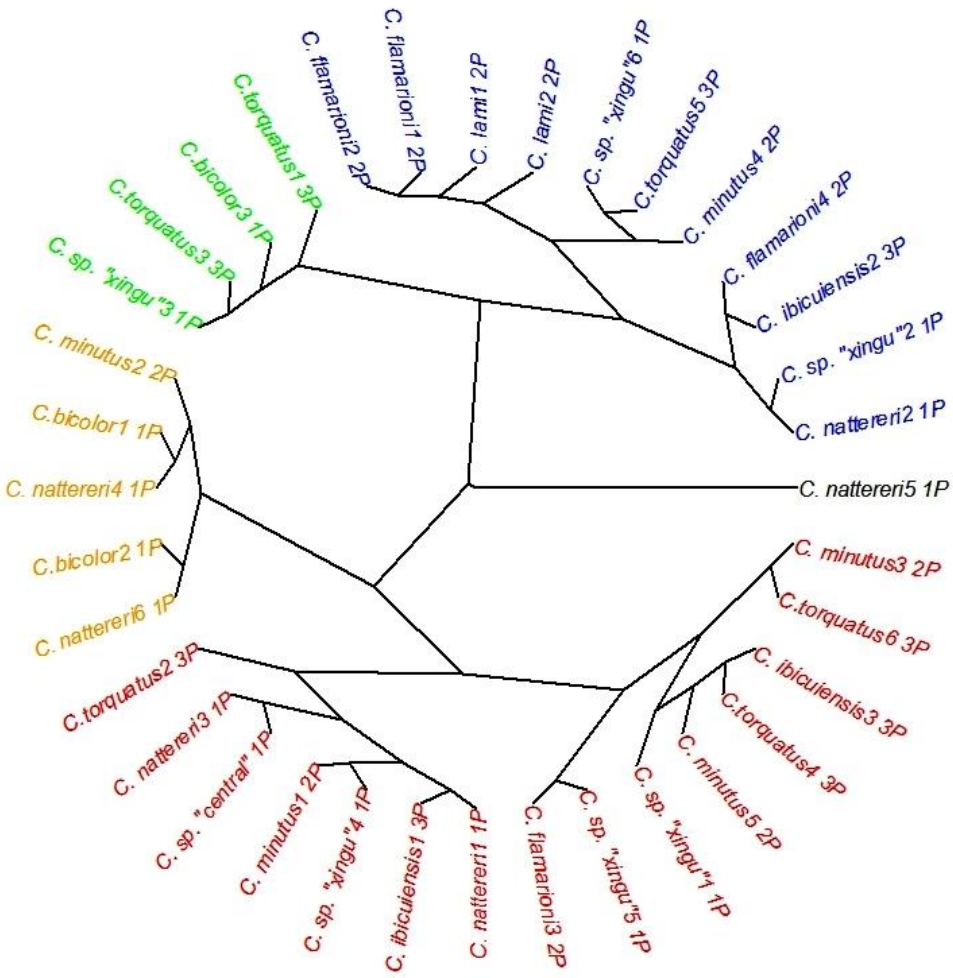

Hierarchical clustering analyses looking for correlations among different species of *Ctenomys* in relation to studied dimension (Face and Nose measurements) obtained by the standardization of Oc-Pat and CBL for each skull.

Appendix III

List of individuals used in this study, their populations, species and species groups (*sensu* Parada *et al.*, 2011 in the case of *Ctenomys*), collection numbers and GenBank accession numbers.

Individual	Population	Species	Species group	Collection No.	Accession No.
CA_06_01	Cáceres - MT	*C. nattereri*	*boliviensis*	TR1429	
CA_07_02	Cáceres - MT	*C. nattereri*	*boliviensis*	TR1430	
CA_08_03	Cáceres - MT	*C. nattereri*	*boliviensis*	TR1431	
CA_09_04	Cáceres - MT	*C. nattereri*	*boliviensis*	TR1432	
SP_77_04	Sapezal - MT	*C. nattereri*	*boliviensis*	TR1871	
SP_78_05	Sapezal - MT	*C. nattereri*	*boliviensis*	TR1872	
NO_50_11	Nova Olimpia - MT	*C.* sp. xingu	*boliviensis*	TR1449	
NU1_31_01	Nova Ubiratã 1 - MT	*C.* sp. xingu	*boliviensis*	TR1453	
NU1_32_02	Nova Ubiratã 1 - MT	*C.* sp. xingu	*boliviensis*	TR1454	
NU1_33_03	Nova Ubiratã 1 - MT	*C.* sp. xingu	*boliviensis*	TR1455	
NU2_56_05	Nova Ubiratã 2 - MT	*C.* sp. xingu	*boliviensis*	TR1475	
FN_67_03	Feliz Natal - MT	*C.* sp. xingu	*boliviensis*	TR1834	
NM_84_04	Nova Mutum - MT	*C.* sp. central	*boliviensis*	TR1878	
PB_40_01	Pimenta Bueno - RO	*C. bicolor*	*boliviensis*	TR1819	
PB_41_02	Pimenta Bueno - RO	*C. bicolor*	*boliviensis*	TR1820	
PB_42_03	Pimenta Bueno - RO	*C. bicolor*	*boliviensis*	TR1821	
TR906	Torquato Severo - RS	*C. torquatus*	*torquatus*	TR906	
TR910	Torquato Severo - RS	*C. torquatus*	*torquatus*	TR910	
TR1403	Dom Pedrito - RS	*C. torquatus*	*torquatus*	TR1403	
TR1068	Manuel Viana - RS	*C. ibicuiensis*	*torquatus*	TR1068	
TR1069	Manuel Viana - RS	*C. ibicuiensis*	*torquatus*	TR1069	
TR1070	Manuel Viana - RS	*C. ibicuiensis*	*torquatus*	TR1070	
TR344	Fazenda dos Freitas - RS	*C. lami*	*torquatus*	TR344	

TR202	Coxilha das Lombas -RS	*C. lami*	*torquatus*	TR202	
TR30	Cidreira - RS	*C. flamarioni*	*mendocinus*	TR30	
TR45	Praia do Barco - RS	*C. flamarioni*	*mendocinus*	TR45	
TR65	Faz Caçapava e Taim - RS	*C. flamarioni*	*mendocinus*	TR65	
TR203	Solidão - RS	*C. flamarioni*	*mendocinus*	TR203	
TR 05	Jaguaruna	*C. minutus*	*torquatus*	TR 05	
TR 35	Tramandai - RS	*C. minutus*	*torquatus*	TR 35	
TR 38	Tramandai - RS	*C. minutus*	*torquatus*	TR 38	
TR 41	Praia do Barco - RS	*C. minutus*	*torquatus*	TR 41	
TR 46	Praia do Barco - RS	*C. minutus*	*torquatus*	TR 46	
O. degus			-	-	XM012515902
mRNA 1	-	*O. degus*			
O. degus			-	-	XM012515909
mRNA 2	-	*O. degus*			
O. degus	-	*O. degus*	-	-	XM012515913
mRNA 4					
O. degus	-	*O. degus*	-	-	XM012515918
mRNA 5					
O. degus	-	*O. degus*	-	-	XM012515919
mRNA 6					
M. musculus	-	*M. musculus*	-	-	NM001271627
mRNA 4					

Considerações finais

A realização desse estudo foi importante para a avaliação de aspectos morfológicos evolutivos de espécies do gênero *Ctenomys*. Ele forneceu evidencias de que houveram alterações (*e.g.* diferenças nos padrões e modularidade) ao longo do tempo, na morfologia das espécias aqui testadas. Logo, proporcionando novos resultados que são de fundamental importância para melhor compreensão do gênero.

Quando foi verificada a correlação entre a morfologia do crânio e mandíbula, foi revelado que espécies com maior força de mordida geralmente habitam solos com maior densidade. A relação entre a força de mordida e a densidade do solo não mostrou-se clara, e houve baixa correlação geral para a maioria das espécies. A força de mordida geralmente foi associada com a forma do crânio (r=0,60). Também verificamos a ocorrência de espécies com força de mordida alta e baixa em solos mais densos e em solos com menor desidade apenas espécies com baixa força de mordida. A varição dos métodos de escavação (*e.g.* cinzel, membros posteriores e anteriores) (Hildebrand, 1985; Hildebrand, 1998, Stein, 2000), podem estar envolvidas com esse padrão.

Ao avaliarmos e compararmos os padrões e magnitudes de integração morfológica em espécies morfologicamente diversas do gênero *Ctenomys*, decobrimos que não houveram mudanças significativas. A integração morfológica variou bastante entre os tuco-tucos, seguindo o padrão já encontrado para mamíferos (Porto et al., 2009). Boa parte da magnitude de integração pode ser atribuída a variação do tamanho. Quando investigamos a covariação dos valores de CR e a forma do crânio encontramos correlacão significativa apenas com dois módulos propostos para o crânio com o tamanho corrigido. As relações filogenéticas correlacionadas com os padrões de modularidade demonstram que possivelmente em conjunto com a evolução do grupo, também houve evolução da modularidade dos crânios.

E por fim, quando foi explorada a relação entre o gene Runx 2 e o comprimento do crânio, não encontramos correlação entre ambos, resultado semelhante ao de Pointer (et. al., 2012). Também encontramos alterações nas repetições do gene, onde Glutaminas foram alteradas para Prolinas. O que possivelmente pode alterar a funcionalidade das proteínas desregulando a funcionalidade do gene (Mundlos et al., 1997; Otto et al., 2002; Hansen et al., 2011; Jaruga et al., 2016). Porém, não podemos afirmar que a substituição de Glutaminas por Prolinas tenha atuado interferindo no comprimento do crânio.

Em síntese, está tese possui grande significância para melhor entendimento da morfologia do gênero *Ctenomys*. Este trabalho remete a novas perspectivas, onde: 1)

Verificar como o desenvolvimento muscular do crânio pode intervir na força de mordida e métodos de escavação, bem como, os diferentes métodos de escavação podem vir a intervir na força de mordida e morfologia; 2) Estudos futuros podem investigar como o ambiente e as relações filogenéticas interferem na mordularidade do crânio; 3) A avalição de outros genes relacionados ao crescimento/alongamento facial (*e.g.* genes Hox).

Referencias
(De acordo com as normas do periódico *Zoological Journal of the Linnean Society*)

Ackermann, RR, Cheverud, JM. 2000. Phenotypic covariance structure in tamarins (genus *Saguinus*): A comparison of variation patterns using matrix correlation and common principal component analysis. *American Journal of Physical Anthropology* **111:** 489–501.

Anderson S, Yates, TL, Cook, JA. 1987. *Notes on Bolivian mammals* 4: The genus *Ctenomys* (Rodentia: Ctenomyidae) in the eastern lowlands. American Museum Novitates.

Atchley, WR, Hall, BK. 1991. A model for development and evolution of complex morphological structures. *Biological Reviews of the Cambridge Philosophical Society* **66:**101-57.

Berg, RL. 1960. The ecological significance of correlation pleiades. *Evolution*. **14:** 171-180.

Bidau CJ. 2015. Family Ctenomyidae. In Patton, J.L., Pardiñas, U.F.J. & D'Elía, G. *Mammals of South America Vol. 2: Rodents*. The University of Chicago Press Books.

Cardini A, Polly, PD. 2013. Larger mammals have longer faces because of size-related constraints on skull form. *Nature Communications* **4:** 24-58.

Becerra, F, Echeverría, A, Vassallo, AI. 2011. Bite force and mandible biomechanics in the subterranean rodent Talas tuco-tuco (*Ctenomys talarum*) (Caviomorpha Octodontoidea). *Canadian Journal of Zoology* **89:** 334-342.

Becerra, F, Echeverría, AI, Casinos, A, Vassallo, AI. 2014. Another one bites the dust: Bite force and ecology in three caviomorph rodents (Rodentia, Hystricognathi). *Journal of Experimental Zoology Part A* **321:** 220–232.

Begall, S, Burda, H, Schleich, CE. 2007. *Subterranean rodents: news from underground.* Berlin: Springer Verlag.

Bookstein, FL. 1989. Principal warps: thin-plate splines and the decomposition of deformations. *IEEE Transactions on Pattern Analysis and Machine Intelligence* **11:** 567–585.

Borges LR, Maestri R, Kubiak BB, Galiano D, Fornel R, Freitas TRO. 2017. The role of soil features in shaping the bite force and related skull and mandible morphology in the subterranean rodents of genus Ctenomys (Hystricognathi: Ctenomyidae). *Journal of Zoology* **301:** 108-117.

Busch, C, Antinuchi, JC, Del Valle, MJ, Kittlein, AI, Malizia, AI, Zenuto RR. 2000. *Population ecology of subterranean rodents.* in: Lacey, E.A., Patton, J.L. & Cameron G.N., eds.) The University of Chicago Press, Chicago, Illinois.

Castillo AH, Cortinas MN, Lessa EP. 2005. Rapid diversification of south american tuco-tucos (Ctenomys; Rodentia, Ctenomyidae): Contrasting mitochondrial and nuclear intron suquences. *Journal of Mammalogy* **86:**170–179.

Cheverud, JM. 1982. Phenotypic, genetic, and environmental morphological integration in the cranium. *Evolution* **36:** 499–516.

Coffman JA. 2003. Runx transcription factors and the developmental balance between cell proliferation and differentiation. *Cell Biology International* **27:** 315–324.

Cook, JA, Anderson, S, Yates, TL. 1990. Notes on Bolivian mammals. The genus *Ctenomys* (Rodentia Ctenomidae) in the highlands. American Museum novitates **2980:** 20–27.

Del Valle, JC, Lohfelt, M, Comparatore, MS, Busch, C. 2001. Feeding selectivity and food preference of *Ctenomys talarum* (tuco-tuco). *Journal of Mammalian Biology* **66:** 165-173.

D'Elía, G, Lessa, EP, Cook, JA. 1999. Molecular phylogeny of tuco-tucos, genus *Ctenomys* (Rodentia, Octodontidae): Evaluation of the mendocinus species group and the evolution of asymmetric sperm. *Journal of Mammalian Evolution* **6:** 19-38.

Falconer, DS; Mackay, TFC. 1996. *Introduction to quantitative genetics.* Longman Group Limited, 4.ed. Edinburgh.

Freitas, TRO, Fernandes, FA, Fornel R, Roratto PA. 2012. An endemic new species of tuco-tuco, genus *Ctenomys* (Rodentia: Ctenomyidae), with a restricted geographic distribution in southern Brazil. *Journal of Mammalogy* **93:** 1355-1367.

Freitas, TRO. 2016. *Family Ctenomyidae (Tuco-tucos). Handbook of the Mammals of the World Volume 6 Lagomorphs and Rodents I.* In: Don E. Wilson; Thomas E. Lacher, Jr; Russell A. Mittermeier. (Org.). 6ed.Barcelona: Lynx Edicions Publications.

Gardner SL, Salazar-Bravo J, Cook JA. 2014. New species of *Ctenomys* (Rodentia: Ctenomyidae) from the lowlands and central valleys of Bolivia. *Special Publication, Museum of Texas Tech University* **62:**1-34.

Goswami, A. 2006. Morphological integration in the carnivoran skull. Evolution: International. *Journal of Organic Evolution* **60:** 169–183.

Hansen, L, Riis, AK; Silahtaroglu, A; Hove, H; Lauridsen, E; Eiberg, H; Kreiborg, S. 2011. RUNX2 analysis of Danish cleidocranial dysplasia families. *Clinical Genetics* **79:** 254–263.

Jaruga, A; Hordyjewska, E; Kandzierski, G; Tylzanowski, P. 2016. Cleidocranial dysplasia and RUNX2-clinical phenotype–genotype correlation. *Clinical Genetics* **90:** 393-402.

Hildebrand, M. 1985. Digging of quadrupeds. In *Functional vertebrate morphology*. Edited by M. Hildebrand, M. Bramble, K.F. Liem, & D.B. Wake. The Belknap Press of Harvard University Press, Cambridge, Mass.

Hildebrand, M. 1998. *Analysis of Vertebrate Structure*. 5th ed. New York: Wiley.

Kashi, Y, King, DG. 2006. Simple sequence repeats as advantageous mutators in evolution. *Trends in Genetics* **22:** 253–9.

Jung, YJ, Bae, HS, Ryoo, HM, Baek, SH. 2017. A novel RUNX2 mutation in exon 8, G462X, in a patient with Cleidocranial Dysplasia. *Journal of Cellular Biochemistry* **119:**1152-1162.

Kim, D, Yukl, ET, Moënne-Loccoz, P, Montellano, PR. 2006. Fungal heme oxygenases: Functional expression and characterization of Hmx1 from Saccharomyces cerevisiae and CaHmx1 from Candida albicans. *Biochemistry* **45:**14772-14780.

King, DG, Soller, M, Kashi, Y. (1997). Evolutionary tuning knobs. *Endeavour.* **21:**36–40.

Koyabu, D, Werneburg, I, Morimoto, N, Zollikofer, CPE, Forasiepi, AM, Endo, H, Kimura, J, Ohdachi SD, Son, NT., Sánchez-Villagra MR. 2014. Mammalian skull heterochrony reveals modular evolution and a link between cranial development and brain size. *Nature Communications* **5:** 3625.

Kubiak, BB, Maestri, R, Almeida, TS, Borges, LR, Galiano, D, Fornel, R, Freitas, TRO. 2018. Evolution in action: soil hardness influences morphology in a subterranean rodent (Rodentia: Ctenomyidae). *Biological Journal of the Linnean Society* XX: 1–11.

Lacey, EA, Patton, JL, Cameron, GN. 2000. *Life Underground.* The University of Chicago Press, Chicago and London.

Lacher, TE, Murphy, WJ, Rogan, J, Smith, AT, Upham, NS. 2016. Evolution, phylogeny, ecology, and conservation of the Clade Glires: Lagomorpha and Rodentia. *Handbook of Mammals of the World, Volume 6: Lagomorphs and Rodents* (ed. by D.E. Wilson, J.T.E. Lacher and R.A. Mittermeier), Lynx Ediciones, Barcelona.

Lessa EP, Cook, JA. 1998. The molecular phylogenetics of tuco-tucos (genus *Ctenomys*, Rodentia: Octodontidae) suggests an early burst of speciation. Molecular Phylogenetics and Evolution **9:** 88-99.

Levanon, D, Negreanu, V, Bernstein, Y, Bar-Am, I, Avivi, L, Groner,Y. 1994. AML1, AML2, and AML3, the human members of the runt domain gene-family: cDNA structure, expression, and chromosomal localization. *Genomics* **23:** 425–432.

Levanon, D, Brenner, O, Otto, F, Groner, Y. 2003. Runx3 knockouts and stomach cancer *EMBO Reports* **4:** 560–564.

Lund, AH, Van-Lohuizen, M. 2002. RUNX: a trilogy of cancer genes. *Cancer Cell* **1:** 213–215.

Maestri, R, Fornel, R, Gonçalves, GL, Geise, L, Freitas, TRO., Carnaval, AC. 2016. Predictors of intraspecific morphological variability in a tropical hotspot: comparing the influence of random and non-random factors. *Journal of Biogeography* **43:** 2160–2172.

Marcy, AE, Hadly, EA, Sherratt, E, Garland, K, Weisbecker, V. 2016. Getting a head in hard soils: Convergent skull evolution and divergent allometric patterns explain shape variation in a highly diverse genus of pocket gophers (*Thomomys*). *BMC Evolutionary Biology* **16:** 207.

Marroig, G, Cheverud, JM. 2001. A comparison of phenotypic variation and covariation patterns and the role of phylogeny, ecology, and ontogeny during cranial evolution of New World Monkeys. *Evolution* **55:** 2576-2600.

Marroig G, Cheverud, JM. 2005. Size as a line of least evolutionary resistance: Diet and adaptive morphological radiation in new world monkeys. *Evolution* **59:** 1128-1142.

Mitteroecker, P, Bookstein, F, 2008. The evolutionary role of modularity and integration in the hominoid cranium. *Evolution* **62:** 943–958.

Moore, WJ. 1981. *The mammalian skull.* Cambridge: Cambridge University Press.

Mundlos, S, Otto, F, Mundlos, C, Mulliken, JB, Aylsworth, AS, Albright, S, Lindhout, D, Cole, WG, Henn, W, Knoll, JHM, Owen, MJ, Mertelsmann, R, Zabel, BU, Olsen, BR. 1997. Mutations involving the transcription factor CBFA1 cause cleidocranial dysplasia. *Cell Press* **89:** 773-779.

Nevo, E. 1979. Adaptive convergence and divergence of subterranean mammals. *Annual Review of Ecology, Evolution, and Systematics* **10:** 269–308.

Newton, AH, Feigin, CY, Pask, AJ. 2017. RUNX2 repeat variation does not drive craniofacial diversity in marsupials. *BMC Evolutionary Biology* 17:110

Nowak, RM. 1999. *Walker's Mammals of the World.* 6th ed. Baltimore (MD): The Johns Hopkins University Press.

Olson, EC, Miller, RL. 1951. A mathematical model applied to a study of the evolution of species. *Evolution: International Journal of Organic Evolution* **5:** 325–338.

Olson, EC, Miller, RL. 1958. *Morphological integration.* Chicago: University of Chicago Press.

Ott, CE, Leschik, G, Trotier, F, Brueton, L, Brunner, HG, Brussel, W, Guillen-Navarro, E, Haase, C, Kohlhase, J, Kotzot, D, Lane, A, Lee-Kirsch, MA, Morlot, S, Simon, MEH, Steichen-Gersdorf, E, Tegay, DH, Peters, H, Mundlos, S, Klopocki, E. 2010. Deletions of the RUNX2 gene are present in about 10% of individuals with cleidocranial dysplasia. *Human Mutation* **31:** 1587-1593.

Otto, F, Thornell, AP, Crompton, T, Denzel, A, Gilmour, KC, Rosewell, IR, Stamp, GW, Beddington, RS, Mundlos, S, Olsen, BR, Selby, PB, Owen, MJ. 1997. Cbfa1, a

candidate gene for cleidocranial dysplasia syndrome, is essential for osteoblast differentiation and bone development. *Cell.* **5:**765-71.

Otto, F; Kanegane, H; Mundlos, S. 2002. Mutations in the RUNX2 Gene in Patients With Cleidocranial Dysplasia. *Human mutation* **19:** 209-216.

Parada, A, D'elia, G, Bidau., C, Lessa, LP. 2011. Species groups and the evolutionary diversification of tuco-tucos, genus *Ctenomys (*Rodentia: Ctenomyidae). *Journal of Mammalogy* **91:** 1313-1321.

Pavlicev, MJP, Kenney-Hunt, EA, Norgard, CC, Roseman, JBW, Cheverud, JM. 2008. Genetic variation in pleiotropy: Differential epistasis as a source of variation in the allometric relationship between long bone lengths and body weight. *Evolution* **62:** 199-213.

Pearson, O, Binsztein, LB, Busch, C, Di Pace, M, Gallopin, G, Penchaszadeh, P, Piantanida, M. 1968. Estructura social, distribuicion espacial y composicion por edaddes de una población de tuco-tucos (*Ctenomys talarum*). *Invest Zoo Chile* **13:** 47-80.

Pelassa, I, Corà, D, Cesano, F, Monje, FJ, Montarolo, PG, Fiumara, F. 2014. Association of polyalanine and polyglutamine coiled coils mediates expansion disease-related protein aggregation and dysfunction. *Human Molecular Genetics* **23:** 3402–20.

Peres-Neto, PR. 1995. *Oecologia Brasiliensis.* Tópicos em Tratamento de Dados Biológicos.

Pointer, M, Kamilar, JM, Warmuth, VSGBC, Delsuc, F, Mundy, NI. 2012. RUNX2 tandem repeats and the evolution of facial length in placental mammals. *BMC Evolutionary Biology* **12:** 103.

Porto A, Oliveira FB, Shirai LT, Conto V, Marroig G. 2009. The Evolution of Modularity in the Mammalian Skull I: Morphological Integration Patterns and Magnitudes. *Evolutionary Biology* **36:** 118–135.

Quack, I, Vonderstrass, B, Stock, M, Avlsworth, AS, Becker, A, Brueton, L, Lee, PJ, Majewski, F, Mulliken, JB, Suri, M, Zenker, M, Mundlos, S, Otto, F. 1999. Mutation analysis of core binding factor A1 in patients with cleidocranial dysplasia. *American Journal of Human Genetics* **65:** 1268-1278.

Raff, RA. 1996. *The Shape of Life: Genes, Development and the Evolution of Animal Form.* University of Chicago Press.

Reig, AO, Busch, C, Ortellis, MO, Contreras, JL. 1990. An overview of evolution, systematica, population biology and molecular biology in *Ctenomys*. In: Nevo, E.; Reig, O.A. (eds) *Biology of subterranean mammals at the organismal and molecular levels.* New York, Allan Liss.

Rennert, J, Coffman, JA, Mushegian, AR, Robertson, AJ. 2003. *BMC Evolutionary Biology* **3:** 4.

Reznick, DN, Ricklefs, RE. 2009. Darwin's bridge between microevolution and macroevolution. *Nature* **457:** 837-842.

Ridley, M. 2006. *Evolução.* 3Ed. Porto Alegre, Artmed.

Ritzman, T., Banovich, N, Buss, K, Guida, J, Rubel, MA, Pinney, J. 2017. Facing the facts: Changes in the Runx2 gene modulates facial morphology in primates. *Journal of Human Evolution* **111:** 139-151.

Rohlf, FJ, Marcus LF, 1993. A revolution in morphometrics. *Trends in Ecology and Evolution* **8:** 129-132.

Rohlf, FJ. 1999. Shape statistics: Procrustes superimpositions and tangent spaces. *Journal of Classification* **16:** 197-223.

Rosi, M, Cona, M, Videla, F, Puig, S, Roig, VG. 2000. Architecture of *Ctenomys mendocinus* (Rodentia) burrows from two habitats differing in abundance and complexity of vegetation. *Acta Theriologica* **45:** 491-505.

Schluter, D. 1996. Adaptive radiation along genetic lines of least resistance. *Evolution* **5:** 1766-1774.

Sears, KE, Goswami, A, Flynn, JJ, Niswander, LA. 2007. The correlated evolution of Runx2 tandem repeats, transcriptional activity, and facial length in carnivora. *Evolution & Development* **9:** 555–565.

Slamovits, CH, Cook, JA, Lessa EP, Rossi, MS. 2001. Recurrent amplification and deletions of satellite DNA accompanied chromosomal diversification in south American tuco-tucos (genus *Ctenomys*, Rodentia: Octodontidae): *A phylogenetic approach. Molecular Biology and Evolution* **18:** 1708–1719.

Smith, KK. 1997. Comparative patterns of craniofacial development in Eutherian and Metatherian mammals. *Evolution* **51:** 1663–1678.

Stein, B. 2000. Morphology of subterranean rodents. In *Life underground: the biology of subterranean rodents.* Lacey, E. A., J. L. Patton, and G. N. Cameron. University of Chicago Press. Chicago, Illinois.

Thirunavukkarasu, K, Mahajan, M, McLarren, KW, Stifani, S, Karsenty, G. 1998. Two domains unique to osteoblast-specific transcription factor Osf2/Cbfa1 contribute to its transactivation function and its inability to heterodimerize with Cbfbeta. *Molecular and Cellular Biology* **18:** 4197–208.

Trevisan, B, Carvalho CA, Loboda, TS. 2017. Processos evolutivos e sistemática. In: *Tópicos de pesquisa em Zoologia.* Instituto de Biociências, Universidade de São Paulo.

Verzi, DH. 2008. Phylogeny and adaptive diversity of rodents of the family Ctenomyidae (Caviomorpha): delimiting lineages and generain the fossil record. *Journal of Zoology* **274:** 386–394.

Wagner, GP, Altenberg, L. 1996. Perspective: Complex adaptations and the evolution of evolvability. *Evolution* **50:** 967-976.

Wagner, GP, Pavlicev, M, Cheverud, JM. 2007. The road to modularity. *Nature Reviews Genetics* **8:** 921–931.

Wagner, GP, Kenney-Hunt, JP, Pavlicev, M, Peck, JR, Waxman, D, Cheverud JM. 2008. Pleiotropic scaling of gene effects and the 'cost of complexity'. *Nature* **452:** 470–473

Williams, BA, Kay, RF, Kirk, EC. 2010. New perspectives on anthropoid origins. *Proceedings of the National Academy of Sciences* **107:** 4797–804.

Zhang, T, Tan, P, Wang, L, Jin, N, Li, Y, Zhang, L, Yang, H, Hu, Z, Zhang, L, Hu, C, Li, C, Qian, K, Zhang, C, Huang, Y, Li, K, Lin, H, Wang, D. 2017. RNALocate: a resource for RNA subcellular localizations. *Nucleic Acids Research* **45:** 135-138.

Ziros, PG, Basdra, EK. 2008. Papavassiliou AG. Runx2: of bone and stretch. *International Journal of Biochemistry & Cell Biology* **40:**1659–1663.

Zhou, G, Chen, Y, Zhou, L, Thirunayukkarasu, K, Hecht, J, Chitayat, D, Gelb, BD, Pirinen, S, Berry, SA, Greenberg, CR, Karsenty, G, Lee, B. 1999. CBFA1 mutation analysis and functional correlation with phenotypic variability in cleidocranial dysplasia. *Human Molecular Genetics* **8:** 2311-2316.

Zhang, YW, Bae, SC, Takahashi, E, Ito, Y. 1997. The cDNA cloning of the transcripts of human PEBP2alphaA/CBFA1 mapped to 6p12.3-p21.1, the locus for cleidocranial dysplasia. *Oncogene* **15:** 367–371.

Zenuto, R, Busch, C. 1995. Influence of the subterranean rodent *Ctenomys australis* (Tuco-tuco) in a sand-dune grassland. *Journal of Mammalian Biology* **60:** 277-285.

Anexo I
Manuscrito publicado no periódico Journal of Zoology

Journal of Zoology

Journal of Zoology. Print ISSN 0952-8369

The role of soil features in shaping the bite force and related skull and mandible morphology in the subterranean rodents of genus *Ctenomys* (Hystricognathi: Ctenomyidae)

L. R. Borges[1], R. Maestri[2], B. B. Kubiak[1], D. Galiano[3], R. Fornel[4] & T. R. O. Freitas[5]

1 Programa de Pós-Graduação em Biologia Animal, Universidade Federal do Rio Grande do Sul, Porto Alegre, RS, Brazil
2 Programa de Pós-Graduação em Ecologia, Universidade Federal do Rio Grande do Sul, Porto Alegre, RS, Brazil
3 Programa de Pós-Graduação em Ciências Ambientais, Universidade Comunitária da Região de Chapecó, Chapecó, SC, Brazil
4 Programa de Pós-Graduação em Ecologia, Universidade Regional Integrada do Alto Uruguai e das Missões, Erechim, RS, Brazil
5 Departamento de Genética, Universidade Federal do Rio Grande do Sul, Porto Alegre, RS, Brazil

Keywords
functional morphology; geometric morphometrics; morphological evolution; phylogenetic comparative methods; rodent skull; soil hardness; subterranean niche; tuco-tucos.

Correspondence
Leandro Rodrigues Borges, Programa de Pós-Graduação em Biologia Animal, Universidade Federal do Rio Grande do Sul, Porto Alegre, RS, Brazil
Email: lborgesbiologia@gmail.com

Editor: Andrew Kitchener

Received 17 May 2016; revised 15 July 2016; accepted 24 August 2016

doi:10.1111/jzo.12398

Abstract

For rodents that live underground, digging in highly compacted soils requires a higher energy expenditure than digging in poorly compacted soils. We tested how soil hardness affects the bite force as well as the shape and size of the skulls and mandibles of tuco-tucos. Our hypothesis is that species that inhabit harder soils would show a stronger bite force, which should be reflected in the shape of the skull and mandible, while species living in softer soils should have a weaker bite force. We used 24 species of the genus *Ctenomys* to estimate bite force (through the incisor strength formula) and quantify the shape and size of the skull and mandible. Information on soil bulk density in the regions occupied by each species was obtained from the literature. We used a combination of geometric morphometric and comparative methods to test our hypothesis. A phylogenetic linear regression (PGLS) between bite force (N) and centroid size was used to account for the dependence of bite force on size. We employed a series of two-block partial least-squares analyses to uncover the covariation between bite force and the shape of the skull and mandible. Finally, we ran five independent PGLS analyses to assess the influence of bulk density on bite force, skull shape and mandible shape, taking into account phylogenetic non-independence. Species with higher bite forces tend to inhabit more-compact soils. However, for most species, the relationship between bite force and soil bulk density was unclear, resulting in a low overall correlation. Nonetheless, differences in skull and mandible shapes were generally associated with bite force ($r = 0.60$). In denser soils, species with high and low bite forces occur, whereas in lower density soils, we found only species with weak bite forces. Differences in the excavation strategies among species may be responsible for this pattern.

Introduction

Knowledge of the factors that guide morphological diversification is of great interest for evolutionary biology (Wainwright, 2007; Diniz-Filho *et al.*, 2009). The morphological variation among species is influenced mainly by two factors, ecology (e.g. environmental variables, biotic interactions) and evolutionary history (Viguier, 2002; Caumul & Polly, 2005; Wiens & Graham, 2005). The ecomorphological concept assumes that a correlation exists between the morphology and the ecology of organisms; that is, the mechanical demands imposed by ecological traits can be reflected in morphological changes in the system involved (Huey, Hertz & Sinervo, 2003; Carrizo, Tulli & Abdala 2014). Mammals possess a variety of body forms, which are often considered to be specific adaptations for specific environments and particular ways of life (Hildebrand, 1985; Biewener, 2003; Carrizo, Tulli & Abdala 2014). Simultaneously, the history of lineages contributes to maintain phylogenetically close species with similar niche characteristics. This phylogenetic niche conservatism is accentuated in small-range mammals living in the tropics (Cooper, Freckleton & Jetz, 2011).

Subterranean rodents have been extensively studied, particularly because they show many specializations (morphological, physiological and behavioral) related to their habitat (Nevo, 1999; Begall, Burda & Schleich, 2007). The genus *Ctenomys* (tuco-tucos) is the most diverse among subterranean rodents (Lacey, Patton & Cameron, 2000). The approximately 70

described species (Gardner, Salazar-Bravo & Cook, 2014; Bidau, 2015) are widely distributed across southern South America. They occupy a wide range of habitat types, especially in open areas including grasslands, steppes, deserts and sand dunes (Redford & Eisenberg, 1992; Bidau, 2006). A few species occur in forest regions (Gardner *et al.*, 2014). These open environments differ widely in the hardness and compaction of the soil, as well as in the amount of resources available. These soil features may influence some aspects of the biology of subterranean rodents (e.g. burrow system characteristics and excavation strategies) (Reichman, Whitham & Ruffner, 1982; Heth, 1989; Rosi *et al.*, 2000; Becerra, Echeverría & Vassallo, 2011; Becerra *et al.*, 2014; Lövy *et al.*, 2015).

Species of *Ctenomys* possess a range of morphological adaptations for digging, which evolved over the last 15 million years after the group separated from its sister family Octodontidae (Lessa *et al.*, 2008). The tuco-tucos, as well as some other subterranean rodents, use their mandibles and incisors to excavate the soil and to sever roots (Hildebrand, 1985; Nevo, 1999). The excavation process involves a high physiological cost, which increases in more-compact soils (Luna & Antinuchi, 2006). The upper incisors of subterranean species are more similar to a chisel than are the incisors of species that inhabit the surface. Excavation using chisel-like teeth is described by some authors as executed primarily by the upper incisors, which break up the soil, while the lower incisors mainly move the soil (Hildebrand, 1998). By acting as a tool, applying a strong force in a restricted area, the incisors are closely involved in the excavation process (Hildebrand, 1998; Stein, 2000), helping to break up the substrate and open the way by cutting roots, tubers and the soft parts of plants (Stein, 2000). However, the differences in excavation strategies among species, and the degree to which each species is affected by the soil that it inhabits, remain largely unexplored (Hildebrand, 1998; Stein, 2000).

In view of the empirical association between soil features and the morphology of subterranean species (Mora, Olivares & Vassallo, 2003; Lessa *et al.*, 2008), we tested how soil hardness affects the bite force as well as the shape and size of the skulls and mandibles of tuco-tucos. The incisor section modulus, a geometrical parameter proportional to bending strength, may be useful for prediction of bite force when direct measurements are not available (Freeman & Lemen, 2008), and was the index used in this study. Our hypothesis is that species that inhabit harder soils would show a stronger bite force, which should be reflected in the shape of the skull and mandible of individuals, while species living in softer soils would have a weaker bite force.

Materials and methods

Sample

We measured the bite force of 167 individuals belonging to 24 species of the genus *Ctenomys* (Supporting Information Appendix S1), deposited in the Recent mammal collection of the Field Museum of Natural History, Chicago, Illinois, USA, and in the Departamento de Genética, Universidade Federal do Rio Grande do Sul, Porto Alegre, Brazil. Only adult specimens were considered: juveniles were identified by their small skulls and were excluded. Additionally, we measured the shape and size of the skull and mandible of 1122 adult specimens for the same 24 species (Supporting Information Appendix S1). These are deposited in the following museums and scientific collections: Departamento de Genética, Universidade Federal do Rio Grande do Sul, Porto Alegre, Brazil (UFRGS); Museo Nacional de História Natural y Antropología, Montevideo, Uruguay (MUNHINA); Museo Argentino de Ciencias Naturales "Bernardino Rivadavia", Buenos Aires, Argentina (MACN); Museo de La Plata, La Plata, Argentina (MLP); Museo de Ciencias Naturales "Lorenzo Scaglia", Mar del Plata, Argentina (MMP); Museum of Vertebrate Zoology, University of California, Berkeley, USA (MVZ); American Museum of Natural History, New York, USA (AMNH); and Field Museum of Natural History, Chicago, USA (FMNH).

Bite force

The bite force was estimated for each individual by the method proposed by Freeman & Lemen (2008). We measured the length and width of the inferior incisor (anterior-posterior length and medial-lateral width, respectively), both taken at the base of the incisor. After taking the measurements, we applied the following formula: $(Zi = ((\text{anterior-posterior length})^2 \times (\text{medial-lateral width}))/6)$, where Zi is the index of incisor strength. This measure is highly correlated with direct measurements of bite force when measured *in vivo*, with a correlation coefficient of 0.96 (Freeman & Lemen, 2008). Bite force values were transformed to Newtons (N), using the regression equation of Freeman & Lemen (2008). See Supporting Information Appendix S2 for bite force values for each species. We then calculated an arithmetic mean of N values for all individuals in each species, and used the mean values for the species in the subsequent analyses.

Geometric morphometrics

Images of each skull in the dorsal, ventral and lateral views, and of the lateral view of the mandible were taken with a digital camera with 3.1 megapixels (2048 × 1536) resolution, in macro function and without flash or zoom. On each image, 29 landmarks (Supporting Information Appendix S3) were digitalized in the dorsal view (Fig. 1a), 30 in the ventral view (Fig. 1b), and 21 in the lateral view of the skull (Fig. 1c) (Fernandes *et al.*, 2009); and 13 were digitalized on the mandible (Fig. 1d) (Fornel, Cordeiro-Estrela & Freitas, 2010). The anatomical landmarks were digitized using the TPSDig2 software version 2.17 (Rohlf, 2015). The resulting matrices of coordinates were superimposed through a Generalized Procrustes Analysis procedure (GPA), which removes the effects of scale, orientation and position. The size of each skull (Supporting Information Appendix S2) was assessed as the square root of the sum of the squares of the distance from each landmark to the centroid of the configuration (Bookstein, 1991), using only the ventral view. We assumed that sexual dimorphism is negligible for the present purposes because interspecific differences are usually greater than the reported sexual dimorphism in both the size and shape of the skull. The means

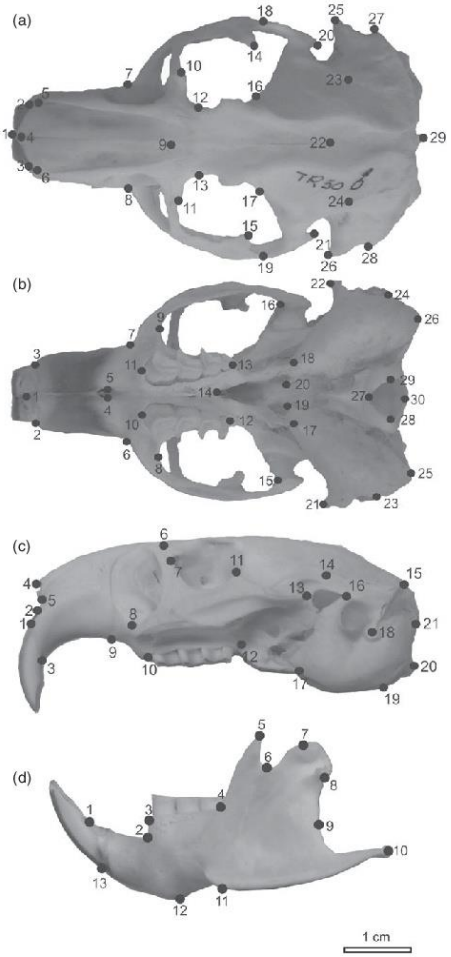

Figure 1 Landmarks used to capture shape from the dorsal, ventral and lateral views of the skull and left side of the mandible, as showed in *Ctenomys flamarioni*.

of shape and size were calculated for all individuals of each species, and used in the subsequent statistical analyses.

Soil compaction

The bulk density (http://soilgrids.org) was chosen as a measurement of soil compaction because it has a direct relationship with soil hardness, as more-compact soils have greater density (Freddi *et al.*, 2007; Reinert *et al.*, 2008; Gubiani, Reinert & Reichert, 2014). Hengl *et al.* (2014) constructed the soil bulk density variable (kg m^{-3}) by compiling previously published soil profile data and environmental layers, at 1-km resolution, and using regression-kriging interpolation at non-sampled locations. The depth at which soil bulk density was compiled by Hengl *et al.* (2014) ranged from 0 to 200 cm. We accessed the information on bulk density for each species using the geographical ranges available from the International Union for Conservation of Nature and Natural Resources (IUCN, 2008). For *Ctenomys minutus* and *Ctenomys ibicuiensis*, the distribution ranges were generated in ArcGIS 10.0 software, based on occurrence records available in the articles by Galiano *et al.* (2014) and Freitas *et al.* (2012), respectively. This was necessary because the information available from the IUCN for *C. minutus* was incorrect (see Galiano *et al.*, 2014 for details), and no information was available for the recently described *C. ibicuiensis*. The bulk density was extracted in ArcGIS 10.0 software for each pixel within the range of each species. Next, we calculated the mean densities of the pixels (mean density of soil) included in the distribution of each species, and used the mean density for each species in the subsequent analysis.

Statistical analyses

Phylogenetic relationships among species were based on the dated phylogenetic hypothesis presented by Freitas *et al.* (2012), pruned to cover the 24 species in our sample (Fig. 2). Details of the phylogenetic construction were described by Freitas *et al.* (2012). We used a phylogenetic generalized least-squares regression between bite force (log-transformed) and centroid size (log-transformed) to account for the dependence of bite force on size. Variables were log-transformed to assure normality and a linear relationship between variables. The phylogenetic covariance matrix used as the error term was based on the Brownian expectation (Grafen, 1989). We expected

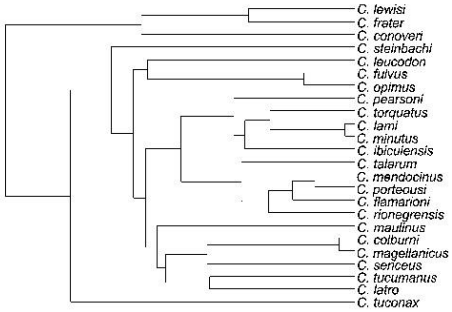

Figure 2 Phylogenetic relationships among species in the genus *Ctenomys*, based on molecular data (Freitas *et al.*, 2012). The original tree was edited to exclude species not investigated here.

larger bodied species to have stronger bites (e.g. Freeman & Lemen, 2008; Nogueira, Peracchi & Monteiro, 2009; Maestri *et al.*, 2016a). To estimate the bite force independently of size, we used the residuals of this regression as a bite force estimate in all subsequent analyses.

We employed a series of two-block partial least-squares analyses (2B-PLS) to find the maximum covariation between bite force and the shape of the skull (in dorsal, ventral and lateral views) and the mandible (Rohlf & Corti, 2000). The significance of this covariation was assessed through 10 000 permutations in MorphoJ 1.06d (Klingenberg, 2011). We then used the PLS shape vectors as new shape variables (because they covary with bite force) to assess the correlation between them and the bulk density, through a phylogenetic generalized least-squares (PGLS) approach as described above.

We ran five independent PGLS analyses to assess the effect of bulk density on bite force (size-corrected), skull shape (PLS shape vectors of dorsal, ventral, and lateral views) and mandible shape (PLS shape vector), taking into account phylogenetic non-independence (Grafen, 1989). The PGLS regressions were performed in the R software (R Core Team, 2016), with the *geomorph* package (Adams & Otárola-Castillo, 2013).

Results

Most of the variation in bite force data was explained by the variation in size: bite force is positively correlated with centroid size ($F_{1,22} = 155.4$; $r^2 = 0.87$; $P < 0.0001$) (Fig. 3). *Ctenomys lewisi*, *C. pearsoni*, *C. steinbachi* and *C. torquatus* showed a stronger bite force than expected for their size. Others including *C. colburni*, *C. ibicuiensis*, *C. magellanicus*, *C. maulinus*, *C. mendocinus*, *C. opimus* and *C. tuconax* showed a weaker bite than expected for their size, deviating from the allometric prediction downward (Fig. 3).

We found a weaker, although positive relationship between bite force and bulk density ($r^2 = 0.23$; Fig. 4a) and between bite force (size-corrected) and bulk density ($r^2 = 0.10$; Table 1; Fig. 4b). Some species, such as *C. lewisi* and *C. steinbachi*, with a stronger bite force, were associated with harder soils, while *C. magellanicus*, *C. maulinus* and *C. colburni*, with a weaker bite force, were associated with softer soils. However, most of the species showed less clear patterns of bite force in relation to bulk density. In general, lower values of bulk density were associated with low bite forces, but higher values of bulk density could be associated with both high and low values of bite force.

The PLS shape vectors derived for the dorsal and lateral views of the skull each showed a higher correlation with the residual bite force than would be expected based on chance (dorsal: $r = 0.64$; $P = 0.03$; lateral: $r = 0.76$; $P = 0.003$) (Figs 5a and 7a, respectively). However, the ventral views of the skull and the mandible did not show a significant correlation with the residual bite force (ventral: $r = 0.60$; $P = 0.07$; mandible: $r = 0.65$; $P = 0.055$), despite their relatively high correlations (Figs 6a and 8a, respectively).

The PGLS analysis showed a significant association between the PLS shape vectors of the dorsal, ventral and lateral views of the skull, and the bulk density of the soil (Table 1). However, the PLS shape vector of the mandible and the residual bite force did not show an association with bulk density (Table 1).

The shape changes described by the PLS shape vector derived from the skull data showed that negative values of residual bite force are associated with a lateral narrowing and lengthy rostrum (Figs 5b and 6b), a lateral narrowing of the

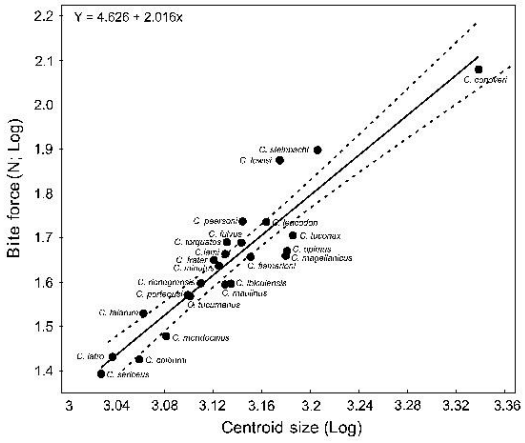

Figure 3 Regression analysis between the bite force (N = Newtons) and the centroid size (log) for 24 species of *Ctenomys*. The dashed lines represent 95% confidence intervals for the predicted line of the phylogenetic generalized least-squares regression.

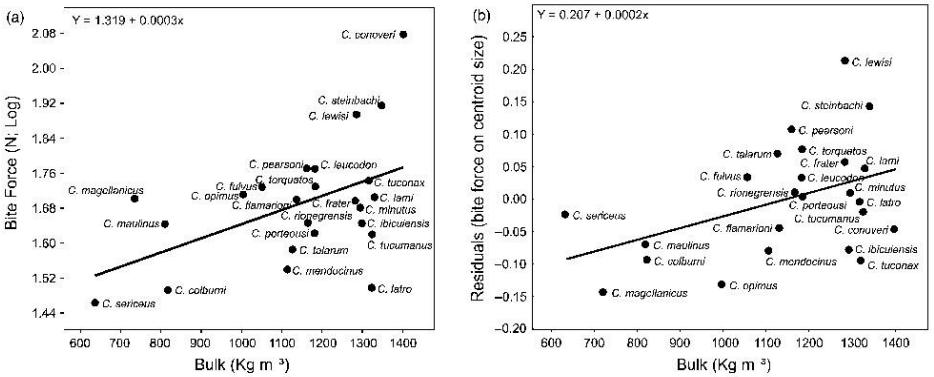

Figure 4 Regression of bite force (log Newtons) on soil bulk density $P = 0.01$ (a), and of bite force (residuals of bite force on centroid size) on soil bulk density $P = 0.03$ (b) for 24 species of *Ctenomys*.

Table 1 Phylogenetic regressions between residual bite forces and the shapes of the skull and mandible, with the soil bulk density of the 24 species of *Ctenomys* found in the Neotropical region

	F	R^2	*P*
Residual bite force			
Bulk	2.51	0.10	0.41
Dorsal PLS shape vector			
Bulk	11.04	0.33	0.001
Ventral PLS shape vector			
Bulk	9.45	0.30	0.001
Lateral PLS shape vector			
Bulk	8.30	0.27	0.001
Mandible PLS shape vector			
Bulk	0.086	0.003	0.874

zygomatic arch, and a perceptible expansion of the braincase (Fig. 7b). At the opposite end of the same shape vector, positive values of residual bite force are associated with a wider skull, especially in the rostrum (Figs 5c and 6c); a relative increase in the skull height (Fig. 7c); a more robust zygomatic arch, particularly in the anterior portion; and a wider interparietal region, as revealed by the convex lateral profile of the occipital (Fig. 7c). Regarding the mandible, negative values of residual bite force were associated with a smaller body of the mandible and a depressed coronoid process (Fig. 8b). Structures of the mandible associated with positive values of residual bite force included a larger condyloid process, a bigger body of the mandible, and a high coronoid process (Fig. 8c).

Discussion

For subterranean rodents, digging in harder soils demands a greater energy expenditure than digging in less-compacted soils, as found for *C. talarum* by Luna & Antinuchi (2006). In turn, increases in bite force are also probably necessary to couple with harder soils. Our study provided evidence that this relationship may affect rodents at a macroevolutionary level, where different species have different bite forces depending on the hardness of the soil that they occupy. Species with stronger bite forces (e.g. *C. conoveri*, *C. lewisi* and *C. steinbachi*) tend to inhabit more-compact soils. However, for most species, the relationship between bite force and bulk density was unclear, resulting in a low overall correlation.

The skull of subterranean rodents is generally more massive and robust than that of surface dwellers (Stein, 2000). The skull projections tend to be compressed to facilitate movement in the burrows (Nevo, 1979). These changes facilitate the process of excavation in a variety of soils, which may be hard or soft (Stein, 2000). The different ways used to dig (chisel teeth and raising the head) (Hildebrand, 1998) are reflected in the different cranial morphologies (Lessa & Thaeler, 1989). In this study, we found a covariation between bite force and skull shape: species with a wider skull and a more-robust mandible have a stronger bite force than species with an elongated and less wide skull and mandible, in agreement with other studies of mammals (Van Valkenburgh & Ruff, 1987; Christiansen & Adolfssen, 2005; Nogueira *et al.*, 2009; Maestri *et al.*, 2016a).

An important factor that restricts the shape and mechanics of the body is its size (Schmidt-Nielsen, 1984). *Ctenomys conoveri* inhabits a region with very compacted soil, although its skull and mandible are less robust according to the PLS analysis. However, the stronger bite force of *C. conoveri* can be explained by its larger body size, which generates sufficient force to dig in harder soil. This suggests that, during the course of evolution, *C. conoveri* did not change the shape of its skull and mandible to adapt to the more-compact soil, but might have changed its body size. Because variation in size is sometimes considered a more labile feature than shape, it is

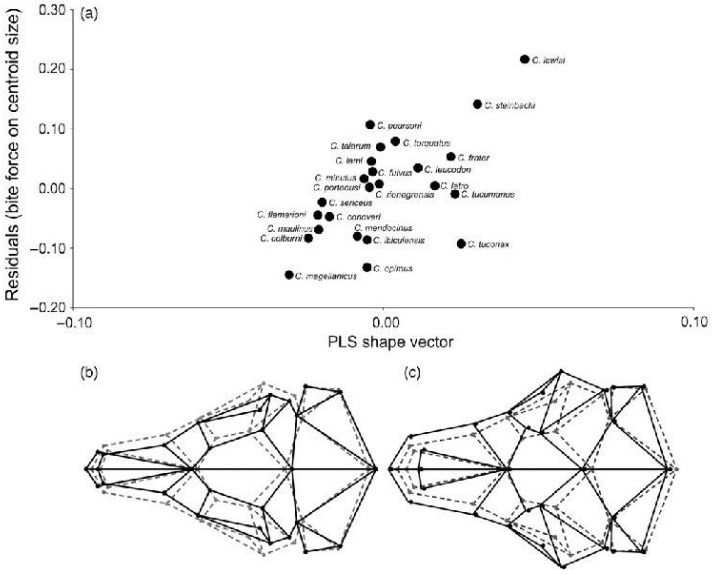

Figure 5 (a) First pair of vectors of a two-block partial least-squares analysis for the association between bite force (residuals of bite force on centroid size) and skull shape in dorsal view for 24 species of *Ctenomys*. Representation of conformational changes associated with (b) negative and (c) positive vectors of PLS (dashed gray lines correspond to the mean shape, and solid black lines correspond to the shape associated with positive and negative scores).

also more susceptible than shape to environmental changes (Thorpe, 1976; Patton & Brylski, 1987; Cardini & Elton, 2009; Maestri *et al.*, 2016b). The cost of burrowing also increases with body size (Vleck, 1981) which generates a trade-off between size increasing and metabolic economy in burrowing. This may be a constraint for species of *Ctenomys* to become larger, which may explain why just *C. conoveri* evolved to a discrepant size compared to others.

In contrast, *C. lewisi* and *C. steinbachi,* which also live in more-compacted soils and have intermediate body sizes, have robust skulls, which probably reflects an adaptation to the compact soils. The shape of the skull and mandible may have changed to increase their bite force in order to facilitate the process of excavation. According to Lacey *et al.* (2000), the genus *Ctenomys* includes species that are widely distributed in South America, exploiting different types of habitats and different types of soil. This ecological diversity, involving distinct functional requirements, may have driven the differentiation in skull morphology and led to a high rate of speciation in the genus (Mora *et al.*, 2003).

Species with both high and low bite forces proved to be present in harder soils, while only species with low bite forces are present in soft soils. This pattern is likely due to the different characteristics of each environment. Environments with lower bulk density (such as sand dunes) have less biomass than higher density soils (sand fields), as soil density is positively related to the amount of biomass available (food source) (Malizia, Vassallo & Busch, 1991; Cutrera *et al.*, 2010; see the results of Galiano *et al.*, 2014; Kubiak, Galiano & Freitas, 2015). The greater availability of food is likely a key factor in the choice of habitat, leading species with lower bite forces to inhabit locations with higher soil bulk density. To make this possible, the species can modify their excavation strategies (Hildebrand, 1998; Vassallo, 1998; Stein, 2000; Becerra *et al.*, 2011, 2014) and/or change the shape and size of their burrow systems (Reichman *et al.*, 1982; Heth, 1989; Rosi *et al.*, 2000; Lövy *et al.*, 2015) in order to access larger amounts of food in smaller home ranges.

In summary, the 24 species of the genus *Ctenomys* studied here showed variations in their skull shape associated with bite force. Studies on the association between bite force and environmental features are expanding knowledge of the interactions between morphology and the environments where these species occur (Verzi *et al.*, 2010; Becerra *et al.*, 2011; Becerra, Casinos & Vassallo, 2013; Becerra *et al.*, 2014; Vassallo *et al.*, 2015). Becerra *et al.* (2014) suggested that, probably, intraspecific differences in the bite force of *C. australis* could be explained mainly by differences in muscle development.

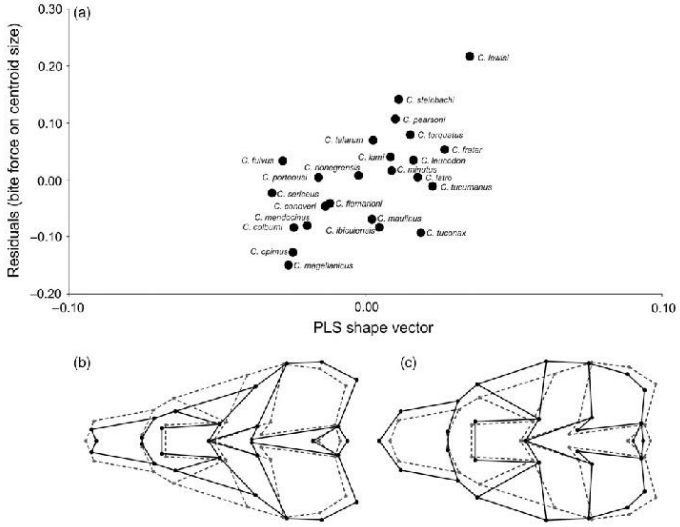

Figure 6 (a) First pair of vectors of a two-block partial least-squares analysis for the association between bite force (residuals of bite force on centroid size) and skull shape in ventral view for 24 species of *Ctenomys*. Representation of conformational changes associated with (b) negative and (c) positive vectors of PLS (dashed gray lines correspond to the mean shape, and solid black lines correspond to the shape associated with positive and negative scores).

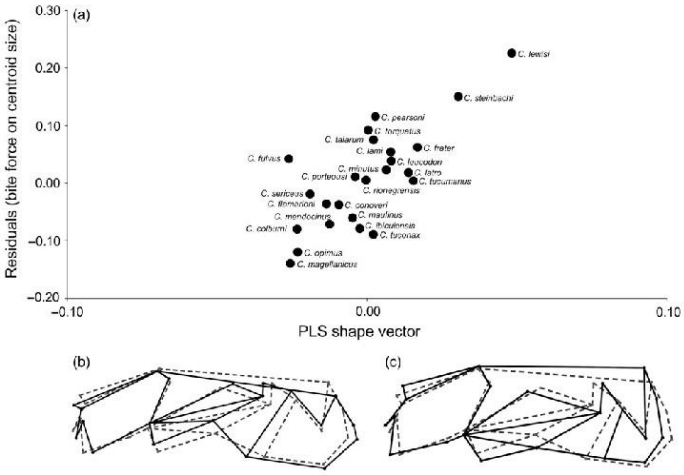

Figure 7 (a) First pair of vectors of a two-block partial least-squares analysis for the association between bite force (residuals of bite force on centroid size) and skull shape in lateral view for 24 species of *Ctenomys*. Representation of conformational changes associated with (b) negative and (c) positive vectors of PLS (dashed gray lines correspond to the mean shape, and solid black lines correspond to the shape associated with positive and negative scores).

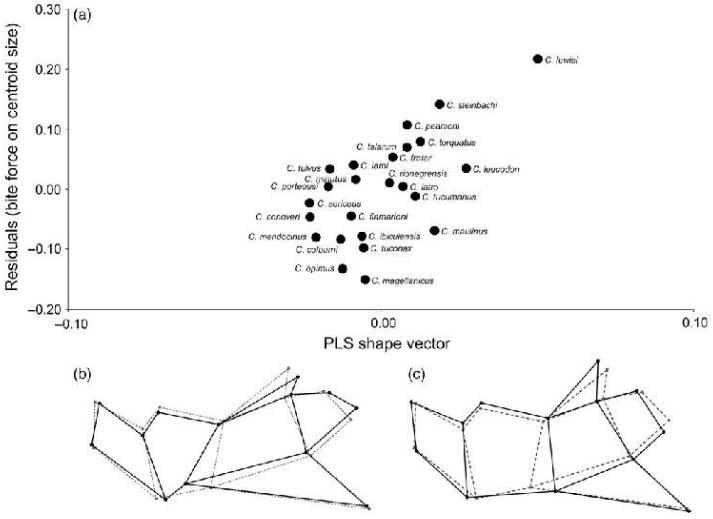

Figure 8 (a) First pair of vectors of a two-block partial least-squares analysis for the association between bite force (residuals of bite force on centroid size) and skull shape in mandible view for 24 species of *Ctenomys*. Representation of conformational changes associated with (b) negative and (c) positive vectors of PLS (dashed gray lines correspond to the mean shape, and solid black lines correspond to the shape associated with positive and negative scores).

This evidence of muscle development in the region of the skull and mandible is likely to contribute to understanding of the bite forces of members of the genus *Ctenomys* and other mammals. Studies of the digging behavior of different species would also be important, providing essential information to better understand the correlation between bite force and the environment.

Acknowledgements

We thank Aldo Vassallo and an anonymous reviewer for the helpful suggestions on the paper. We are grateful to our colleagues of the Laboratório de Citogenética e Evolução for their support in various stages of this study. Our thanks to all curators and collection managers who provided access to specimens of *Ctenomys*: Enrique González (MUNHINA), Olga B. Vacaro and Esperança A. Varela (MACN), Diego H. Verzi and A. Itatí Olivares (MLP), A. Damián Romero (MMP), James L. Patton, Eileen A. Lacey, and Christopher Conroy (MVZ), Eileen Westwig (AMNH), and Bruce D. Patterson (FMNH). L.R.B and R.M. received student scholarships from the Coordenação de Aperfeiçoamento de Pessoal de Nível Superior (CAPES), and B.B.K. and D.G. received student grants from the Conselho Nacional de Desenvolvimento Científico e Tecnológico (CNPq). T.R.O.F. received research support from CNPq, CAPES and the Fundação de Amparo à Pesquisa do Rio Grande do Sul (FAPERGS).

References

Adams, D.C. & Otárola-Castillo, E. (2013). Application geomorph: an R package for the collection and analysis of geometric morphometric shape data. *Methods Ecol. Evol.* **4**, 393–399.

Becerra, F., Echeverría, A. & Vassallo, A.I. (2011). Bite force and mandible biomechanics in the subterranean rodent Talas tuco-tuco (*Ctenomys talarum*) (Caviomorpha Octodontoidea). *Can. J. Zool.* **89**, 334–342.

Becerra, F., Casinos, A. & Vassallo, A.I. (2013). Biting performance and skull biomechanics of a chisel tooth digging rodent (*Ctenomys tuconax*; Caviomorpha; Octodontoidea). *J. Exp. Zool. A Ecol. Genet. Physiol.* **319**, 74–85.

Becerra, F., Echeverría, A.I., Casinos, A. & Vassallo, A.I. (2014). Another one bites the dust: Bite force and ecology in three caviomorph rodents (Rodentia, Hystricognathi). *J. Exp. Zool. A Ecol. Genet. Physiol.* **321**, 220–232.

Begall, S., Burda, H. & Schleich, C.E. (2007). *Subterranean rodents: news from underground*. Berlin: Springer Verlag.

Bidau, C.J. (2006). Familia Ctenomyidae. In *Mamíferos de Argentina: sistemática y distribución*: 212–231. Bárquez, R.J., Díaz, M.M. & Ojeda, R.A. (Eds). Tucumán, Argentina: SAREM (Sociedad Argentina para el Estudio de los Mamíferos).

Bidau, C.J. (2015). Family Ctenomyidae lesson, 1842. In *Mammals of South America*, Vol. 2: 818–877. Patton, J.L.,

Pardiñas, U.F.J. & D'Elía, E. (Eds). Chicago and London: The University of Chicago Press.
Biewener, A.A. (2003). *Animal locomotion*. Oxford, UK: Oxford University Press.
Bookstein, F.L. (1991). *Morphometric tools for landmark data: geometry and biology*. London, UK: Cambridge University Press.
Cardini, A. & Elton, S. (2009). Geographical and taxonomic influences on cranial variation in red colobus monkeys (Primates, Colobinae): introducing a new approach to 'morph' monkeys. *Glob. Ecol. Biogeogr.* **18**, 248–263.
Carrizo, L.V., Tulli, M.J. & Abdala, V. (2014). An ecomorphological analysis of forelimb musculotendinous system in sigmodontine rodents (Rodentia, Cricetidae, Sigmodontinae). *J. Mammal.* **95**, 843–854.
Caumul, R. & Polly, P.D. (2005). Phylogenetic and environmental components of morphological variation: skull, mandible, and molar shape in marmots (Marmota, Rodentia). *Evolution* **59**, 2460–2472.
Christiansen, P. & Adolfssen, J.S. (2005). Bite forces, canine strength and skull allometry in carnivores (Mammalia, Carnivora). *J. Zool.* **266**, 133–151.
Cooper, N., Freckleton, R.P. & Jetz, W. (2011). Phylogenetic conservatism of environmental niches in mammals. *Proc. R. Soc. B* **278**, 2384–2391.
Cutrera, A.P., Mora, M.S., Antenucci, C.D. & Vassallo, A.I. (2010). Intra- and interspecific variation in home-range size in sympatric tuco-tucos, *Ctenomys australis* and *Ctenomys talarum*. *J. Mammal.* **91**, 1425–1434.
Diniz-Filho, J.A., Bini, L.M., Rangel, T.F.L.B., Loyola, R.D., Hof, C., Nogués-Bravo, D. & Araújo, M.B. (2009). Partitioning and mapping uncertainties in ensembles of forecasts of species turnover under climate changes. *Ecography* **32**, 1–10.
Fernandes, F.A., Fornel, R., Cordeiro-Estrela, P. & Freitas, T.R.O. (2009). Intra- and interspecific skull variation in two sister species of the subterranean rodent genus *Ctenomys* (Rodentia, Ctenomyidae): coupling geometric morphometrics and chromosomal polymorphism. *Zool. J. Linn. Soc.* **155**, 220–237.
Fornel, R., Cordeiro-Estrela, P. & Freitas, T.R.O. (2010). Skull shape and size variation in *Ctenomys minutus* (Rodentia: Ctenomyidae) in geographical, chromosomal polymorphism, and environmental contexts. *Biol. J. Linn. Soc.* **101**, 705–720.
Freddi, O.S., Centurion, J.F., Beutler, A.N., Aratani, R.G., Leonel, C.L. & Silva, A.P. (2007). Soil compaction and least limiting water range on development and productivity of maize. *Bragantia*, Campinas **66**, 477–486.
Freeman, P.W. & Lemen, C.A. (2008). A Simple Morphological Predictor of Bite Force in Rodents. *J. Zool.* **275**, 418–422.
Freitas, T.R.O., Fernandes, F.A., Fornel, R. & Roratto, P.A. (2012). An endemic new species of tuco-tuco, genus *Ctenomys* (Rodentia: Ctenomyidae), with a restricted geographic distribution in southern Brazil. *J. Mammal.* **93**, 1355–1367.
Galiano, D., Kubiak, B.B., Overbeck, G.E. & Freitas, T.R.O. (2014). Effects of rodents on plant cover, soil hardness, and soil nutrient content: a case study on tuco-tucos (*Ctenomys minutus*). *Acta Theriol.* **59**, 583–587.
Gardner, S.L., Salazar-Bravo, J. & Cook, J.A. (2014). New Species of Ctenomys Blainville 1826 (Rodentia: Ctenomyidae) from the Lowlands and Central Valleys of Bolivia. *Faculty Publications from the Harold W. Manter Laboratory of Parasitology*. Paper 722.
Grafen, A. (1989). The phylogenetic regression. *Philos. Trans. R. Soc. Lond. B Biol. Sci.* **326**, 119–157.
Gubiani, P.I., Reinert, D.J. & Reichert, J.M. (2014). Critical values of soil bulk density evaluated by boundary conditions. *Ciênc. Rural* **44**, 994–1000.
Hengl, T., Jesus, J.M., MacMillan, R.A., Batjes, N.H., Heuvelink, G.B.M., Ribeiro, E., Samuel-Rosa, A., Kempen, B., Leenaars, J.G.B., Walsh, M.G. & Ruiperez Gonzalez, M. (2014). SoilGrids1 km — Global Soil Information Based on Automated Mapping. *PLoS One* **9**, e105992.
Heth, G. (1989). Burrow patterns of the mole-rat *Spalax ehrenbergi* in two soil types (terra-rossa and rendzina) in Mount Carmel, Israel. *J. Zool.* **217**, 39–56.
Hildebrand, M. (1985). Digging of quadrupeds. In *Functional vertebrate morphology*: 89–109. Hildebrand, M., Bramble, M., Liem, K.F. & Wake, D.B. (Eds). Cambridge, Massachusetts: The Belknap Press of Harvard University Press.
Hildebrand, M. (1998). *Analysis of vertebrate structure*. 5th edn. New York: Wiley.
Huey, R.B., Hertz, P.E. & Sinervo, B. (2003). Behavioral drive versus behavioral inertia in evolution: a null model approach. *Am. Nat.* **161**, 357–366.
IUCN (2008). Red List. Available at: http://www.iucnredlist.org/technical-documents/spatial-data.
Klingenberg, C.P. (2011). MorphoJ: an integrated software package for geometric morphometrics. *Mol. Ecol. Resour.* **11**, 353–357.
Kubiak, B.B., Galiano, D. & Freitas, T.R.O. (2015). Sharing the Space: Distribution, Habitat Segregation and Delimitation of a New Sympatric Area of Subterranean Rodents. *PLoS One* **10**, e0123220.
Lacey, E.A., Patton, J.L. & Cameron, G.N. (2000). *Life underground*. Chicago and London: The University of Chicago Press.
Lessa, E. & Thaeler, C. (1989). A reassessment of morphological specialization for digging in pocket gophers. *J. Mammal.* **70**, 689–698.
Lessa, E.P., Vassallo, A.I., Verzi, D.H. & Mora, M.S. (2008). Evolution of morphological adaptations for digging in living and extinct ctenomyid and octodontid rodents (Caviomorpha, Octodontoidea). *Biol. J. Linn. Soc.* **95**, 267–283.
Lövy, M., Šklíba, J., Hrouzková, E., Dvořáková, V., Nevo, E. & Šumbera, R. (2015). Habitat and Burrow System Characteristics of the Blind Mole Rat *Spalax galili* in an Area of Supposed Sympatric Speciation. *PLoS One* **10**, e0133157.

Luna, F. & Antinuchi, C.D. (2006). Cost of foraging in the subterranean rodent *Ctenomys talarum*: effect of soil hardness. *Can. J. Zool.* **84**, 661–667.
Maestri, R., Patterson, B.D., Fornel, R., Monteiro, L.R. & de Freitas, T.R.O. (2016a). Diet, bite force and skull morphology in the generalist rodent morphotype. *J. Evol. Biol.* (Online DOI: 10.1111/jeb.12937)
Maestri, R., Fornel, R., Gonçalves, G.L., Geise, L., de Freitas, T.R.O. & Carnaval, A.C. (2016b). Predictors of intraspecific morphological variability in a tropical hotspot: comparing the influence of random and non-random factors. *J. Biogeogr.* (Online DOI: 10.1111/jbi.12815)
Malizia, A.I., Vassallo, A.I. & Busch, C. (1991). Population and habitat characteristics of two sympatric species of *Ctenomys* (Rodentia: Octodontidae). *Acta Theriol.* **36**, 87–94.
Mora, M., Olivares, A.I. & Vassallo, A.I. (2003). Size, shape and structural versatility of the skull of the subterranean rodent *Ctenomys* (Rodentia, Caviomorpha): functional and morphological analysis. *Biol. J. Linn. Soc.* **78**, 85–96.
Nevo, E. (1979). Adaptive Convergence and Divergence of Subterranean Mammals. *Annu. Rev. Ecol. Syst.* **10**, 269–308.
Nevo, E. (1999). *Mosaic evolution of subterranean mammals – Regression, progression, and global convergence*. New York: Oxford University Press.
Nogueira, M.R., Peracchi, A.L. & Monteiro, L.R. (2009). Morphological correlates of bite force and diet in the skull and mandible of phyllostomid bats. *Funct. Ecol.* **23**, 715–723.
Patton, J.L. & Brylski, P.V. (1987). Pocket gophers in alfalfa fields: causes and consequences of habitat-related body size variation. *Am. Nat.* **130**, 493–506.
R Core Team (2016). *R: a language and environment for statistical computing*. Vienna, Austria: R Foundation for Statistical Computing. Available at: https://www.R-project.org/.
Redford, K.H. and Eisenberg, J.F. (1992). *Mammals of the Neotropics*. Vol. 2. *The Southern Cone: Chile, Argentina, Uruguay, Paraguay*. Chicago: University of Chicago Press.
Reichman, O.J., Whitham, T.G. & Ruffner, G.A. (1982). Adaptive geometry of burrow spacing in two pocket gopher populations. *Ecology* **63**, 687–695.
Reinert, D.J., Albuquerque, J.A., Reichert, J.M., Aita, C. & Andrada, M.M.C. (2008). Bulk density critical limits for normal root growth of cover crops. *Rev. Bras. Ciênc. Solo* **32**, 1805–1816.
Rohlf, F.J. (2015). The tps series of software. *Hystrix* **26**, 9–12.
Rohlf, F.J. & Corti, M. (2000). Use of two-block partial least-squares to study covariation in shape. *Syst. Biol.* **49**, 740–753.
Rosi, M.I., Cona, M.I., Videla, F., Puig, S. & Roig, V.G. (2000). Architecture of *Ctenomys mendocinus* (Rodentia) burrows from two habitats differing in abundance and complexity of vegetation. *Acta Theriol.* **45**, 491–505.
Schmidt-Nielsen, K. (1984). *Scaling: why is animal size so important?* Cambridge, UK: Cambridge University Press.
Stein, B. (2000). Morphology of subterranean rodents. In *Life underground: the biology of subterranean rodents*: 19–61. Lacey, E.A., Patton, J.L. & Cameron, G.N. (Eds). Chicago: University of Chicago Press.
Thorpe, R.S. (1976). Biometric analysis of geographic variation and racial affinities. *Biol. Rev.* **51**, 407–452.
Van Valkenburgh, B. & Ruff, C.B. (1987). Canine tooth strength and killing behaviour in large carnivores. *J. Zool.* **212**, 379–397.
Vassallo, A.I. (1998). Functional morphology, comparative behaviour, and adaptation in two sympatric subterranean rodents genus Ctenomys (Caviomorpha: Octodontidae). *J. Zool.* **244**, 415–427.
Vassallo, A.I., Becerra, F., Echeverría, A.I. & Casinos, A. (2015). Ontogenetic integration between force production and force reception: a case study in Ctenomys (Rodentia: Caviomorpha). *Acta Zool.* **97**, 232–240.
Verzi, D.H., Álvarez, A., Olivares, A.I., Morgan, C.C. & Vassallo, A.I. (2010). Ontogenetic trajectories of key morphofunctional cranial traits in South American subterranean ctenomyid rodents. *J. Mammal.* **91**, 1508–1516.
Viguier, B. (2002). Is the morphological disparity of lemur skulls (Primates) controlled by phylogeny and/or environmental constraints? *Biol. J. Linn. Soc.* **76**, 577–590.
Vleck, D. (1981). Burrow structure and foraging costs in the fossorial rodent, *Thomomys bottae*. *Oecologia* **49**, 391–396.
Wainwright, P.C. (2007). Functional versus morphological diversity in macroevolution. *Annu. Rev. Ecol. Evol. Syst.* **38**, 381–401.
Wiens, J.J. & Graham, C.H. (2005). Niche conservatism: integrating evolution, ecology, and conservation biology. *Annu. Rev. Ecol. Evol. Syst.* **36**, 519–539.

Supporting Information

Additional Supporting Information may be found in the online version of this article:

Appendix S1. List of species of *Ctenomys* and sample size used to investigate the skull and mandible shape, and the number of individuals used to measure the incisor strength index (bite force).
Appendix S2. The 24 species of the genus *Ctenomys* studied, their bite forces (N = Newtons), centroid size values, and bulk density values.
Appendix S3. Definition of landmarks with numbers and locations for each view of the cranium and mandible of *Ctenomys* (shown in Fig. 1 in the main text).